

IPELS-16, Garching, August 3, 2024

Paradigmatic liquid-metal experiments on geo- and astrophysical phenomena

Frank Stefani

With thanks to:

Agris Gailitis (Riga), Gunter Gerbeth, André Giesecke, Thomas Gundrum, Vivaswat Kumar, George Mamatsashvili, Ashish Mishra, Jude Ogbonna, Federico Pizzi, Sebastian, Günther Rüdiger (Potsdam), Martin Seilmayer, Rodion Stepanov (Perm), Tom Weier...

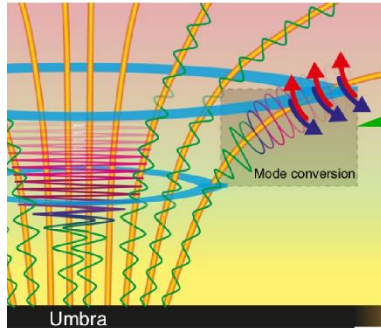


HZDR

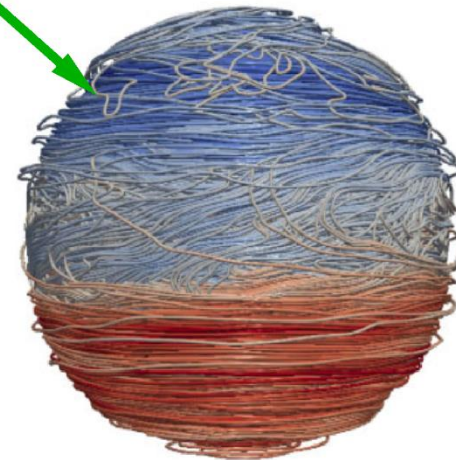
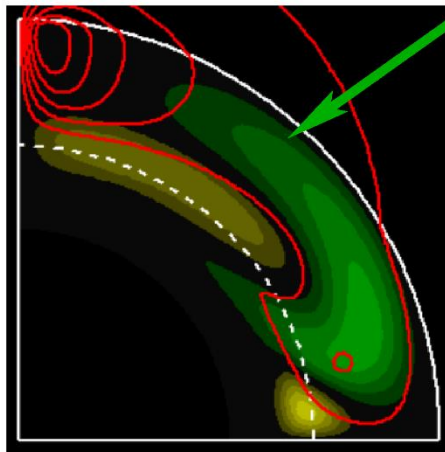
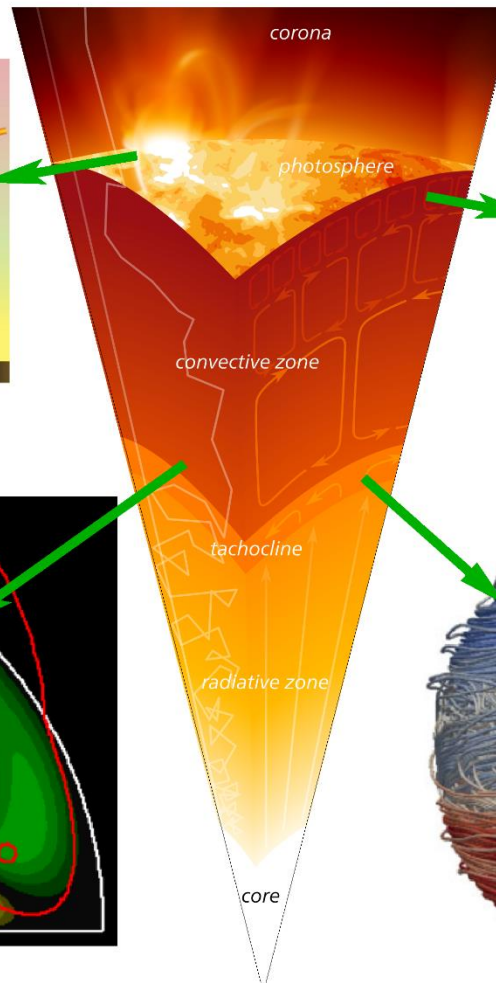
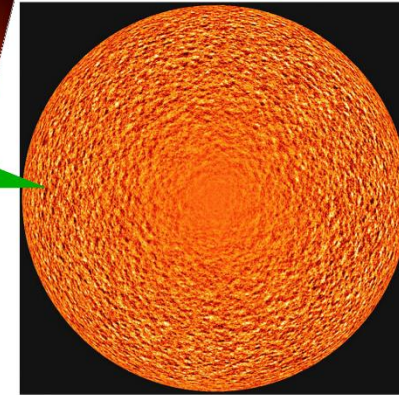
 **HELMHOLTZ**
ZENTRUM DRESDEN
ROSSENDORF

Motivation and schedule

1) Alfvén waves



2) Convection

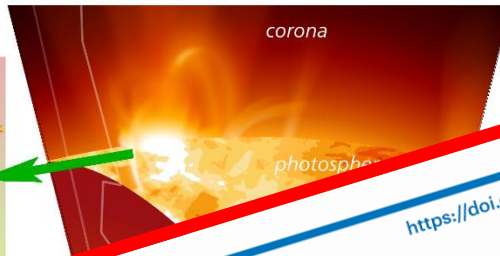
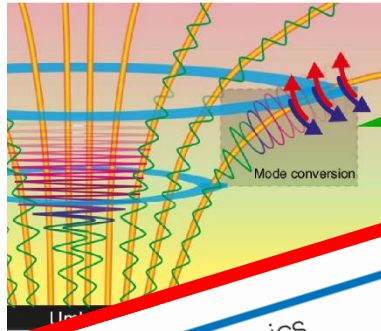


4) Dynamo

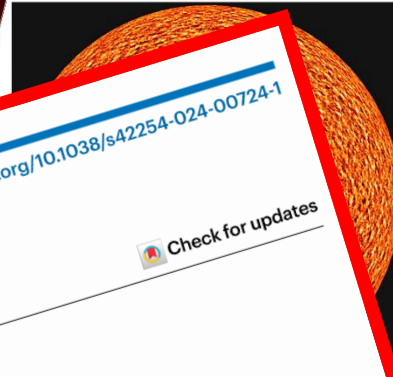
3) MRI etc...

Motivation and schedule

1) Alfvén waves



2) Convection



4) Dynamo

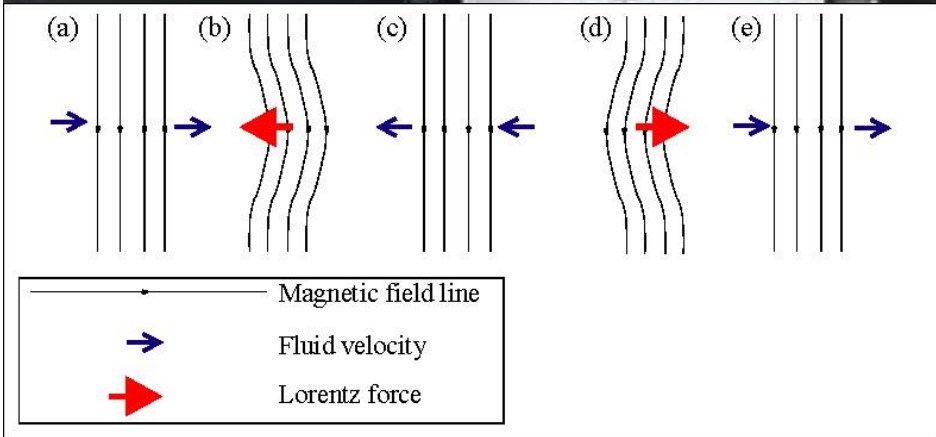
3) MRI etc...

core



Alfvén waves

Alfvén waves: Prediction by H. Alfvén 1942 (Nobel prize 1970)



... but, not in a direction determined by the direction of the stimulus—and often producing an aggregating effect superficially similar to that of a taxis; and an *orientation*, which is the placing of the body (usually if not always animal) in a direction determined by the direction of the stimulus. To these three classes many of the cases can be referred.

But the responses of sessile plant organs do not seem to be so conveniently classified. The thigmotropism of *Clematis* tendrils appears to warrant that name, for the response is a directional one. But the same cannot be said of the so-called 'thigmotropism' of *Mimosa* leaflets, *Mimulus* stigma or *Berberis*

* Evans, A. E., "Flora of Cambridgeshire", 165 (1939).
 † Bagnall, J. E., "Flora of Staffordshire", 57 (1901).
 ‡ Britton, C. E., *J. Bot.*, 48, 186 (1910).

Existence of Electromagnetic-Hydrodynamic Waves

If a conducting liquid is placed in a constant magnetic field, every motion of the liquid gives rise to an E.M.F. which produces electric currents. Owing to the magnetic field, these currents give mechanical forces which change the state of motion of the liquid.

Thus a kind of combined electromagnetic-hydrodynamic wave is produced which, so far as I know, has as yet attracted no attention.

The phenomenon may be described by the electrodynamic equations

$$\begin{aligned} \text{rot } H &= \frac{4\pi}{c} i \\ \text{rot } E &= -\frac{1}{c} \frac{dB}{dt} \\ B &= \mu H \\ i &= \sigma(E + \frac{v}{c} \times B); \end{aligned}$$

together with the hydrodynamic equation

$$\rho \frac{dv}{dt} = \frac{1}{c} (i \times B) - \text{grad } p,$$

where σ is the electric conductivity, μ the permeability, ρ the mass density of the liquid, i the electric current, v the velocity of the liquid, and p the pressure.

Consider the simple case when $\sigma = \infty$, $\mu = 1$ and the imposed constant magnetic field H_0 is homogeneous and parallel to the z -axis. In order to study a plane wave we assume that all variables depend upon the time t and z only. If the velocity v is parallel to the x -axis, the current i is parallel to the y -axis and produces a variable magnetic field H' in the x -direction. By elementary calculation we obtain

$$\frac{d^2 H'}{dz^2} = \frac{4\pi\sigma}{H_0^2} \frac{d^2 H'}{dt^2},$$

which means a wave in the direction of the z -axis with the velocity

$$V = \frac{H_0}{\sqrt{4\pi\sigma}}$$

Waves of this sort may be of importance in solar physics. In a region of the sun where the magnetic field, and as solar matter is a good conductor, the conditions for the existence of electromagnetic-hydrodynamic waves are satisfied. If in a region of the sun we have $H_0 = 15$ gauss and $\sigma = 0.005$ gm. cm.⁻¹, the velocity of the waves amounts to

$$V \sim 60 \text{ cm. sec.}^{-1}.$$

This is about the velocity with which the sunspot zone moves towards the equator during the sunspot cycle. The above values of H_0 and σ refer to a distance of about 10¹⁰ cm. below the solar surface where the original cause of the sunspots may be found. Thus it is possible that the sunspots are associated with a magnetic and mechanical disturbance proceeding as an electromagnetic-hydrodynamic wave.

The matter is further discussed in a paper which will appear in *Arkiv för matematik, astronomi och fysik*.

H. ALFVÉN.

Kgl. Tekniska Högskolan,
Stockholm.

Energy of Dissociation of Carbon Monoxide

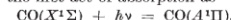
THE energies of dissociation of a number of diatomic molecules have been determined from spectroscopic data, apparently with high accuracy, by the observation of predissociation limits. During the last few years the following values have been proposed for CO: $D(\text{CO}) = 6.92^1, 8.41^2, 9.14^3, 10.45^4$ e.v.; while values of 9.85 and 11.11 also appear possible⁵. Controlled electron experiments suggest 9.6⁶.

The value obtained by extrapolation of the vibra-

tional levels of the ground state is about 11, and support for this value has been given by Kynch and Penney⁵. Herzberg⁷ has recently summarized evidence favouring 9.14.

At first sight, the strongest argument for 9.14 is the observation by Faltings, Groth and Harteck⁸ that CO is decomposed by the xenon line at 1295 Å., not by that at 1470 Å., from which they conclude that $8.44 < D(\text{CO}) < 9.57$. This conclusion is not based on an examination of the initial act of absorption. The only known absorption in the 295 Å. region is that corresponding to the fourth positive bands. The origins of the (9,0) and (10,0) bands lie at 76,839 cm.⁻¹ and 78,010 cm.⁻¹. The xenon line 1295 Å. = 77,172 cm.⁻¹ falls between these bands and, if absorbed from the lowest vibrational level of CO, would correspond approximately to the line P(35) of (10,0). This gives as the upper limit of $D(\text{CO})$ (when the rotational energy is taken into account) a value of 79,722 cm.⁻¹ = 9.88 e.v. (not 9.57 e.v. as stated by Herzberg⁷). Actually, it is doubtful whether such a high rotational line as P(35) would be observed at room temperature, and absorption, if it is due to CO, would probably occur from a higher vibrational level, corresponding perhaps to the (13,2) band, in which case the dissociation limit may be placed as high as 10.1.

Taking the first act of absorption as



and assuming a life not less than 10⁻⁸ sec. for A¹Π, then at atmospheric pressure each molecule experiences at least 100 collisions before radiating. It seems to us that this gives a reasonable chance for a reaction such as



to proceed with quantum efficiency approaching unity. The state of the carbon atom might be either ¹D or P; the former if spin is to be conserved, the latter if not. In either case the reaction is strongly exothermic. The failure of the xenon line 1470 to induce photodissociation may be due to the reaction requiring an activation energy.

Estimates of $D(\text{CO})$ less than 10 take no account of the non-crossing rule of Hund, and Neumann and Wigner⁹. This rule states that potential energy curves of molecular states of identical species cannot cross. Whether the rule is rigorous when the nuclear and electronic motions are not separated needs further examination, but at least we see no reason for anticipating a failure of the rule in the lowest energy curve of CO. If this curve has only one turning point then the non-crossing rule requires unequivocally that $D(\text{CO}) > 10.3$, and would agree well with the predissociation limit at 11.11 e.v.

The dissociation energy of CO⁺ is 2.6 e.v. less than that of CO ($D(\text{CO}^+) = D(\text{CO}) + I(\text{C}) - I(\text{CO})$). Three electronic states of CO⁺ are known, namely, X²Σ⁺, A¹Π and B²Σ⁺, extrapolating to dissociation limits of about 9.8 (a very long extrapolation), 9.2 and 9.4 e.v. respectively. Since the two ²Σ⁺ states must give different products of dissociation, it would appear, on the evidence of the B²Σ⁺ state, that $D(\text{CO}^+) = 7.4$, and $D(\text{CO})$ is about 10, and on the evidence of the A¹Π state that $D(\text{CO}^+) = 9.2$ and $D(\text{CO})$ is 11.8. All that may fairly be deduced from present evidence on CO⁺ is that $D(\text{CO})$ is unlikely to be much less than 10.

We have also re-examined nitrogen. The accepted value $D(\text{N}_2) = 7.38$ is based on the identification of the upper state of the Vegard-Kaplan bands with the

Alfvén waves: Prediction by H. Alfvén 1942 (Nobel prize 1970)

Many experiments in liquid metal and plasma

- S. Lundquist, Nature **164**, 146 (1949)
- B. Lehnert, Phys.Rev. **94** (1954), 815
- A. Jameson, J. Fluid Mech. **19** (1964), 513
- K. Iwai et al, Magnetohydrodynamics **39**, 245 (2003)
- T. Alboussiere et al., Phys. Fluids **23** (2011), 096601
- Z. Tigrine et al., Geophys. J. Int. **219**, S83 (2019)
- S. Lalloz et al., arXiv: 2405.04276

W. Gekelman et al., Phys. Plasmas **18** (2011), 055501

...and quite a number of talks at this conference!

This a kind of combined electromagnetic-hydrodynamic wave is produced which, so far as I know, has as yet attracted no attention.

The phenomenon may be described by the electrodynamic equations

$$\text{rot } H = \frac{4\pi}{c} i$$

$$\text{rot } E = -\frac{1}{c} \frac{dB}{dt}$$

$$B = \mu H$$

$$i = \sigma(E + \frac{v}{c} \times B);$$

together with the hydrodynamic equation

$$\partial \frac{dv}{dt} = \frac{1}{c} (i \times B) - \text{grad } p,$$

where σ is the electric conductivity, μ the permeability, ∂ the mass density of the liquid, i the electric current, v the velocity of the liquid, and p the pressure.

Consider the simple case when $\sigma = \infty$, $\mu = 1$ and the imposed constant magnetic field H_0 is homogeneous and parallel to the z -axis. In order to study a plane wave we assume that all variables depend upon the time t and z only. If the velocity v is parallel to the x -axis, the current i is parallel to the y -axis and produces a variable magnetic field H' in the x -direction. By elementary calculation we obtain

$$\frac{d^2 H'}{dz^2} = \frac{4\pi\partial}{H_0^2} \frac{d^2 H'}{dt^2},$$

which means a wave in the direction of the z -axis with the velocity

$$V = \frac{H_0}{\sqrt{4\pi\partial}}.$$

Waves of this sort may be of importance in solar physics. In the neighbourhood of the sun's magnetic field, and as solar matter is a good conductor, the conditions for the existence of electromagnetic-hydrodynamic waves are satisfied. If in a region of the sun we have $H_0 = 15$ gauss and $\partial = 0.005$ gm. cm.⁻³, the velocity of the waves amounts to

$$V \sim 60 \text{ cm. sec.}^{-1}.$$

This is about the velocity with which the sunspot zone moves towards the equator during the sunspot cycle. The above values of H_0 and ∂ refer to a distance of about 10^{10} cm. below the solar surface where the original cause of the sunspots may be found. Thus it is possible that the sunspots are associated with a magnetic and mechanical disturbance proceeding as an electromagnetic-hydrodynamic wave.

The matter is further discussed in a paper which will appear in *Arkiv för matematik, astronomi och fysik*.

H. ALFVÉN.

Kgl. Tekniska Högskolan,
Stockholm.

Energy of Dissociation of Carbon Monoxide

THE energies of dissociation of a number of diatomic molecules have been determined from spectroscopic data, apparently with high accuracy, by the observation of predissociation limits. During the last few years the following values have been proposed for CO: $D(\text{CO}) = 6.92^1, 8.41^2, 9.14^3, 10.45^4$ e.v.; while values of 9.85 and 11.11 also appear possible⁵. Controlled electron experiments suggest 9.6⁶.

The value obtained by extrapolation of the vibra-

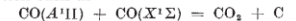
tional levels of the ground state is about 11, and support for this value has been given by Kynch and Penney⁵. Herzberg⁷ has recently summarized evidence favouring 9.14.

At first sight, the strongest argument for 9.14 is the observation by Faltings, Groth and Harteck⁸ that CO is decomposed by the xenon line at 1295 Å., but not by that at 1470 Å., from which they conclude that $8.44 < D(\text{CO}) < 9.57$. This conclusion is not based on an examination of the initial act of absorption. The only known absorption in the 295 Å. region is that corresponding to the fourth positive bands. The origins of the (9,0) and (10,0) bands lie at 76,839 cm.⁻¹ and 78,010 cm.⁻¹. The xenon line 1295 Å. = 77,172 cm.⁻¹ falls between these bands and, if absorbed from the lowest vibrational level of CO, would correspond approximately to the line P(35) of (10,0). This gives as the upper limit of $D(\text{CO})$ (when the rotational energy is taken into account) a value of 79,722 cm.⁻¹ = 9.88 e.v. (not 9.57 e.v. as stated by Herzberg⁷). Actually, it is doubtful whether such a high rotational line as P(35) would be observed at room temperature, and absorption, if it is due to CO, would probably occur from a higher vibrational level, corresponding perhaps to the (13,2) band, in which case the dissociation limit may be placed as high as 10.1.

Taking the first act of absorption as

$$\text{CO}(X^1\Sigma) + h\nu = \text{CO}(A^1\Pi),$$

and assuming a life not less than 10^{-8} sec. for $A^1\Pi$, then at atmospheric pressure each molecule experiences at least 100 collisions before radiating. It seems to us that this gives a reasonable chance for a reaction such as



to proceed with quantum efficiency approaching unity. The state of the carbon atom might be either 1D or 3P ; the former if spin is to be conserved, the latter if not. In either case the reaction is strongly exothermic. The failure of the xenon line 1470 to induce photodissociation may be due to the reaction requiring an activation energy.

Estimates of $D(\text{CO})$ less than 10 take no account of the non-crossing rule of Hund, and Neumann and Wigner⁹. This rule states that potential energy curves of molecular states of identical species cannot cross. Whether the rule is rigorous when the nuclear and electronic motions are not separated needs further examination, but at least we see no reason for anticipating a failure of the rule in the lowest energy curve of CO. If this curve has only one turning point then the non-crossing rule requires unequivocally that $D(\text{CO}) > 10.3$, and would agree well with the predissociation limit at 11.11 e.v.

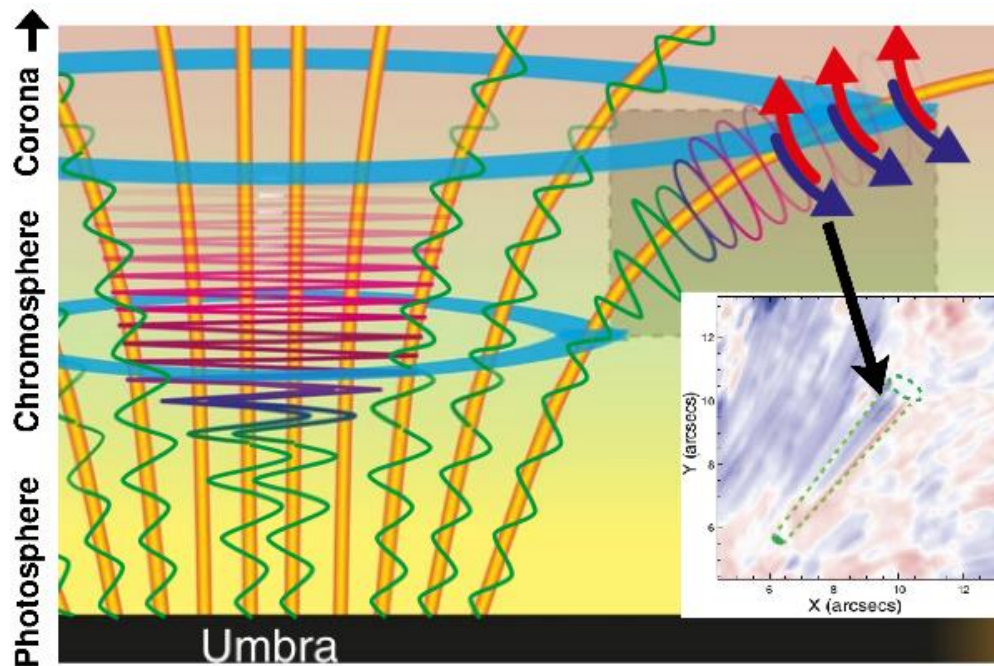
The dissociation energy of CO^+ is 2.6 e.v. less than that of CO ($D(\text{CO}^+) = D(\text{CO}) + I(\text{C}) - I(\text{CO})$). Three electronic states of CO^+ are known, namely, $X^2\Sigma^+$, $A^1\Pi$ and $B^2\Sigma^+$, extrapolating to dissociation limits of about 9.8 (a very long extrapolation), 9.2 and 9.4 e.v. respectively. Since the two $^2\Sigma^+$ states must give different products of dissociation, it would appear, on the evidence of the $B^2\Sigma^+$ state, that $D(\text{CO}^+)$ is 7.4, and $D(\text{CO})$ is about 10, and on the evidence of the $A^1\Pi$ state that $D(\text{CO}^+)$ is 9.2 and $D(\text{CO})$ is 11.8. All that may fairly be deduced from present evidence on CO^+ is that $D(\text{CO})$ is unlikely to be much less than 10.

We have also re-examined nitrogen. The accepted value $D(\text{N}_2) = 7.38$ is based on the identification of the upper state of the Vegard-Kaplan bands with the

An underexplored aspect of Alfvén waves...

...is related to the **heating of the solar corona** which relies on transformation of **sound waves into Alfvén waves** via parametric resonance, or swing excitation (at a point where **sound speed = Alfvén speed**, or plasma $\beta \sim 1$)

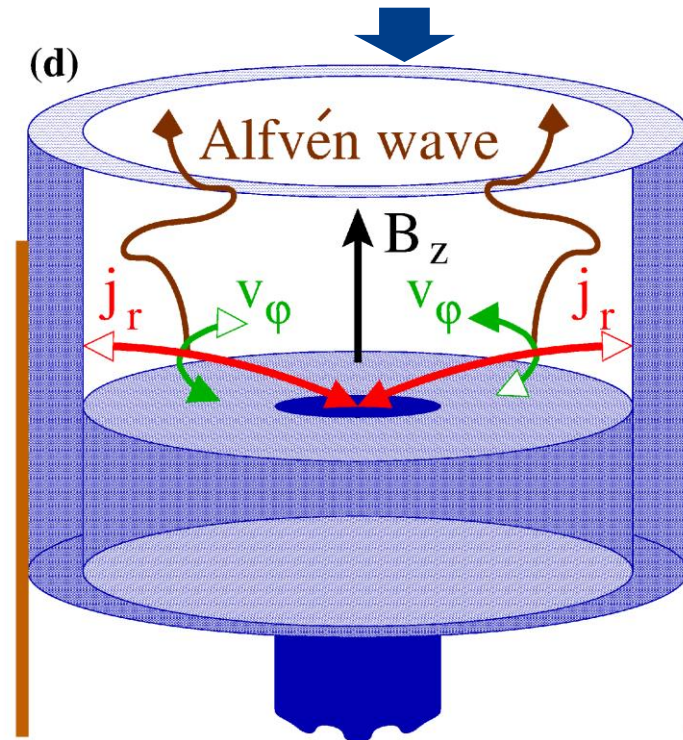
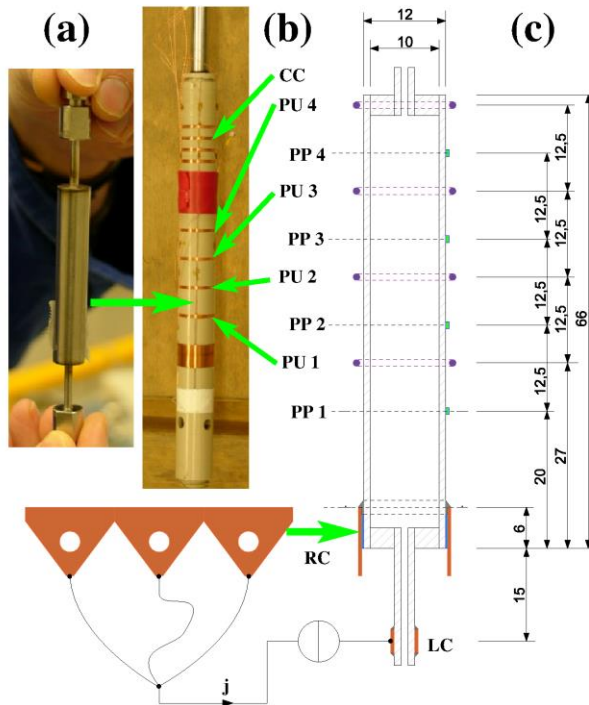
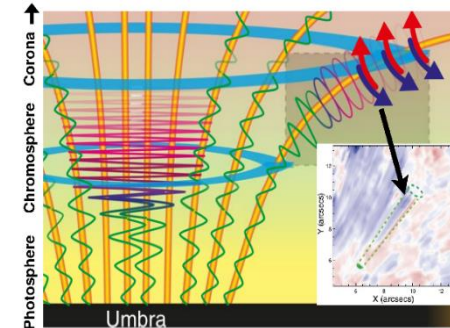
T. Zaqarashvili, ApJ 552 (2001) L81



Grant et al., Nature Phys. 14 (2018), 480;
Srivastava et al., Sci. Rep. 7 (2017), 43147

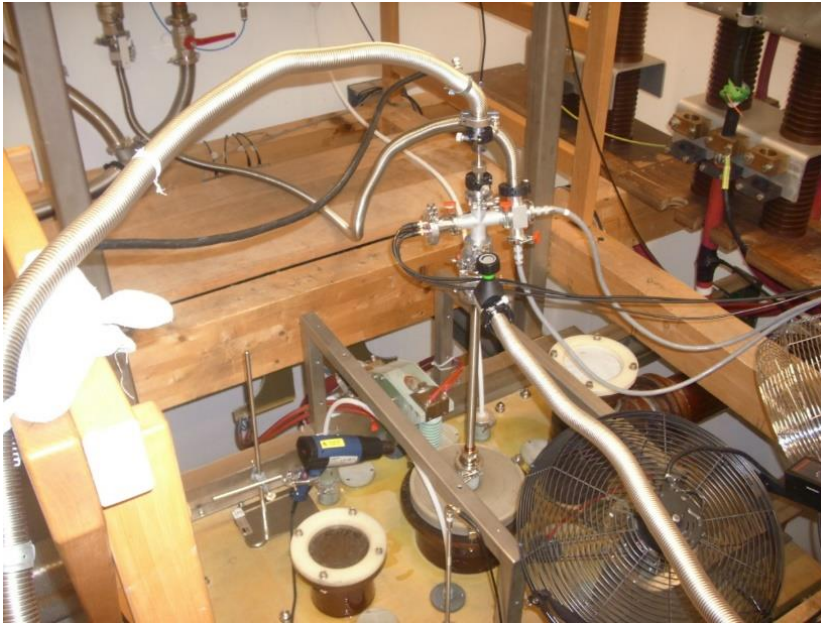
Alfvén wave experiments at High Magnetic Field Lab at HZDR

For liquid Rubidium (dangerous!!!) we obtain **Sound speed = Alfvén speed** (plasma $\beta=1$) at $B=54$ T

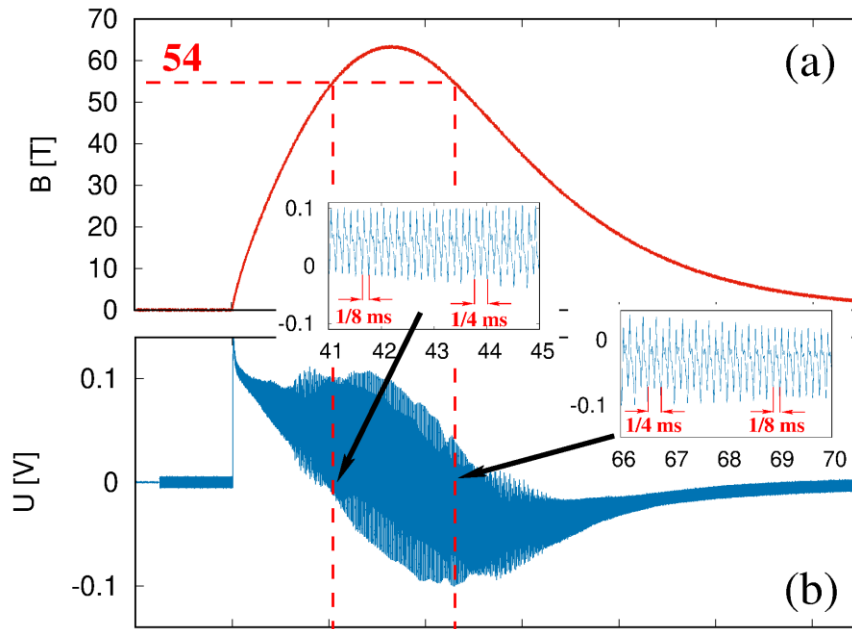


$\mathbf{j} \times \mathbf{B}$ excitation of torsional Alfvén waves in B up to 63 T

Alfvén wave experiments at High Magnetic Field Lab at HZDR

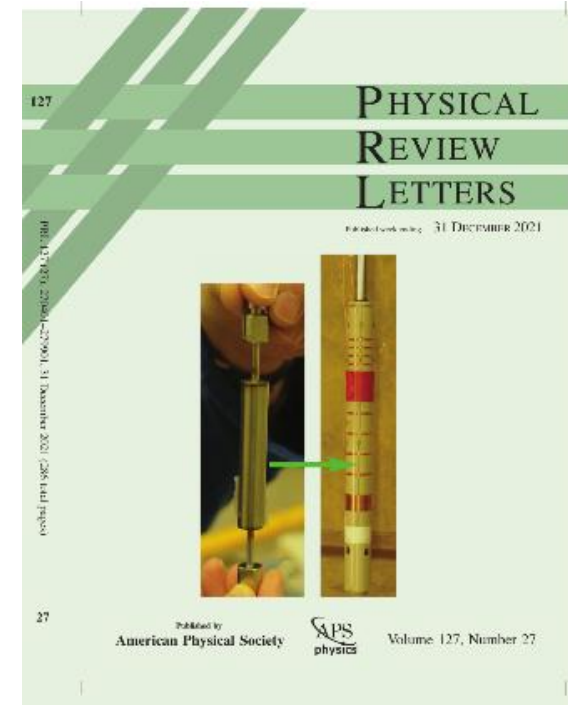


CW excitation: Voltage over bottom contact



Some rough estimates:

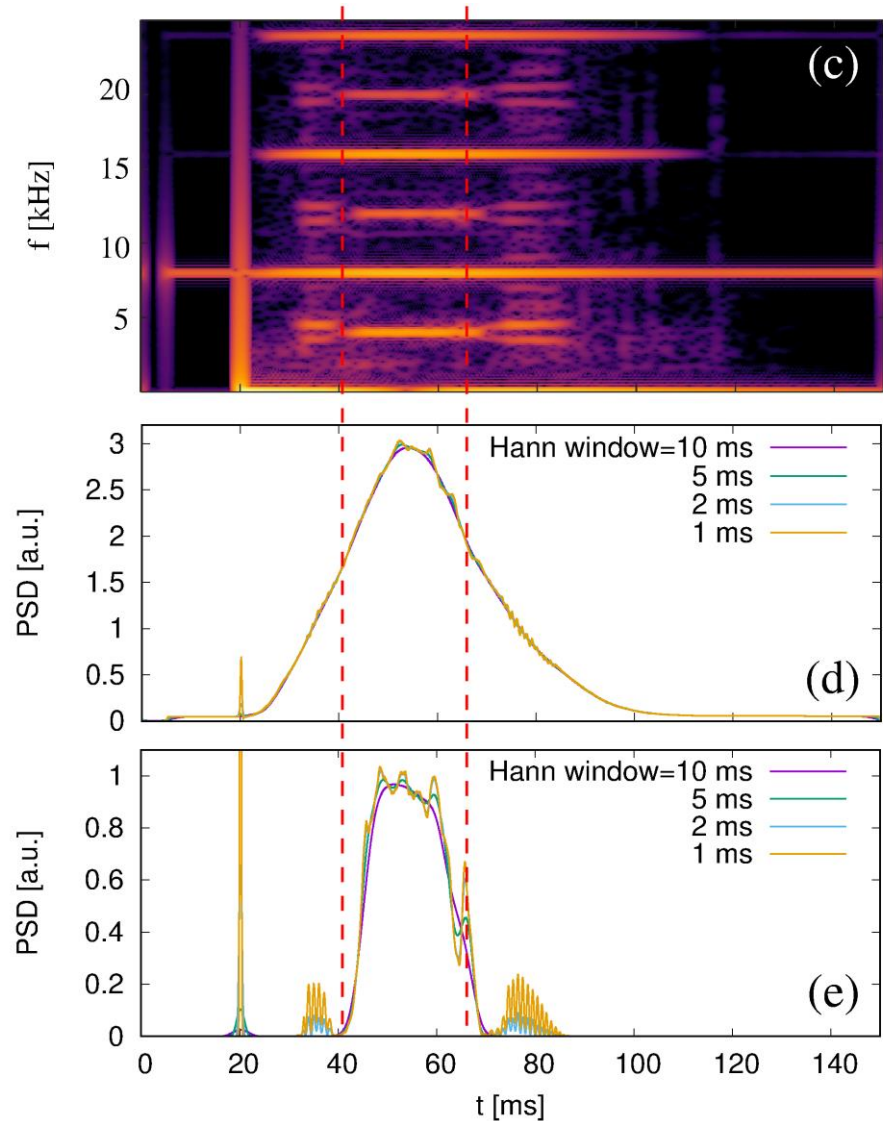
- Excitation current: 5 A, 8 kHz CW
- Current density: $\sim 100 \text{ kA/m}^2$
- Azimuthal acceleration: $j B/\rho \sim 3000 \text{ m/s}^2$
- Flow velocity: $\sim a T/2 \sim 20 \text{ cm/s}$
- Induced voltage: $\sim vBr \sim 50 \text{ mV}$



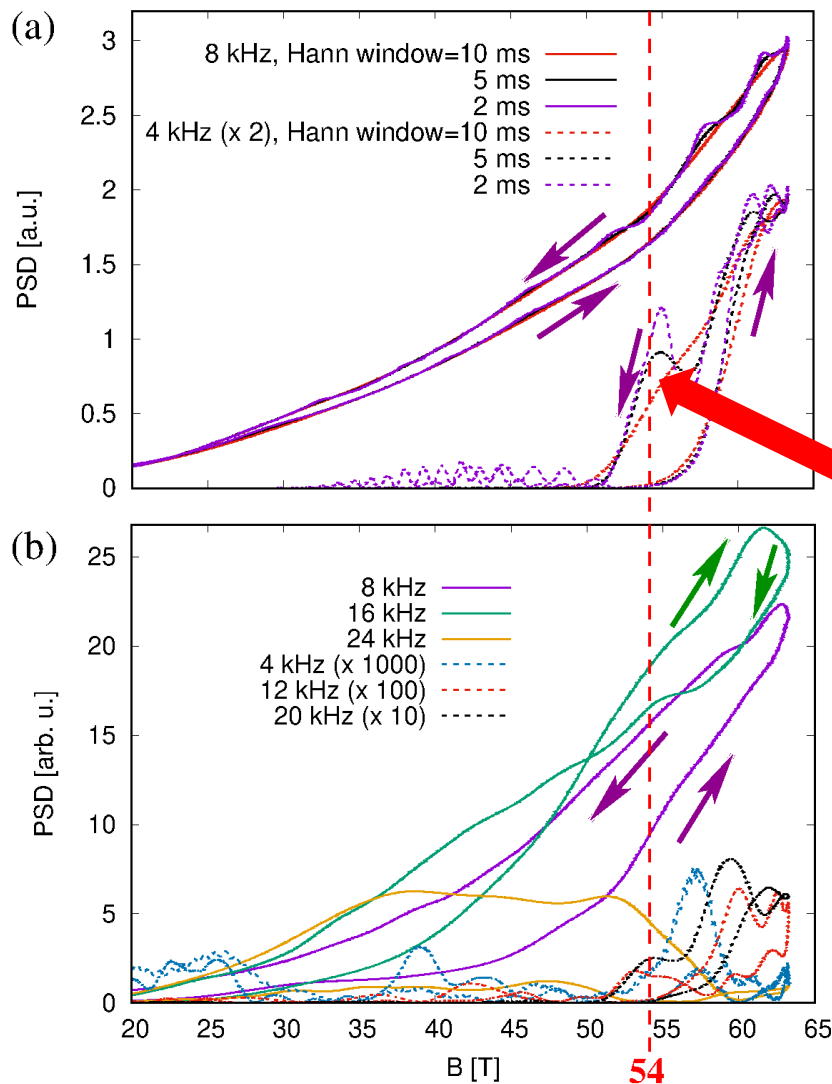
F.S. et al, Phys. Rev. Lett. 127 (2021), 275001

CW excitation: Voltage over bottom contact

- Gabor transform (short time Fourier) with von Hann window 5 ms
- PSD of 8 kHz stripe is very smooth and roughly $\sim B^2$
- PSD of 4 kHz stripe appears only for $B=54$ T (and larger)



CW excitation: Dependence on magnetic field



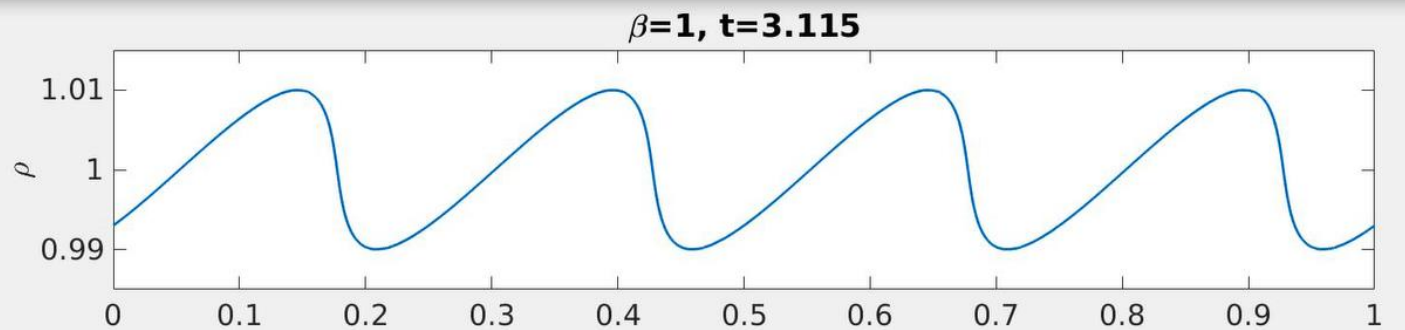
Voltage over bottom contact
(indicative of Alfvén wave):
PSD's for 8 kHz and 4 kHz

**Period doubling due to
parametric resonance
(swing excitation)!!!**

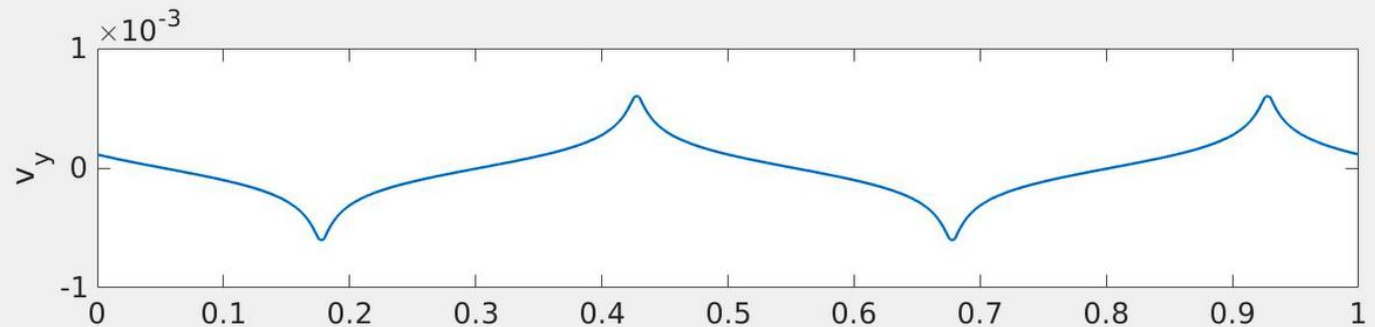
Voltage at pick-up coil 2
(indicative of magnetosonic waves):
PSD's for $n \cdot 4$ kHz

First simulations of parametric resonance at $\beta=1$

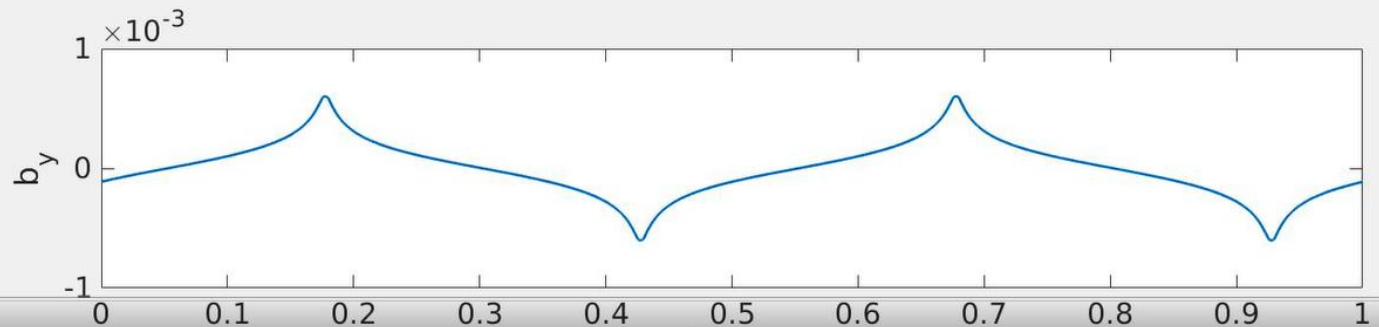
Density



Velocity



Magnetic field



T. Zaqarashvili, ApJ
552 (2001) L81

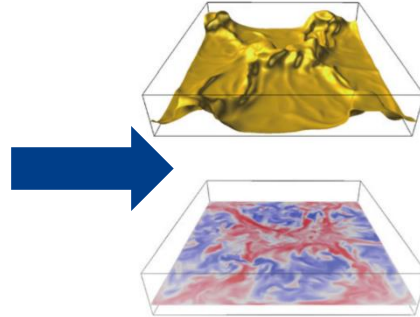
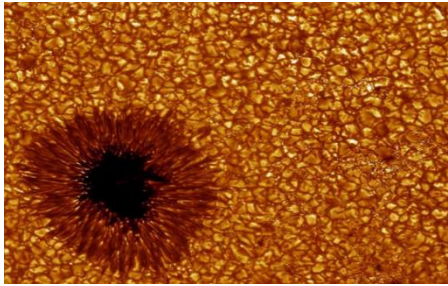


G. Mamatsashvili et al.,
in preparation

Convection

Convection at small Prandtl numbers

Turbulent superstructures in shallow geometry

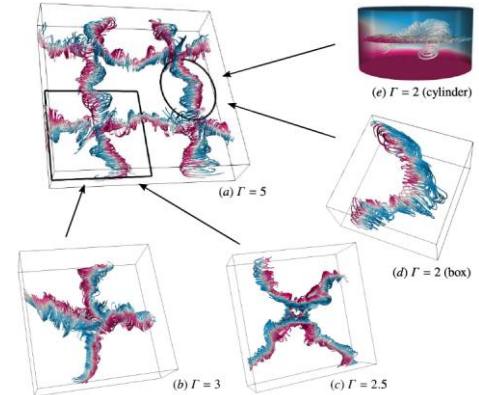


Akashi et al., J. Fluid Mech. 932, A27 (2022)

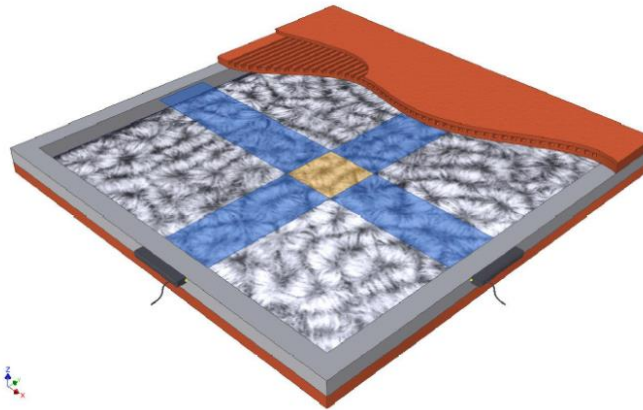
Jump rope vortex, detected first in...

Vogt et al., PNAS 115, 12674 (2018)

...turns out to be a universal feature

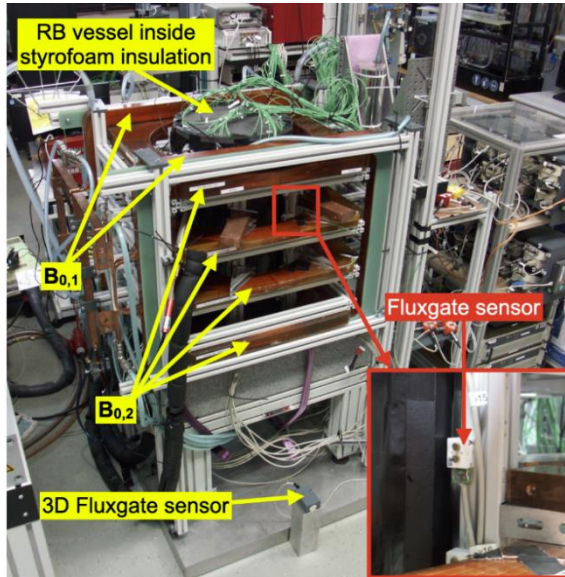


New experiment with $\Gamma=25$

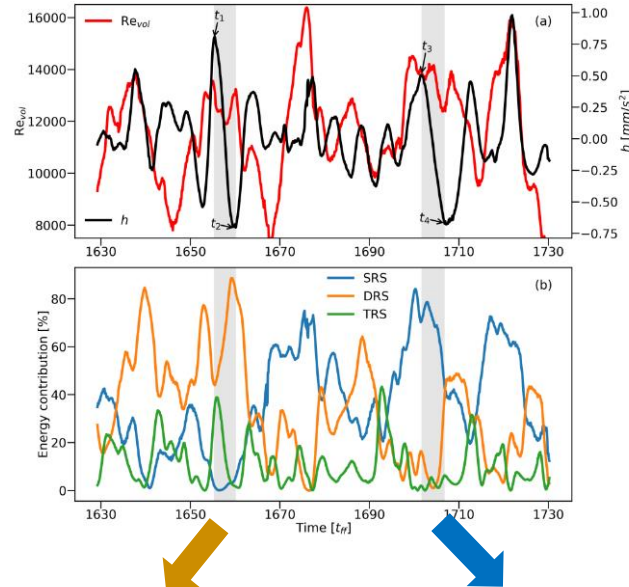


Convection at small Prandtl numbers

Collaps of large-scale coherent flow in **tall geometry**

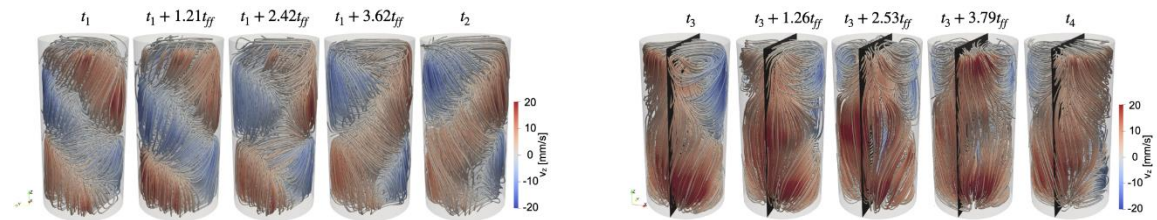


Application of **Contactless Inductive Flow Tomography** for flow reconstruction



Chaotic transitions between single, double, and triple rolls

T. Wondrak et al.,
J. Fluid Mech.
974, A48 (2023)



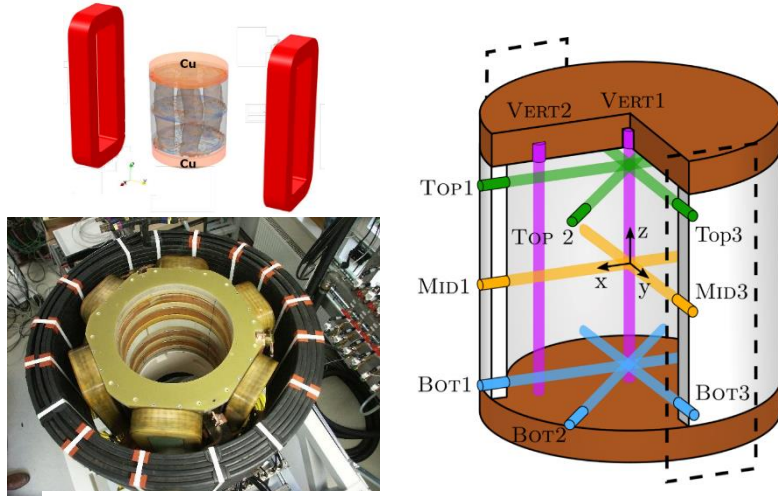
Helicity oscillations (with nearly no energy change) for **Double Roll Structure** und **Single Roll Structure**

R. Mitra et al., Phys. Fluids 36, 066611(2024)

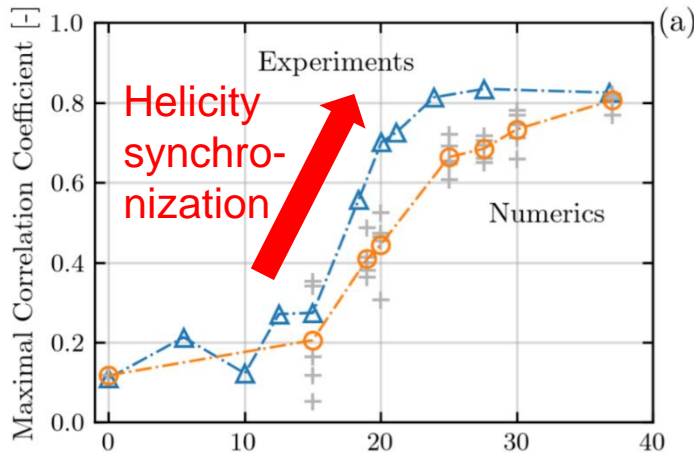
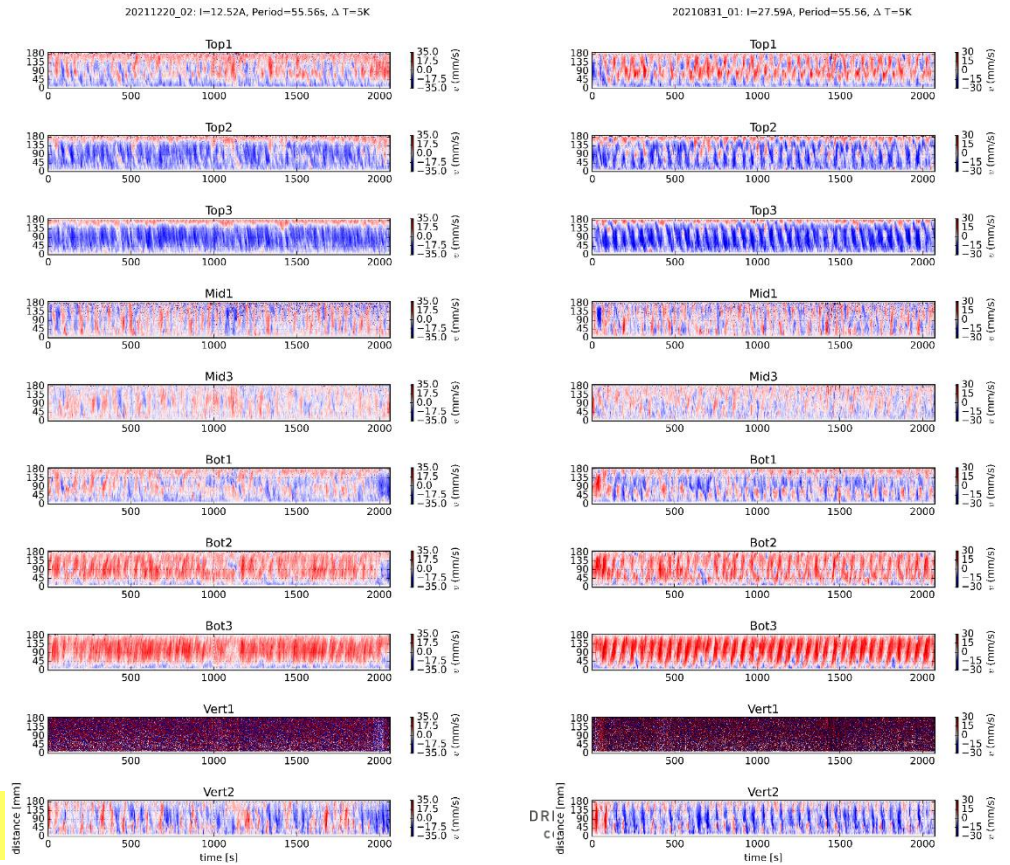


Helicity synchronization in a Rayleigh-Bénard flow

Goal: resonant excitation of the helicity of the sloshing $m=1$ mode (single roll structure) by a **tide-like** ($m=2$) electromagnetic force



Synchronization of helicity
12.5 A \longrightarrow **27.5 A**



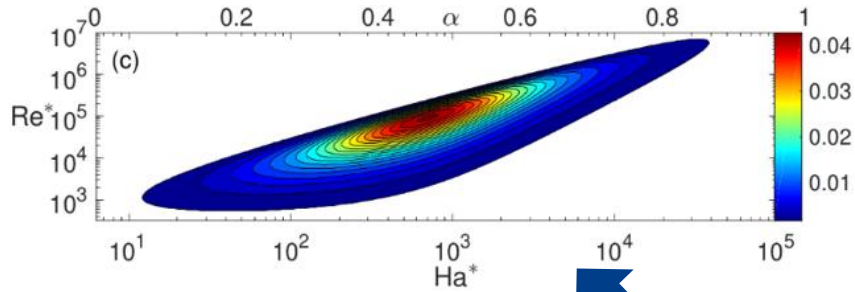
Jüstel et al., Phys. Fluids 34, 104115 (2022)

(The many facets of)

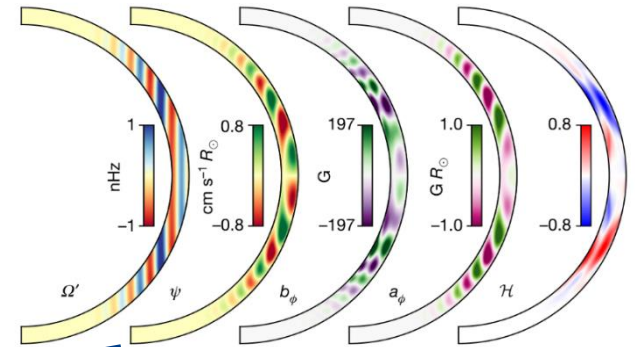
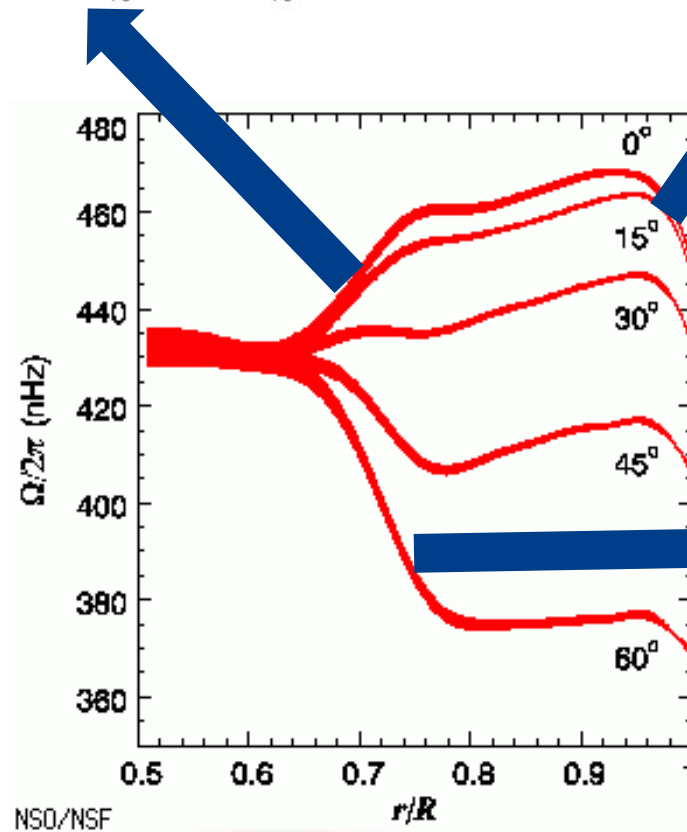
magnetorotational instability

(MRI)

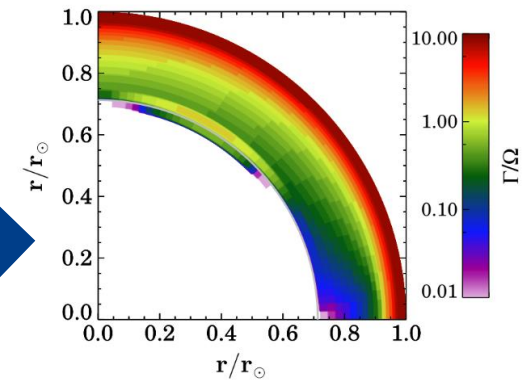
MRI in the Sun?



G. Mamatsashvili,
F.S., R. Hollerbach,
G. Rüdiger, Phys.
Rev. Fluids 4
(2019), 103905



G.M. Vasil et al.,
Nature 628, 769
(2024)



D. Kagan, G.C. Wheeler,
ApJ 782, 21 (2014)

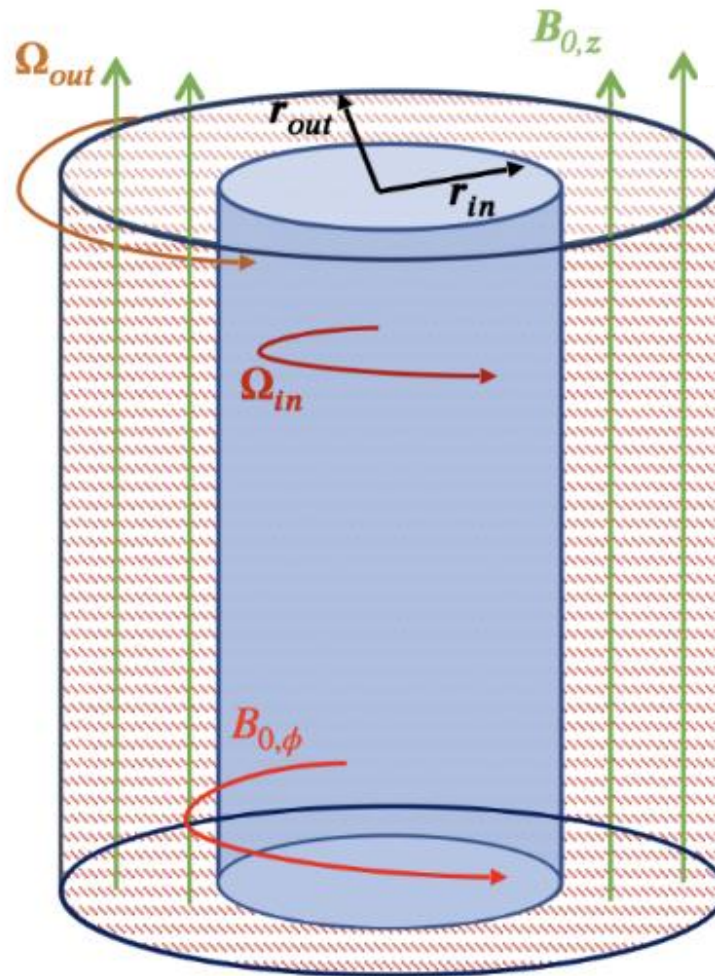
A quick guide through the MRI-zoo

HMRI

$$\Omega_{out} < \Omega_{in}$$

$$\mathbf{B}_{\phi} \sim \mathbf{B}_z$$

$$m=0$$



AMRI

$$\Omega_{out} < \Omega_{in}$$

$$\mathbf{B}_{\phi} \gg \mathbf{B}_z$$

$$m=1$$

SMRI

$$\Omega_{out} < \Omega_{in}$$

$$\mathbf{B}_{\phi} \ll \mathbf{B}_z$$

$$m=0$$

Super-HMRI

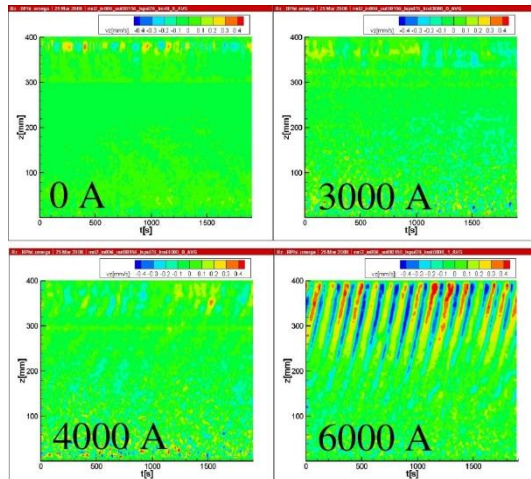
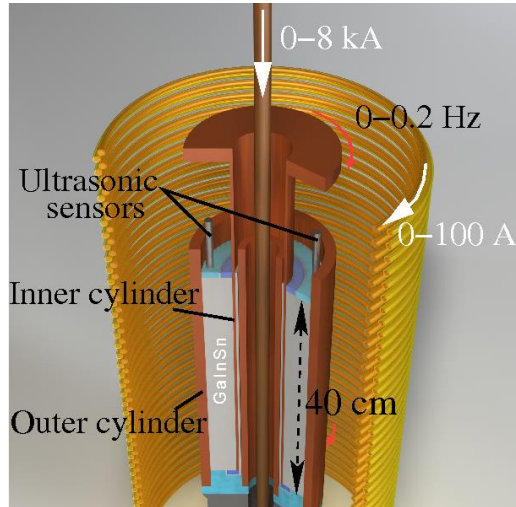
$$\Omega_{out} > \Omega_{in}$$

$$\mathbf{B}_{\phi} \sim \mathbf{B}_z$$

$$m=0$$

Helical MRI, Azimuthal MRI, Taylor instability (TI) at HZDR

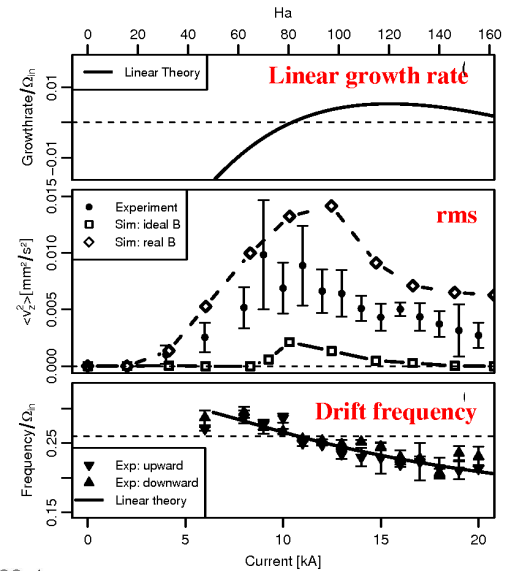
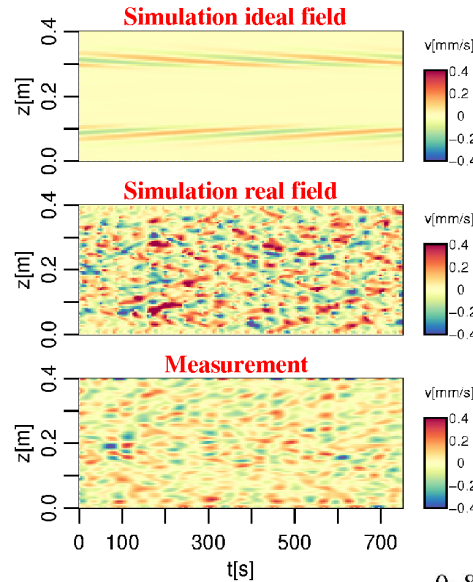
2006: HMRI



F.S. et al., PRL 97 (2006), 184502;
PRE 80 (2009), 066303

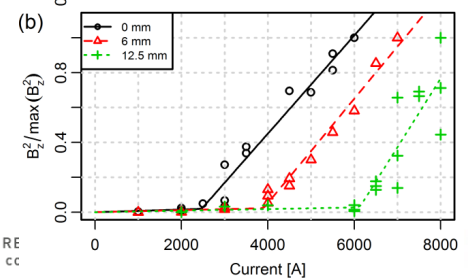
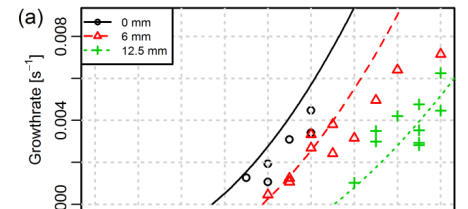
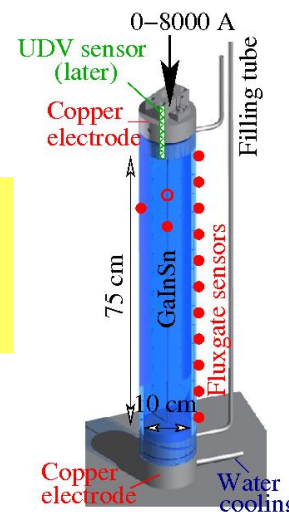
2014: AMRI

Seilmayer et al., PRL113 (2014), 024505



2012: TI

Seilmayer et al.,
PRL 108 (2012),
244501

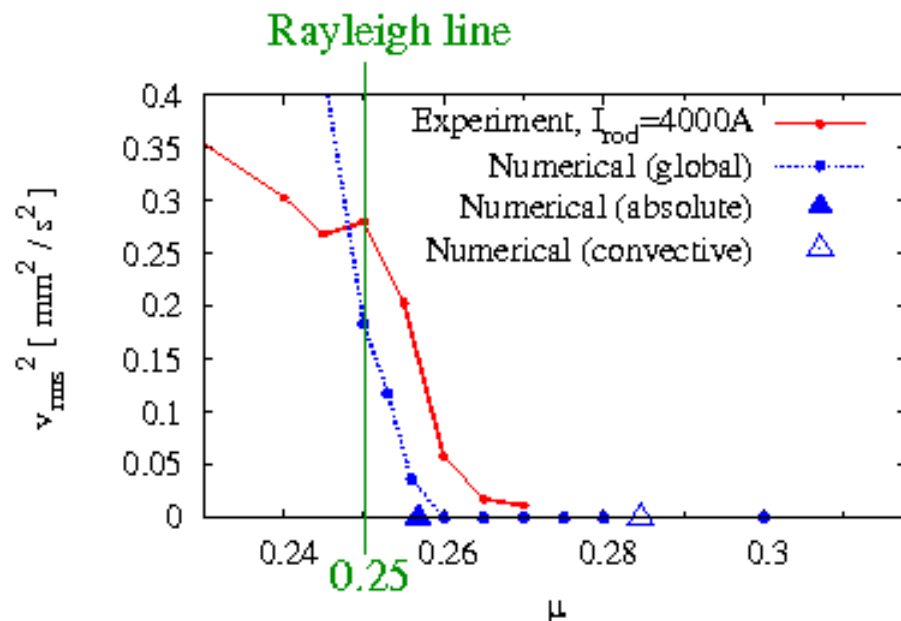
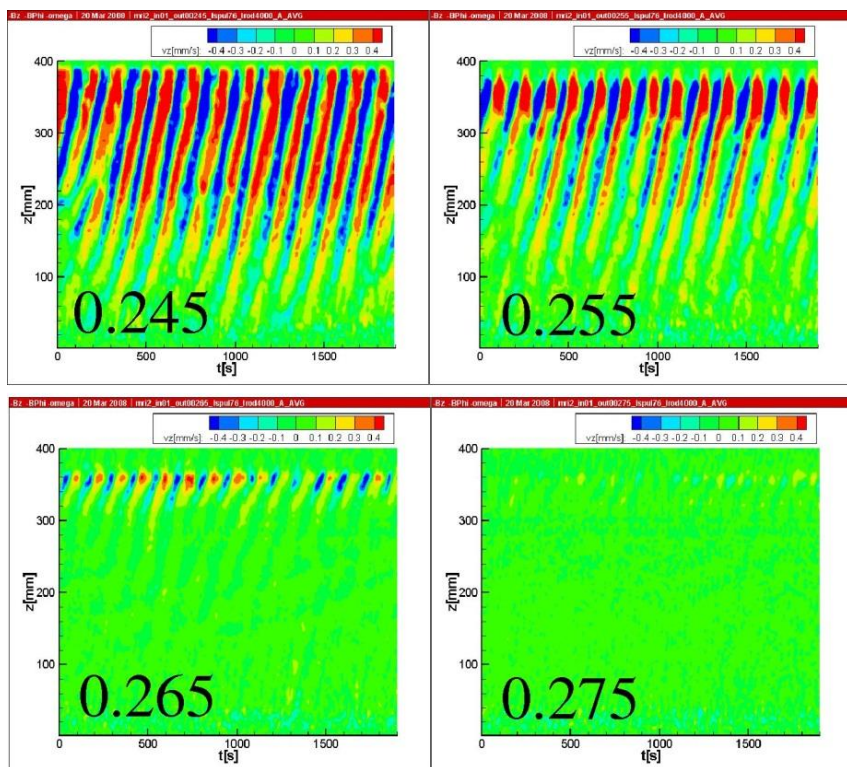


PROMISE: Selected results for HMRI

Example 1: Increase of the ratio

$$\mu = \Omega_{\text{out}} / \Omega_{\text{in}}$$

Observed MRI is indeed an absolute (global) instability, and not only a convective one

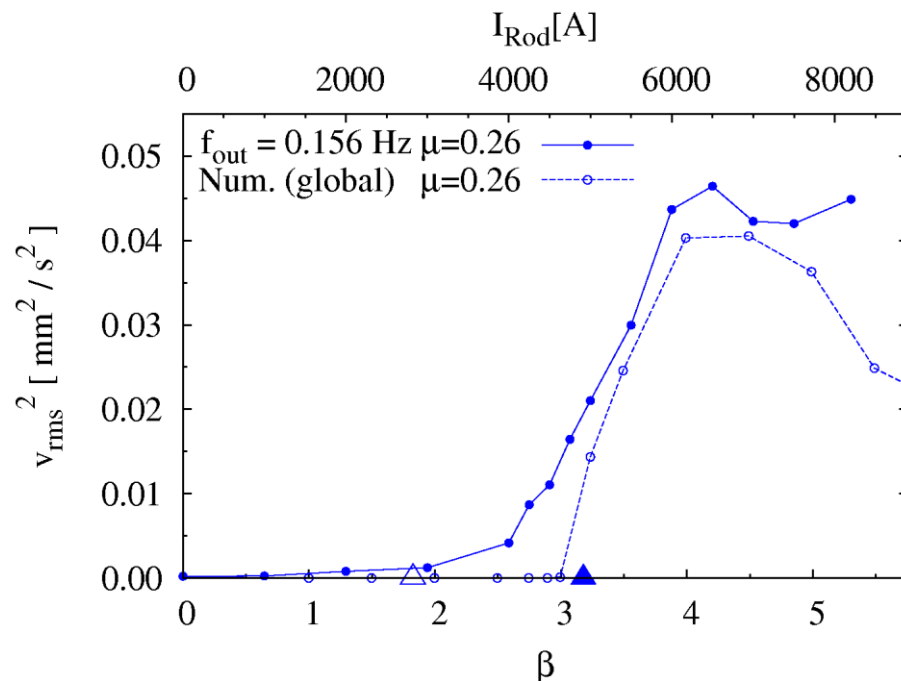
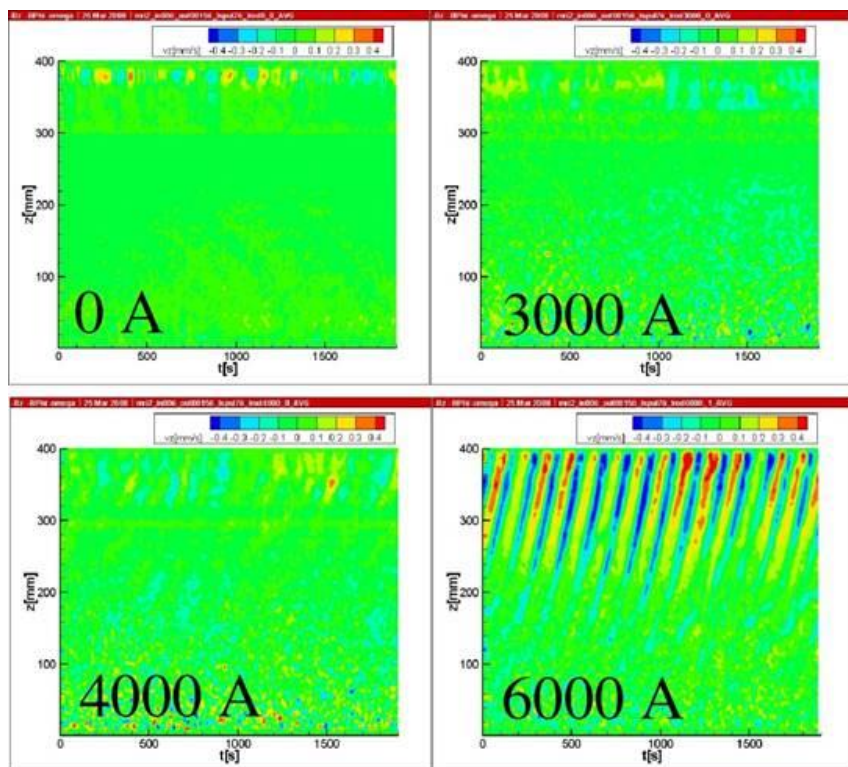


Stefani et al., Phys. Rev. E 80 (2009), 066303

PROMISE: Selected results for HMRI

Example 2: Increase of axial current (i.e. of the ratio $\beta=B_\varphi/B_z$)

Again, observed MRI is indeed an absolute (global) instability, and not only a convective one



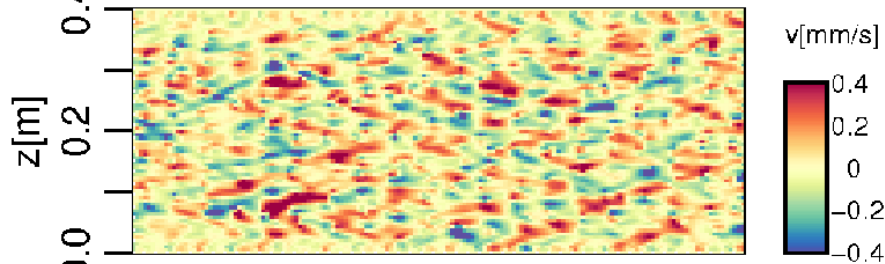
Stefani et al., Phys. Rev. E 80 (2009), 066303

AMRI: $m=1$ mode under influence of (pure, or dominant) B_ϕ

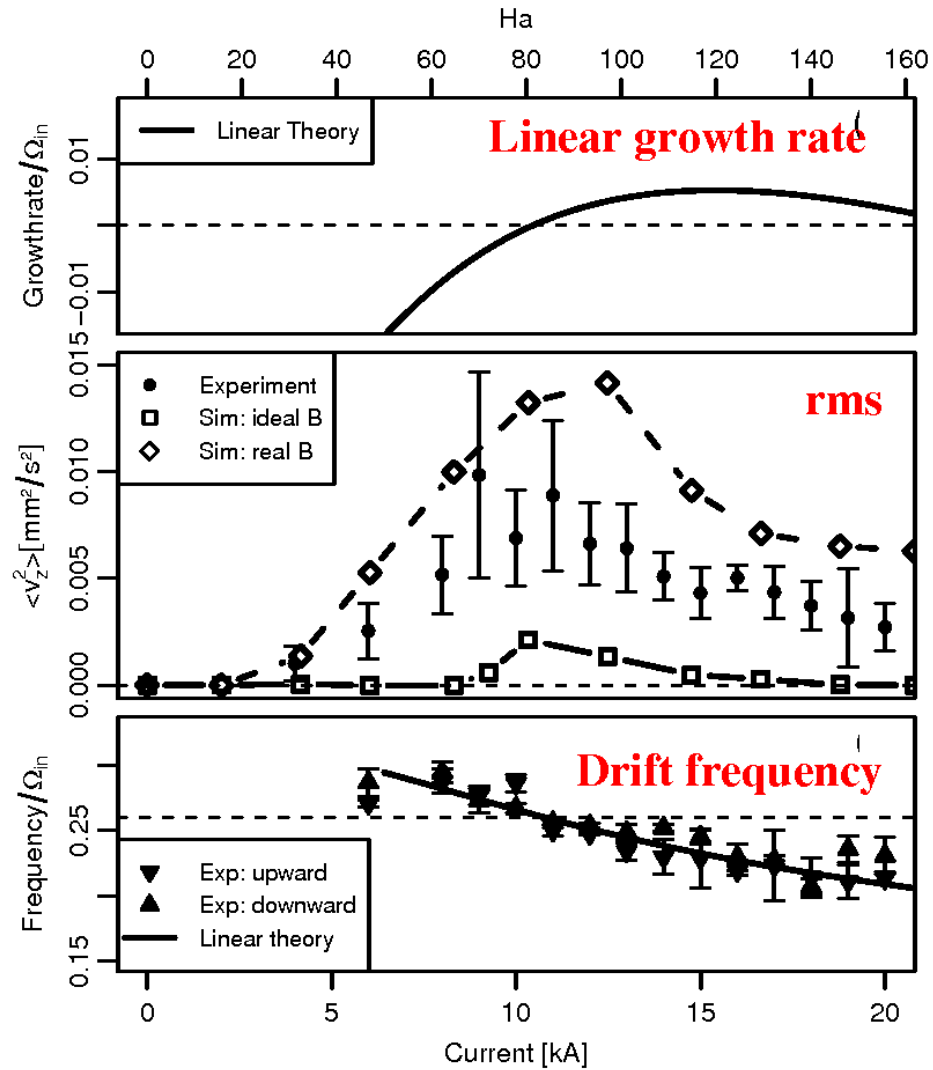
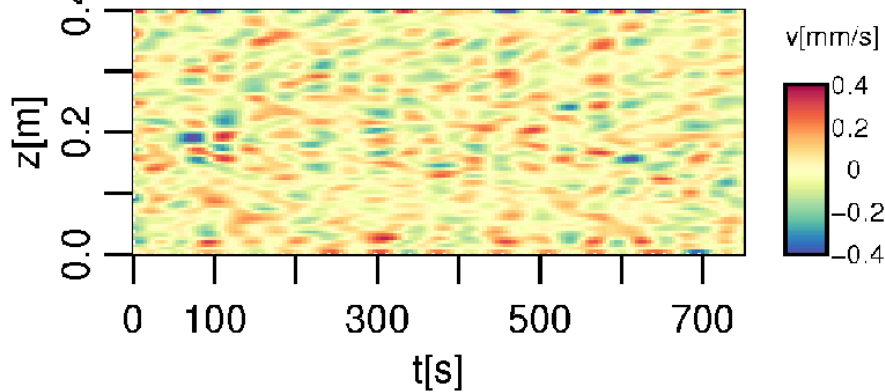
Simulation ideal field



Simulation real field



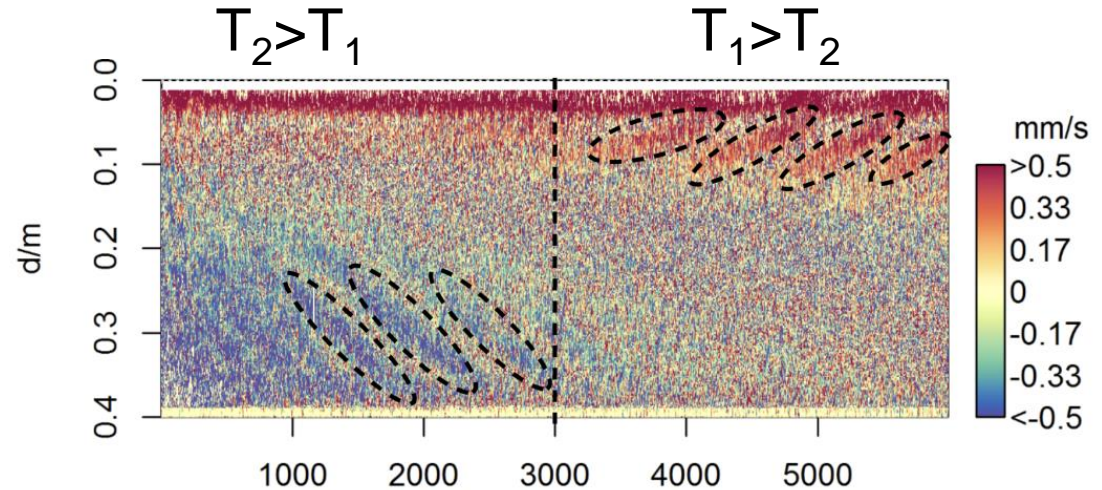
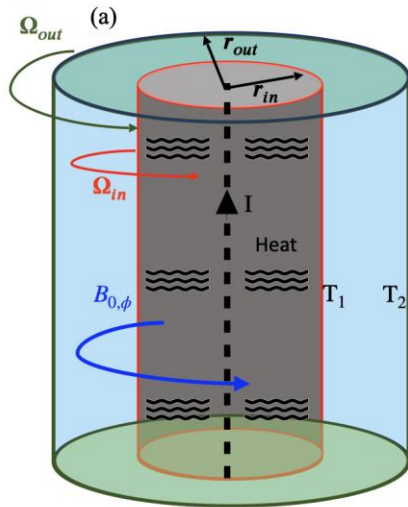
Measurement



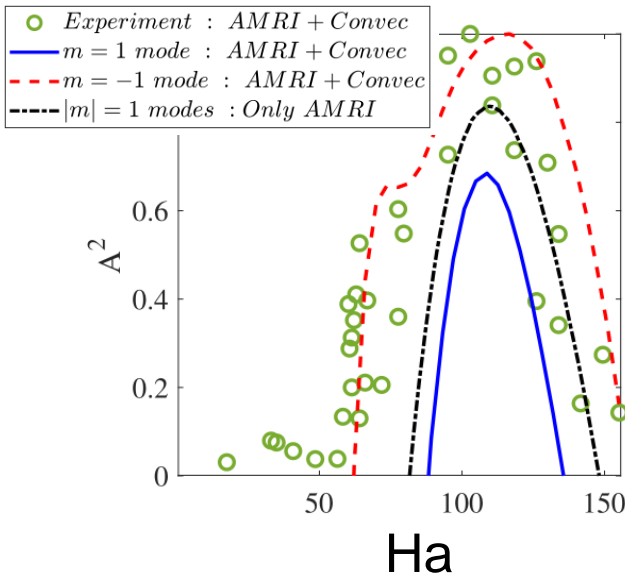
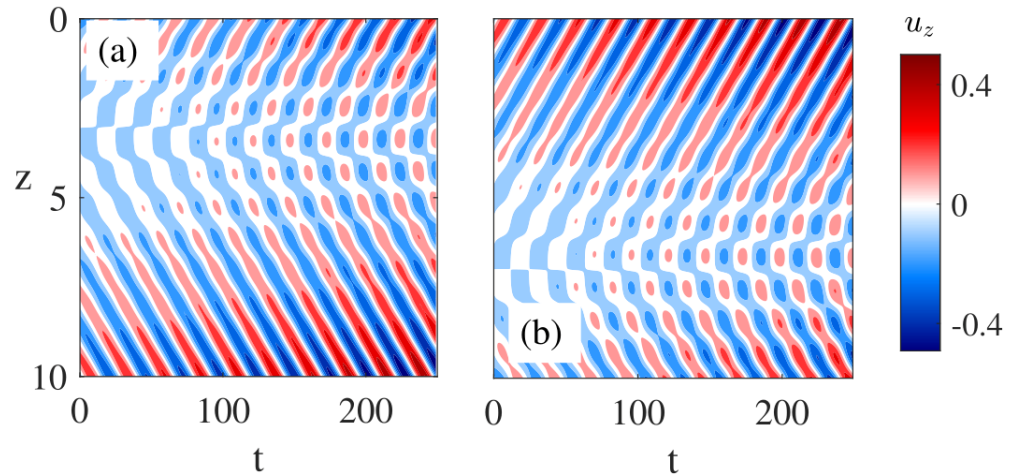
M. Seilmayer et al., PRL113 (2014), 024505

New results for AMRI+Convection: „One-winged butterflies“

Experiment with changing radial heat flux

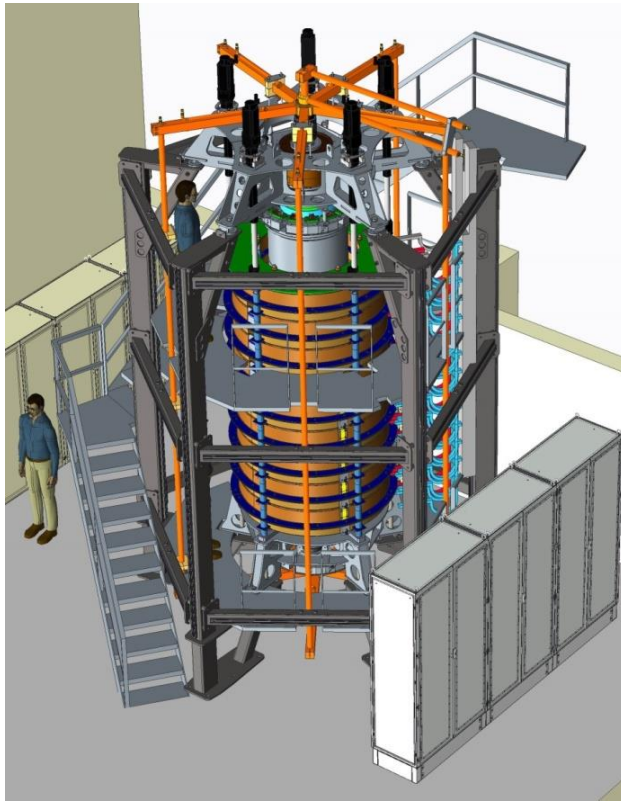


Simulation

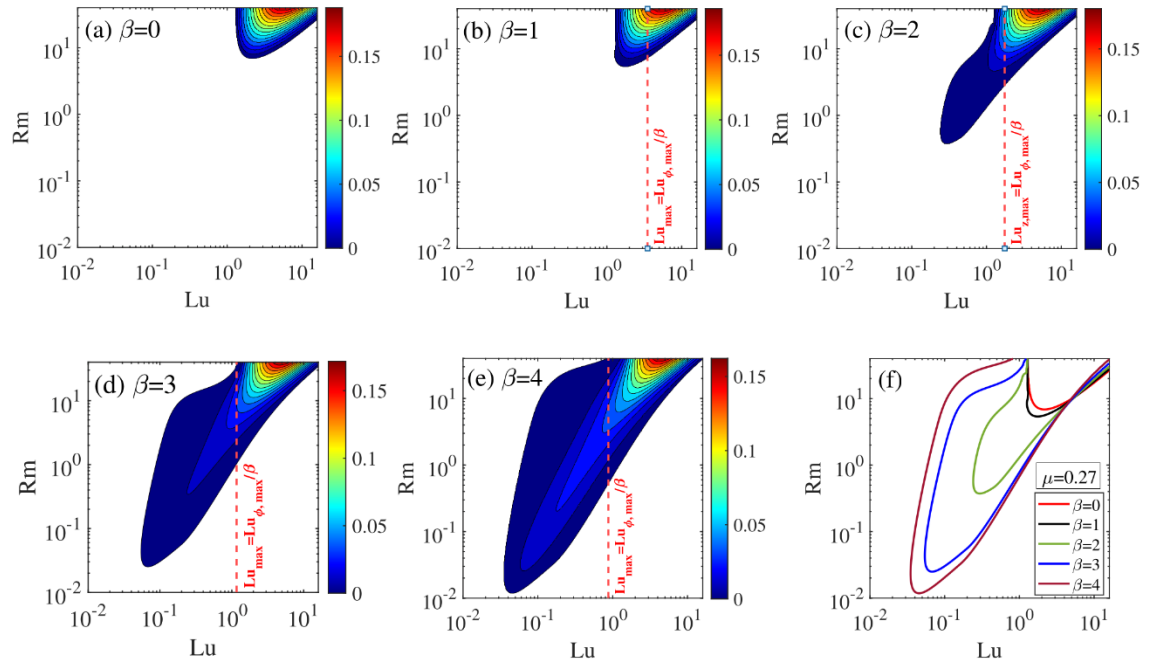


Seilmayer et al., Magnetohydrodynamics 56 (2020), 225; Mishra et al., J. Fluid Mech. (in press)

Planned experiment for SMRI, HMRI, AMRI, Super-HMRI and TI



Design of the planned MRI/TI-experiment

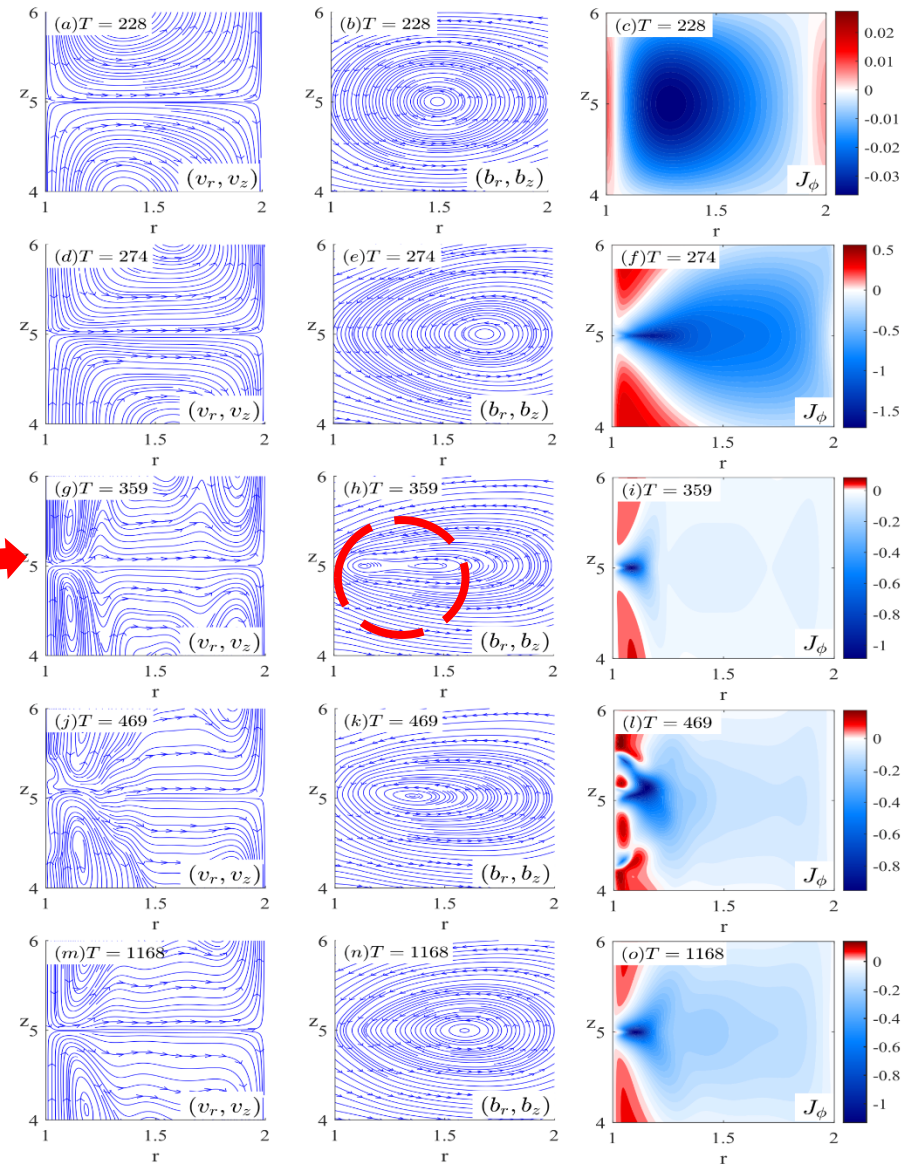
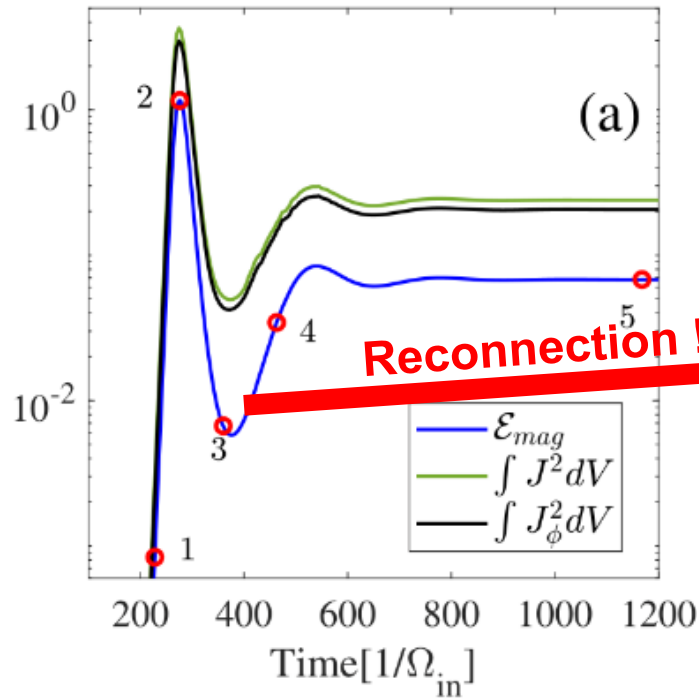


Main goal: follow the monotonic transition from HMRI to SMRI for decreasing $\beta=B_\varphi/B_z$

Mishra et al., Phys. Rev. Fluids 7 (2022), 064802

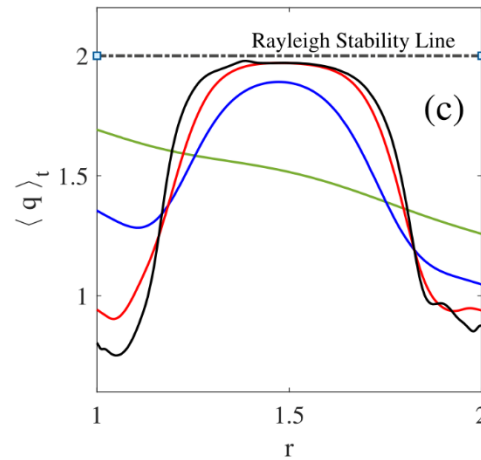
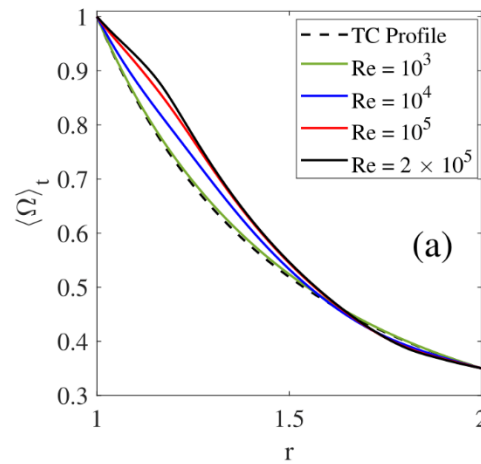
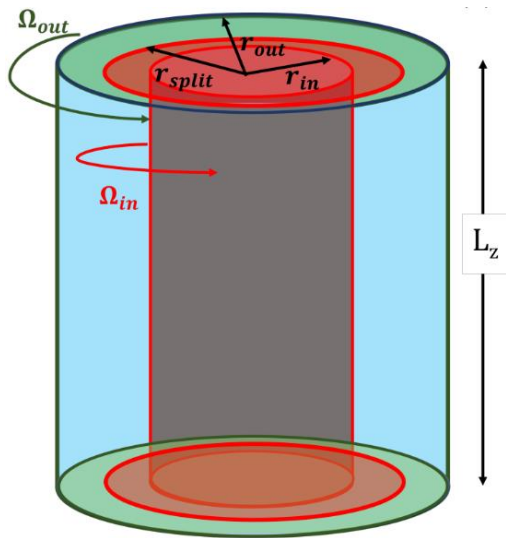
Preparations of MRI experiment: nonlinear simulations for $m=0$

Saturation of MRI via magnetic reconnection



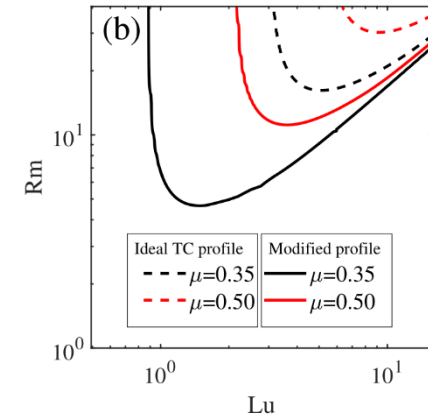
A. Mishra et al, Phys. Rev. Fluids 8, 083902 (2023)

That's all pretty nice, but what happens with real endcaps?

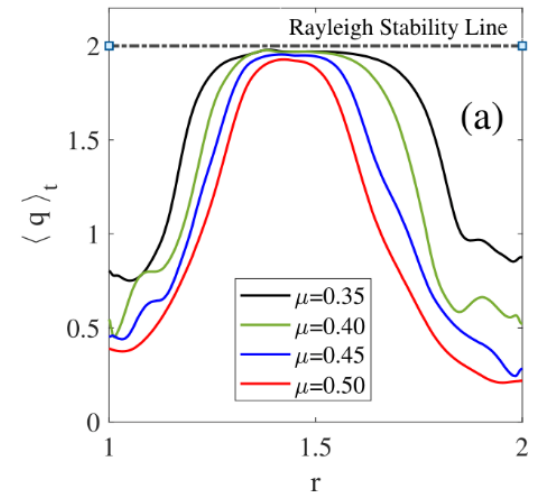


A. Mishra, Dissertation and Phys. Rev. Fluids 9, 033904 (2024)

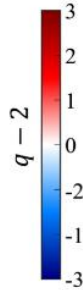
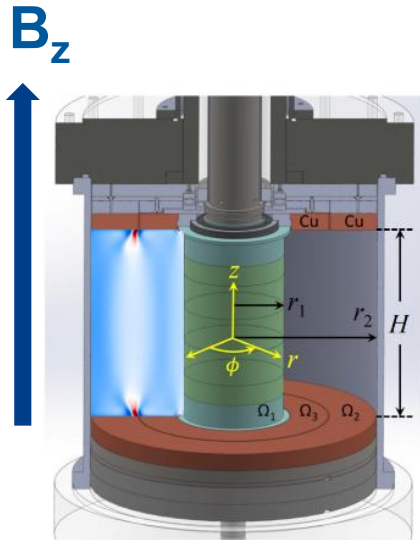
Ideal profile \rightarrow real flow: **Critical Rm and Lu drop by factor of ~ 3**



Replacing $\mu=0.35$ by $\mu=0.5$, the original critical values are retained



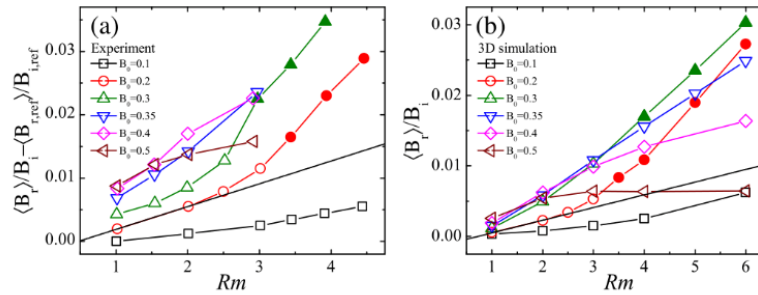
The Princeton experiment on SMRI (talk by Y. Wang yesterday)



PHYSICAL REVIEW LETTERS 129, 115001 (2022)
 Editors' Suggestion Featured in Physics

Observation of Axisymmetric Standard Magnetorotational Instability in the Laboratory

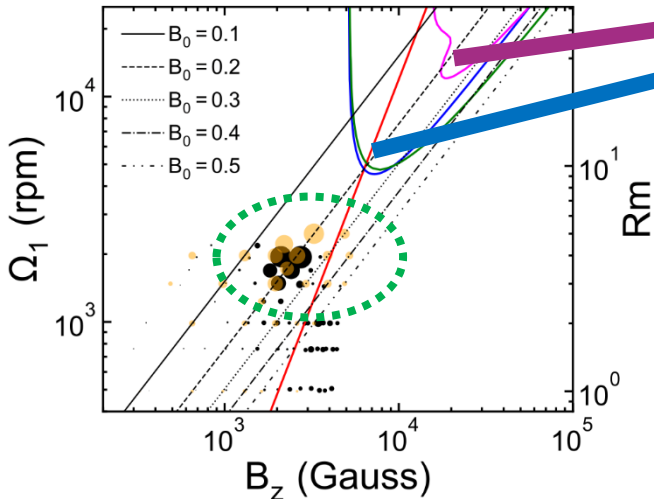
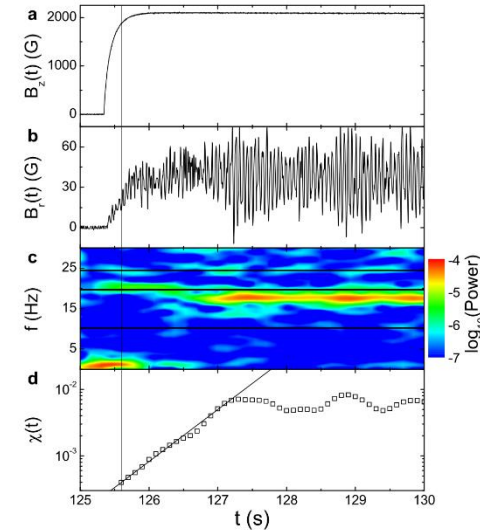
Yin Wang^{1,2}, Erik P. Gilson¹, Fatima Ebrahimi^{1,2}, Jeremy Goodman², and Hantao Ji^{1,2}
¹Princeton Plasma Physics Laboratory, Princeton University, Princeton, New Jersey 08543, USA
²Department of Astrophysical Sciences, Princeton University, Princeton, New Jersey 08544, USA



nature communications

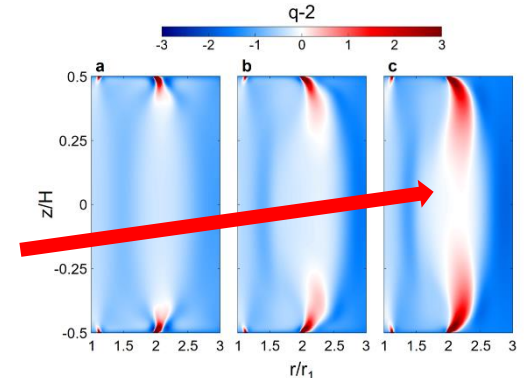
Identification of a non-axisymmetric mode in laboratory experiments searching for standard magnetorotational instability

Received: 4 April 2022 Accepted: 25 July 2022
 Yin Wang¹, Erik P. Gilson¹, Fatima Ebrahimi^{1,2}, Jeremy Goodman², Kyle J. Casper¹, Himawan W. Winarto² & Hantao Ji^{1,2}



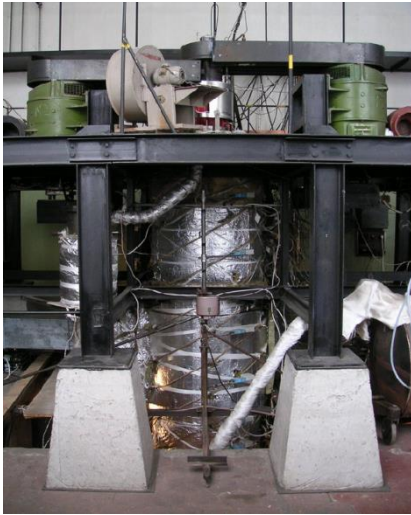
MRI detected for 10-times (m=1) or 3-times (m=0) too small values of Rm und Lu

Similar problem:
 Flow-induced currents in copper-lids modify the flow profile, which may become Rayleigh unstable ($q > 2$)



Rüdiger et al., J. Plasma Phys. 90 (2024), 905900105

Dynamos

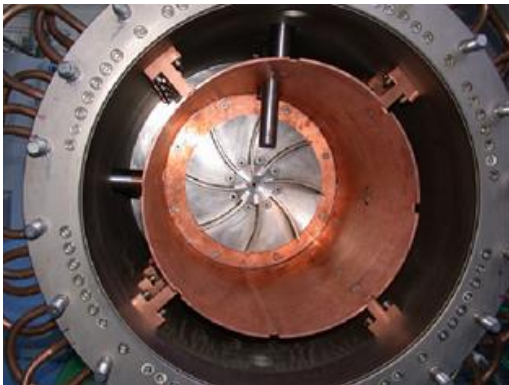


Riga

Karlsruhe



Dynamos



VKS



DRESDYN

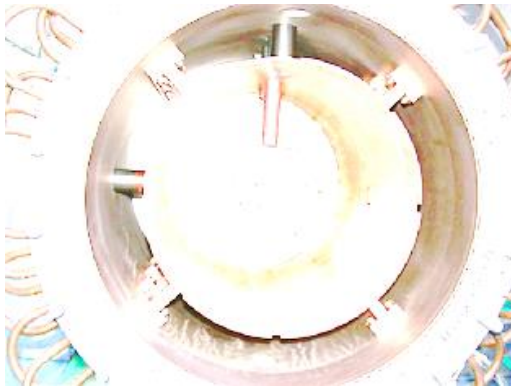


Riga

Karlsruhe



Dynamos

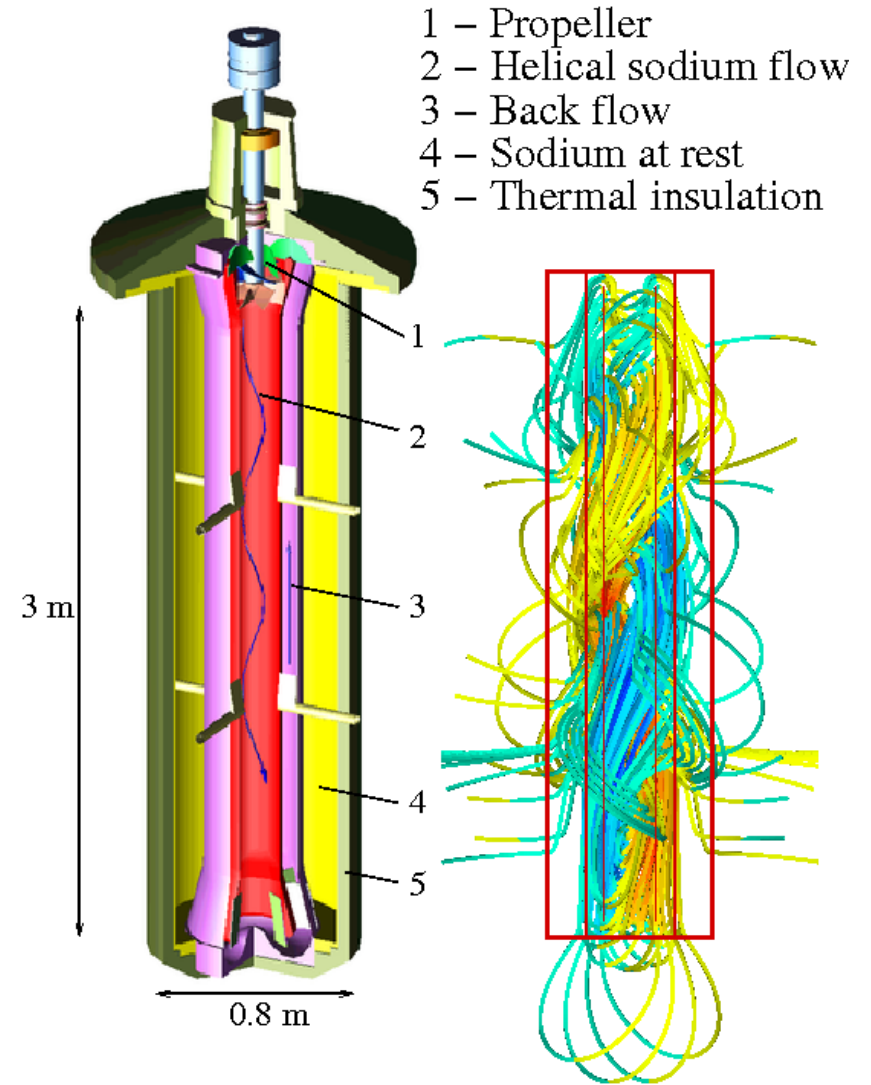
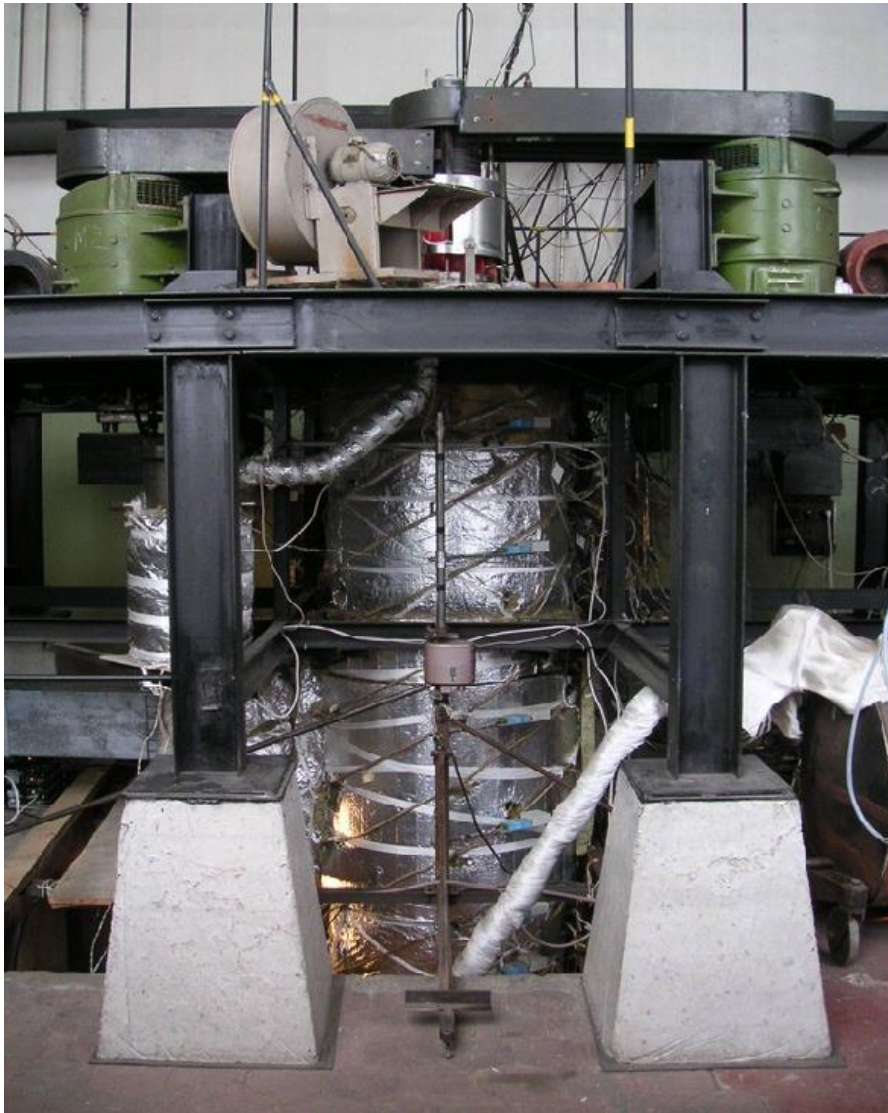


VKS



DRESDYN

Riga dynamo experiment



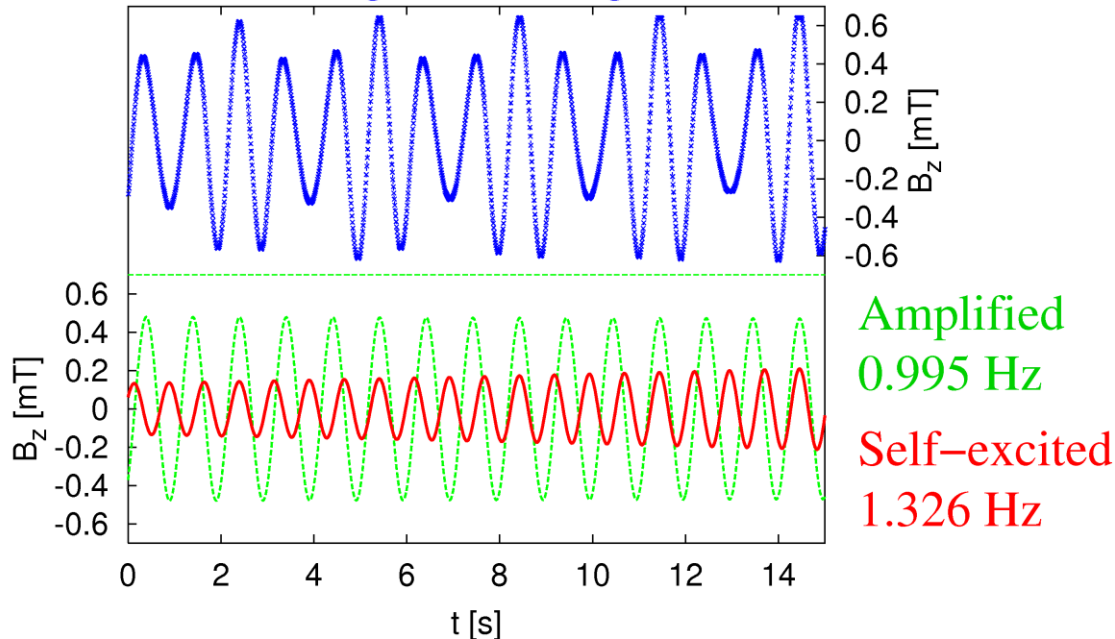
Dynamo
module

Simulated
eigenfield

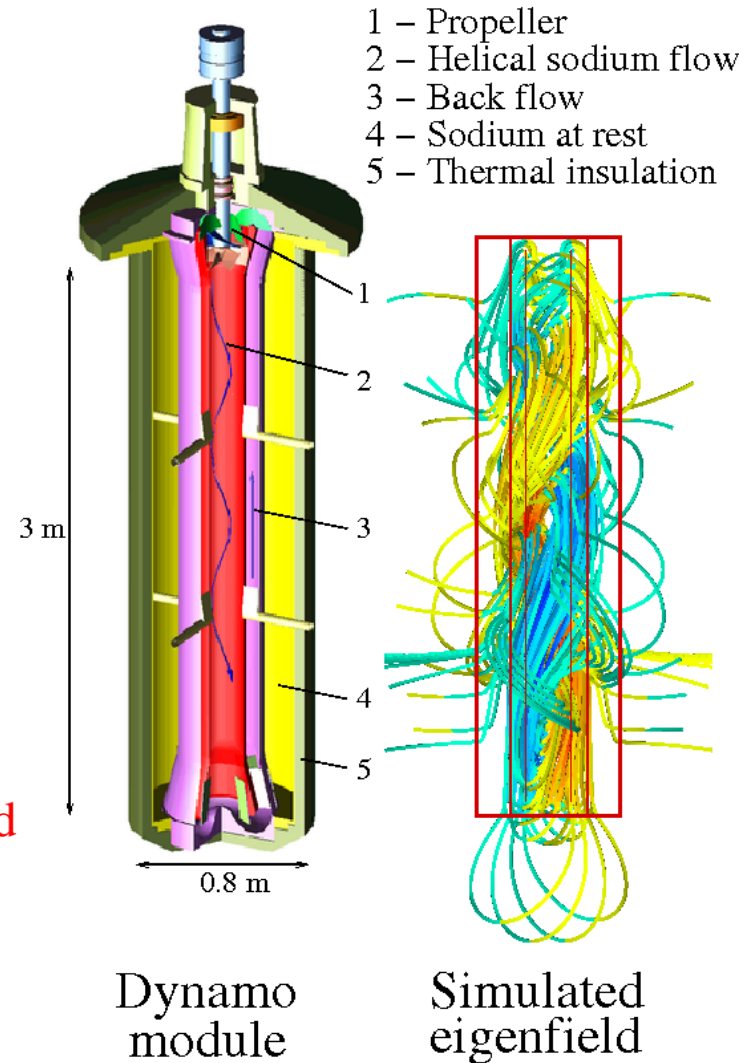
Riga dynamo experiment

First experimental realization of magnetic field self-excitation in a liquid metal flow
(11 November 1999)

Measured signal at flux gate sensor

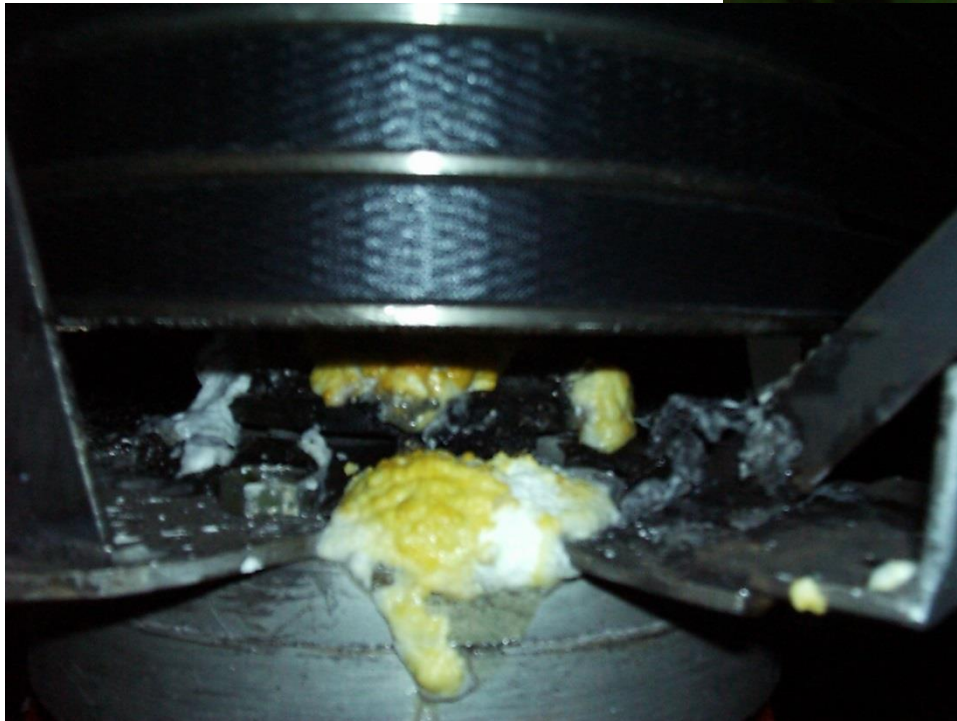


Gailitis et al., Phys. Rev. Lett. 84 (2000) 4365



Come on baby light my SODIUM fire...

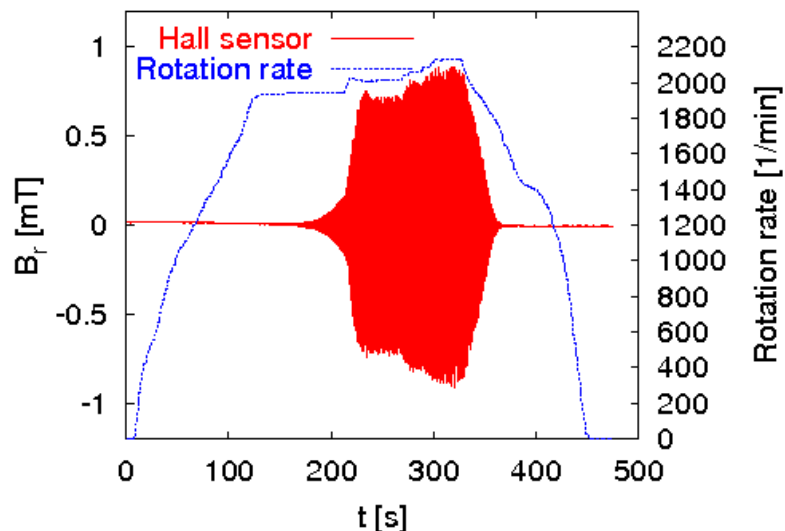
Evening of 11th
November 1999



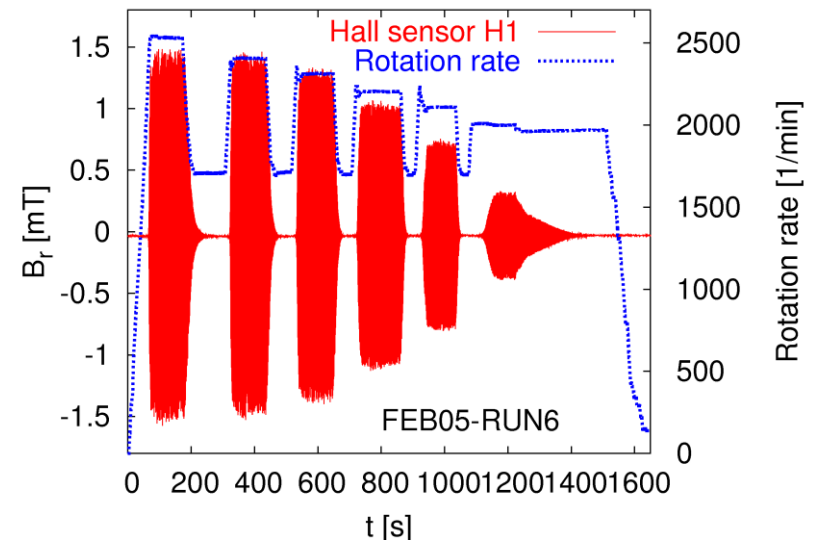
...and the day
after...

Riga dynamo experiment

From the kinematic to the saturated regime (July 2000)



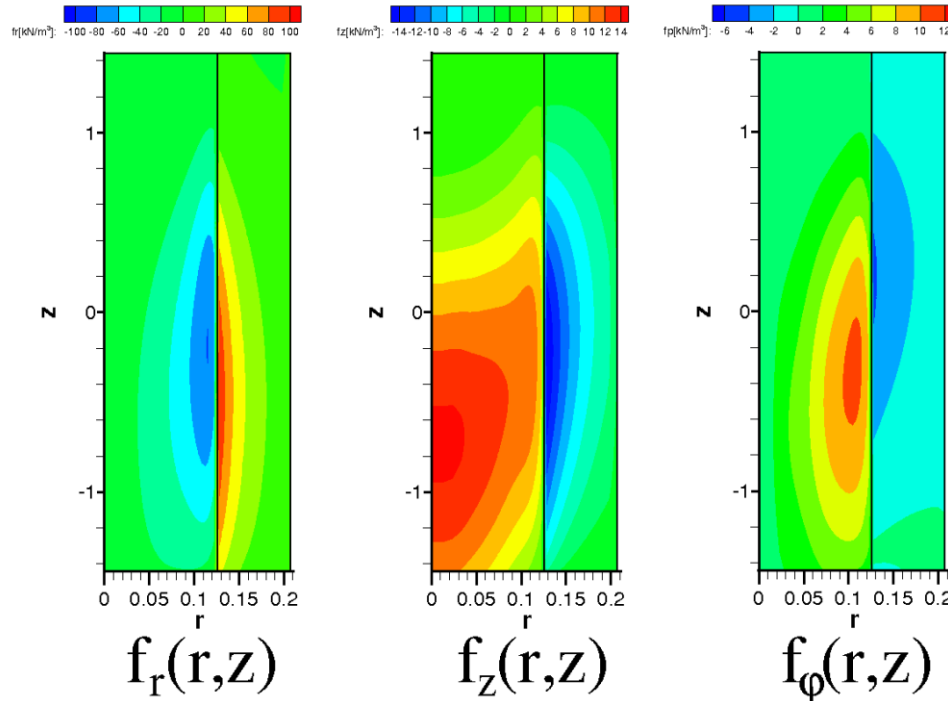
Switching the dynamo on and off (February 2005)



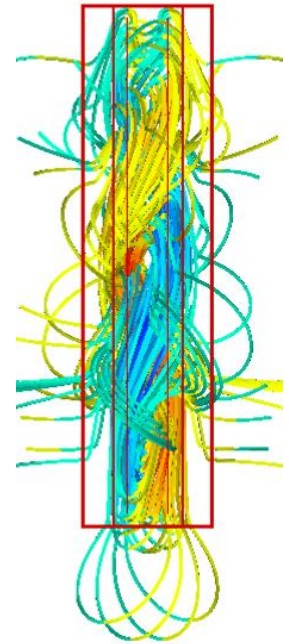
Gailitis et al., Phys. Rev. Lett. 84 (2000) 4365; Phys. Rev. Lett. 86 (2001) 3024; Rev. Mod. Phys. 74 (2002) 973 ; Phys. Plasmas 11 (2004) 2838; Compt. Rend. Phys. 9 (2008), 721; **J. Plasma Phys. 84, 735840301 (2018)**

Riga dynamo experiment: Back-reaction illustrates Lenz's rule

Lorentz force components resulting from self-excited eigenfield

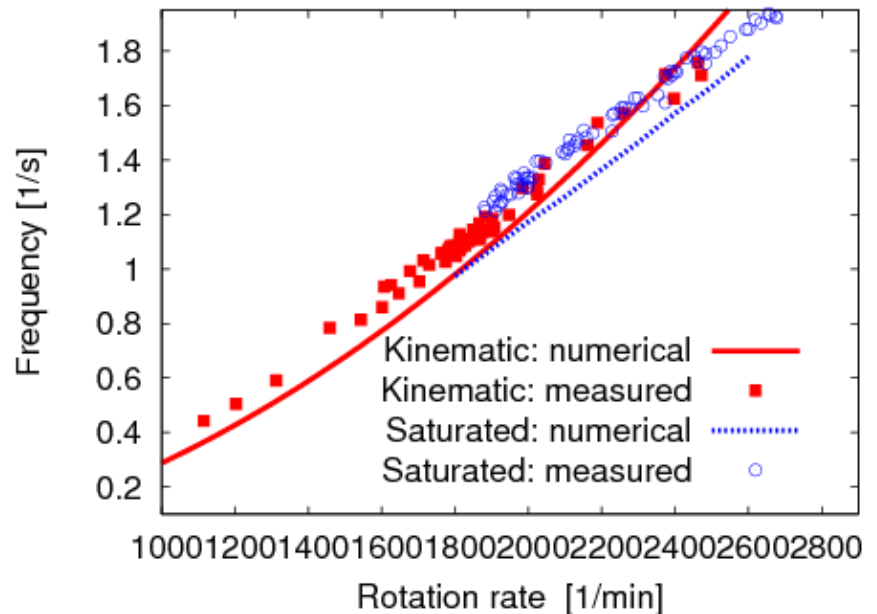
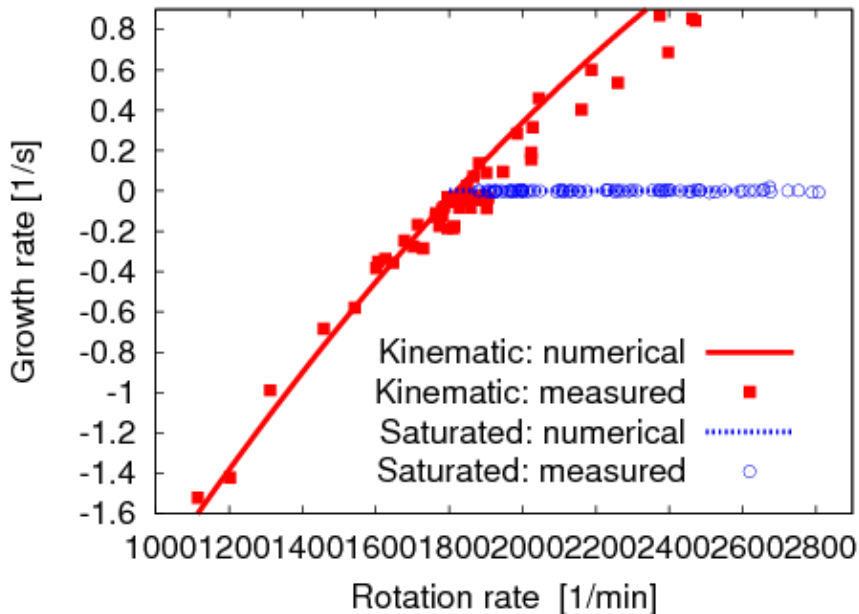


$$\frac{\partial \mathbf{B}}{\partial t} = \nabla \times (\mathbf{v} \times \mathbf{B}) + \frac{1}{\mu_0 \sigma} \Delta \mathbf{B}$$



$$\frac{\partial \mathbf{v}}{\partial t} + (\mathbf{v} \cdot \nabla) \mathbf{v} = -\frac{\nabla p}{\rho} + \frac{1}{\mu_0 \rho} (\nabla \times \mathbf{B}) \times \mathbf{B} + \nu \Delta \mathbf{v} + \mathbf{f}_{extern}$$

Riga dynamo experiment: Growth rates and frequencies



Numerical predictions (with correct vacuum boundary conditions) of the kinematic dynamo were accurate to some 5 per cent

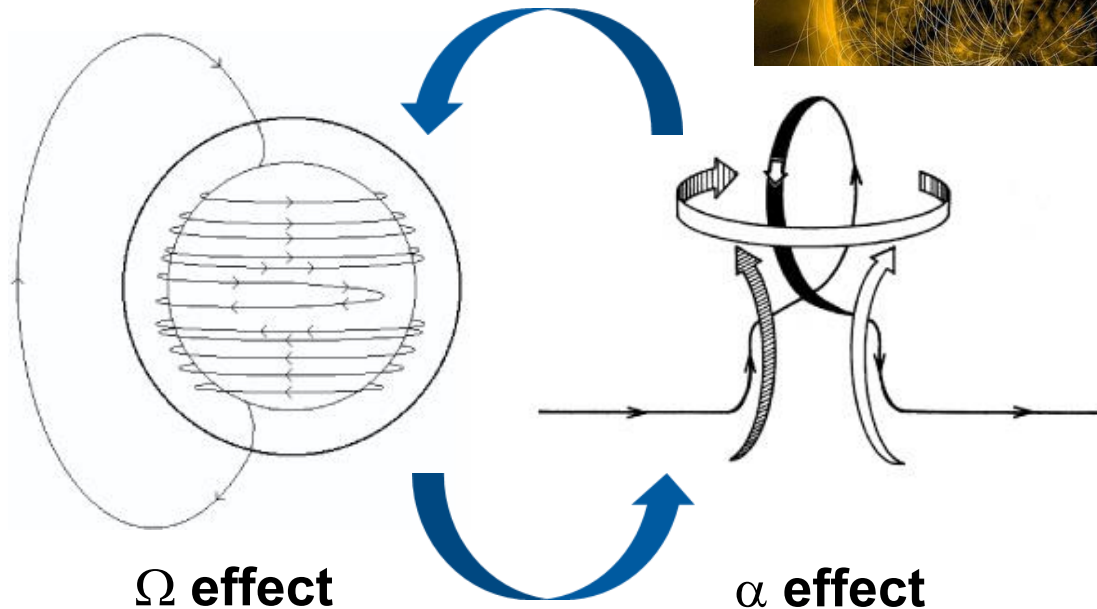
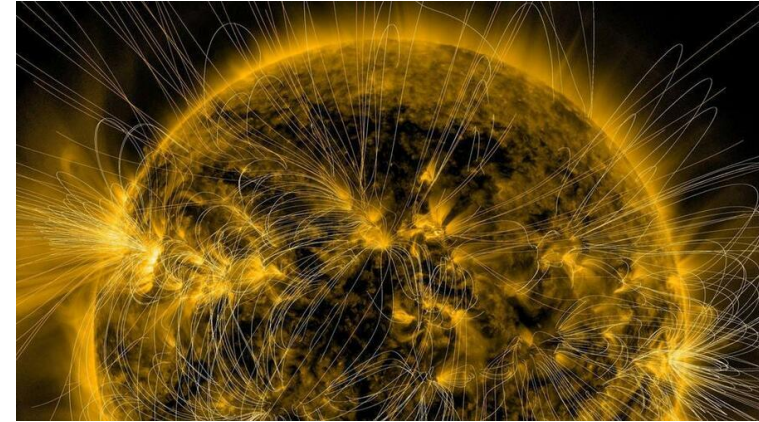
Simplified back-reaction model (Lorentz forces acting along streamlines) gives very reasonable field amplitudes and structures in the saturation regime

Gailitis et al. J. Plasma Phys. 84, 735840301 (2018)

A short diversion into theory: The solar dynamo

Any solar dynamo needs:

- some Ω effect to wind up toroidal field from poloidal field
- some α effect to regenerate poloidal field from toroidal field



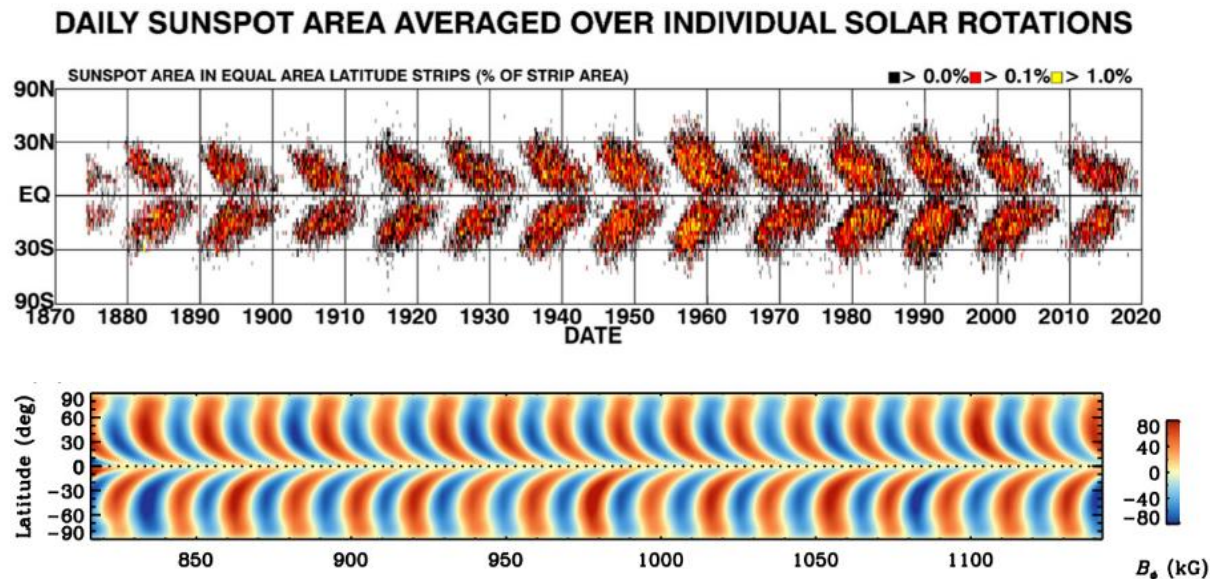
Parker, *Astrophys J.* 122, 293 (1955)

Solar dynamo: Conventional modelling

With appropriate models, (including meridional circulation), and some parameter fitting, one obtains

- a reasonable **period of the Hale cycle** (22 years)
- a reasonable **shape of the butterfly diagram** of sunspots

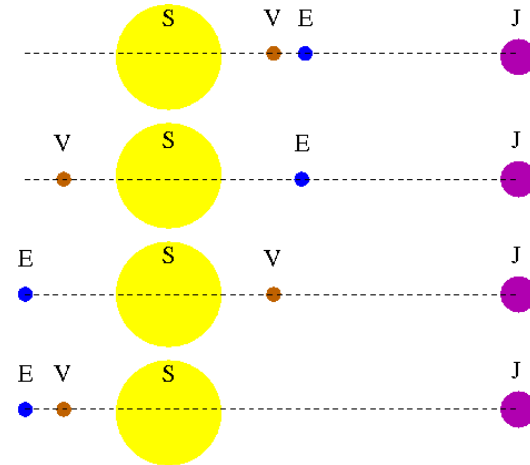
<http://www.solarcyclescience.com/solarcycle.html>



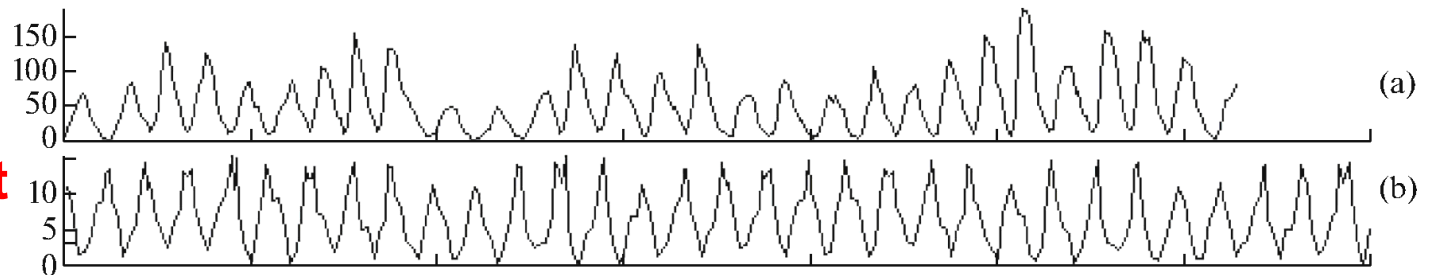
Karak, B.B., Miesch, M., ApJ 847 (2017), 69

Is there a problem at all with the solar dynamo? Perhaps yes...

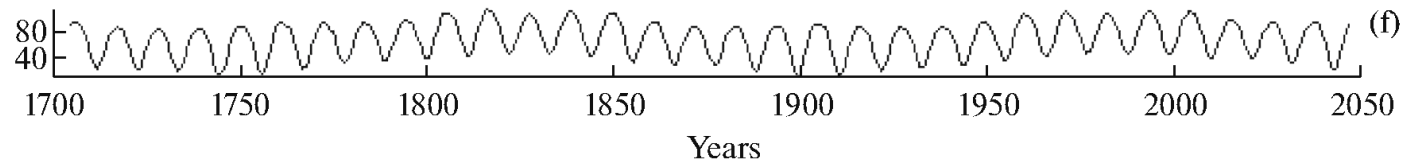
Conspicuous synchronization of the solar Schwabe cycle with the **11.07-yr period of three-planet syzygies** of the tidally dominant **Venus-Earth-Jupiter system** (despite weak tidal forces!)



Sunspots
VEJ alignment index

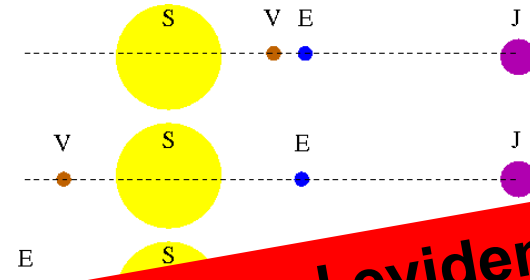


Bollinger, Proc. Okla. Acad. Sci. 33 (1952), 307; Takahashi, Solar. Phys. 3 (1968), 598; Wood, Nature 240 (1972), 91; **Wilson, Pattern Recogn. Phys. 1 (2013), 147**; Okhlopov, Mosc. U. Bull. Phys. B. 69 (2014), 257; **Okhlopov, Mosc. U. Bull. Phys. B. 71 (2016), 444**; Scafetta, Pattern Recogn. Phys. 2 (2014), 1; Vos et al. 2004



Is there a problem at all with the solar dynamo? Perhaps yes...

Conspicuous synchronization of the solar Schwabe cycle with the **11.07-yr period of three-planet syzygies** of the tidally dominant **Venus-Earth-Jupiter system** (despite weak tidal forces!)



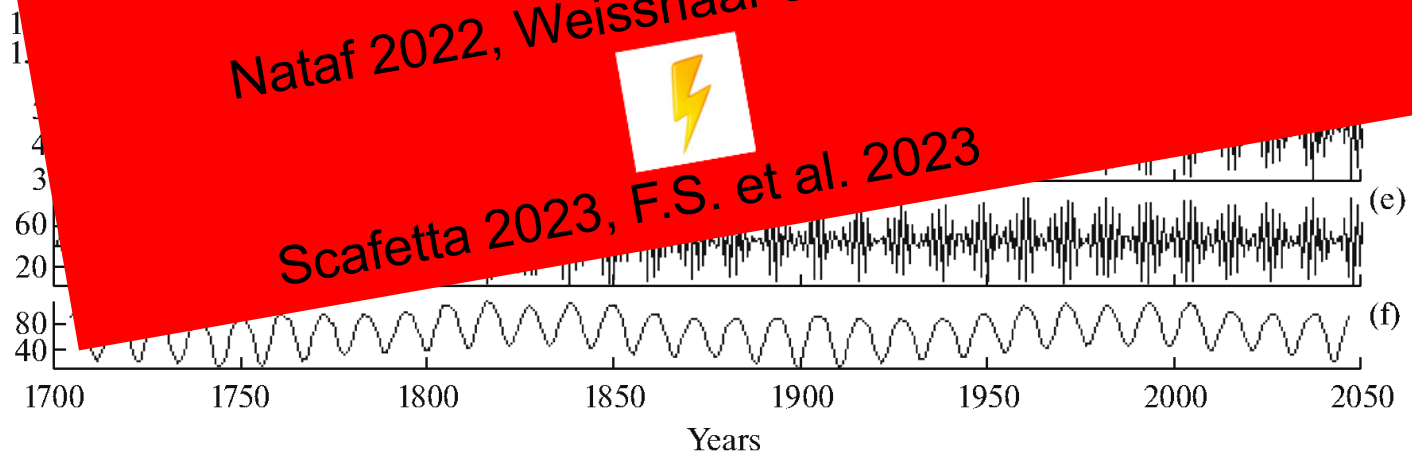
Heavy discussion about empirical evidence of phase-stability (and synchronization)

Dicke 1978, Schove 1983, F.S. et al. 2016, 2019, 2022

Nataf 2022, Weisshaar et al. 2023

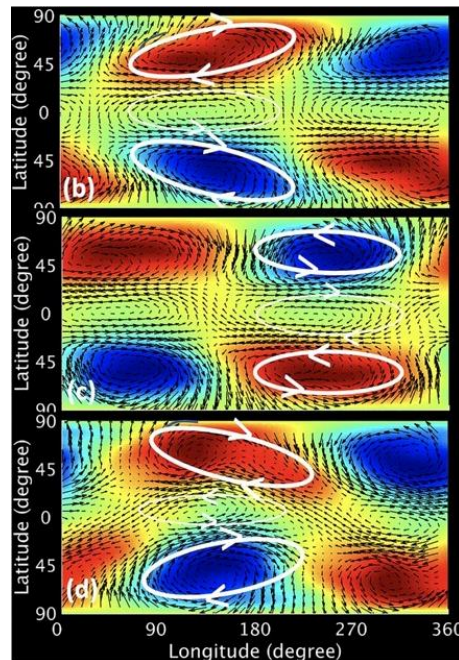
Scafetta 2023, F.S. et al. 2023

Sunspots
VEJ alignment index

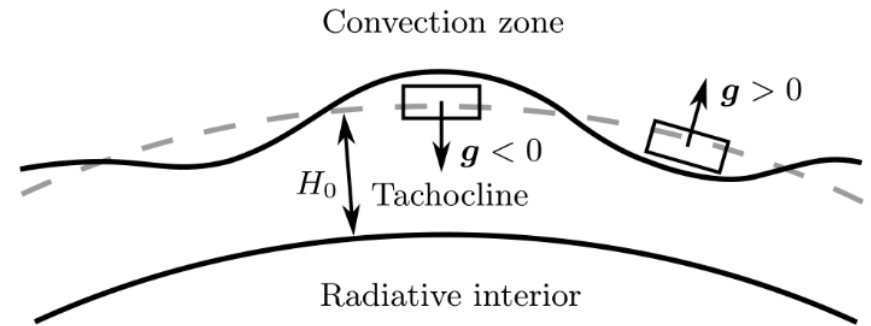


New ansatz: Tidal synchronization of magneto-Rossby waves

magneto-Rossby
waves



M. Dikpati, S.W. McIntosh,
Space Weather 18 (2020),
e2018SW002109



Shallow water approximation
with azimuthal magnetic field
under the influence of tidal
forces

G. Horstmann et al., *Astrophys. J.* 944
(2023), 48; F.S. et al., *Solar Physics*
299 (2024), 51

New ansatz: Tidal synchronization of magneto-Rossby waves

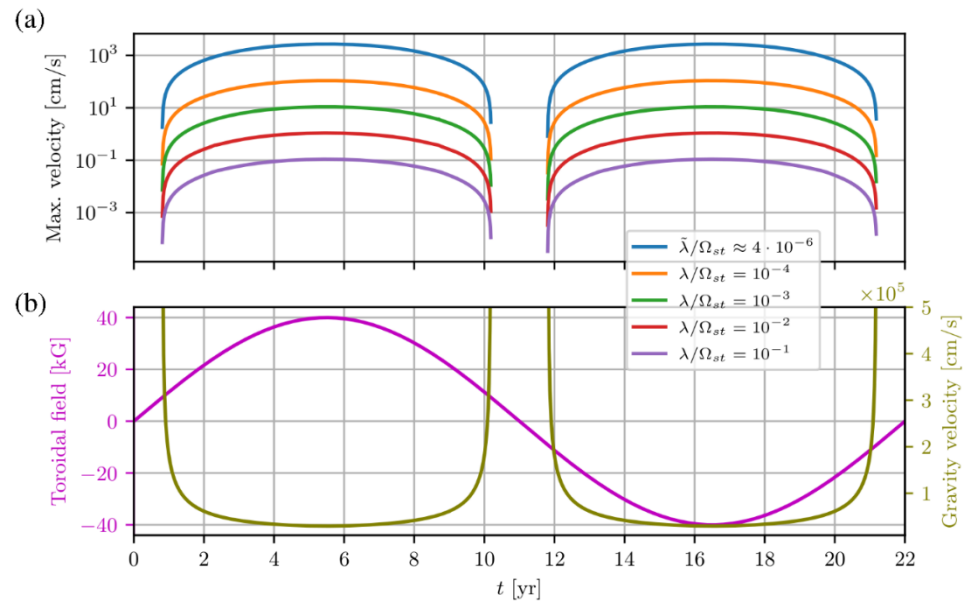
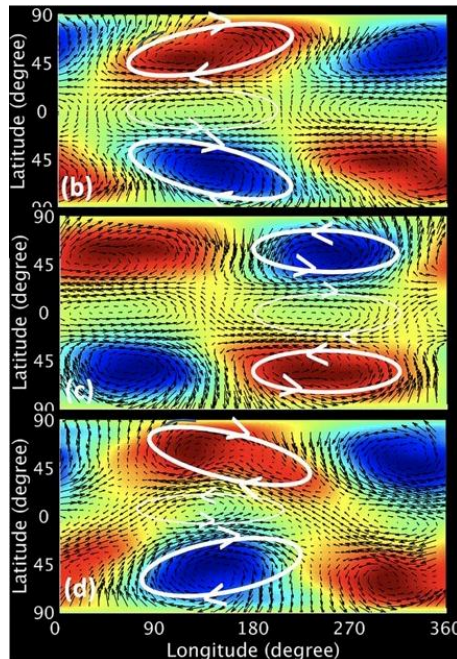
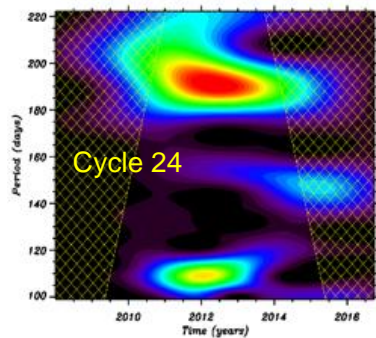
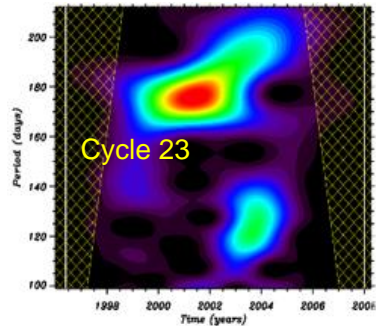
$$\square_{v_A}^2 v - C_0^2 \square_{v_A} \Delta v + f_0^2 \frac{\partial^2 v}{\partial t^2} - C_0^2 \beta \frac{\partial}{\partial x} \frac{\partial v}{\partial t} + 2\lambda \frac{\partial}{\partial t} \square_{v_A} v - \lambda C_0^2 \Delta \frac{\partial v}{\partial t} + \lambda^2 \frac{\partial^2 v}{\partial t^2} = f_0 \frac{\partial}{\partial x} \frac{\partial^2 V}{\partial t^2} - \lambda \frac{\partial}{\partial y} \frac{\partial^2 V}{\partial t^2} - \frac{\partial}{\partial t} \frac{\partial}{\partial y} \square_{v_A} V$$

$$= \left[f_0 \Omega + 2\Omega^2 - \frac{2v_A^2}{R_0^2} + \frac{2f_0 \Omega}{R_0} y \right] \frac{4K\Omega}{R_0} \sin\left(\frac{2x}{R_0} - 2\Omega t\right) + \frac{4K\lambda\Omega^2}{R_0} \cos\left(\frac{2x}{R_0} - 2\Omega t\right)$$

Rieger-type periods magneto-Rossby waves



Analytical solution



Example: Venus-Jupiter spring tide, period 118 days; wave **velocities of up to 1-100 m/s are possible** for realistic tides

E. Gurgenashvili et al.,
A&A 653, A146 (2021)

M. Dikpati, S.W. McIntosh,
Space Weather 18 (2020),
e2018SW002109

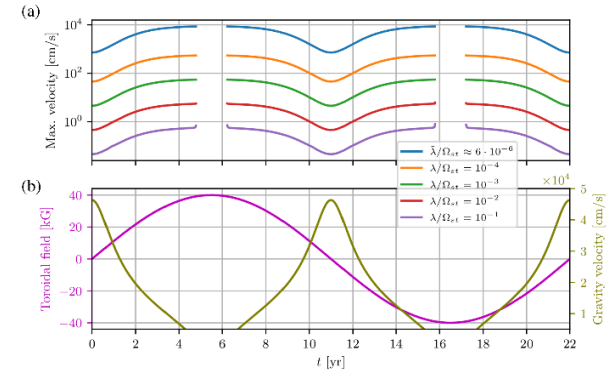
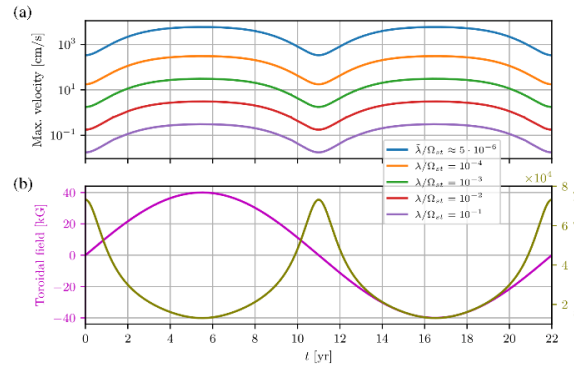
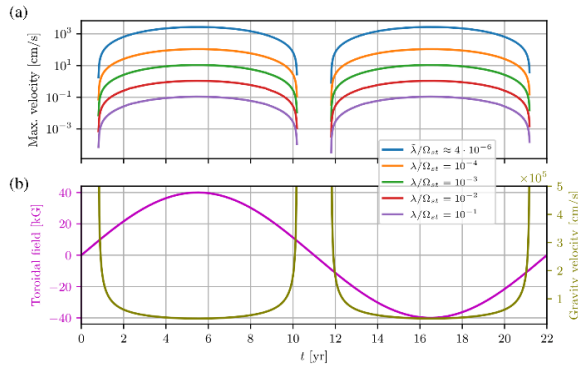


New ansatz: Tidal synchronization of magneto-Rossby waves

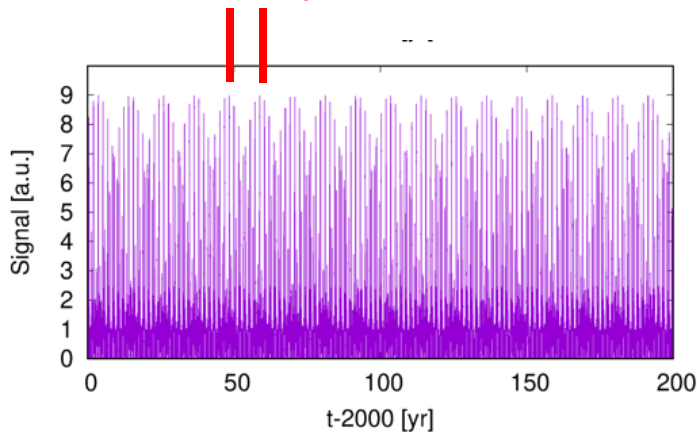
Venus-Jupiter spring tide
with period 118 days

Earth-Jupiter spring tide
with period 199 days

Venus-Earth spring tide
with period 292 days



11.07 years



$$s(t) = \left[\cos\left(2\pi \cdot \frac{t - t_{VJ}}{0.5 \cdot P_{VJ}}\right) + \cos\left(2\pi \cdot \frac{t - t_{EJ}}{0.5 \cdot P_{EJ}}\right) + \cos\left(2\pi \cdot \frac{t - t_{VE}}{0.5 \cdot P_{VE}}\right) \right]^2$$

Any **dynamo-relevant effect** (helicity, α -effect, zonal flow, pressure...) will be a **quadratic functional** of the waves. This comprises a significant **part with 11.07-year period**.

F.S. et al., Solar Physics
299 (2024), 51

A „realistic“ 2D α - Ω -dynamo model with meridional circulation...

$$\frac{\partial B}{\partial t} = \tilde{\eta} D^2 B + \frac{1}{s} \frac{\partial(sB)}{\partial r} \frac{\partial \tilde{\eta}}{\partial r} - R_m s \mathbf{u}_p \cdot \nabla \left(\frac{B}{s} \right) + C_\Omega s (\nabla \times (A \mathbf{e}_\phi)) \cdot \nabla \Omega,$$

$$\frac{\partial A}{\partial t} = \tilde{\eta} D^2 A - \frac{R_m}{s} \mathbf{u}_p \cdot \nabla (sA) + C_\alpha^c \alpha^c B + C_\alpha^p \alpha^p B,$$

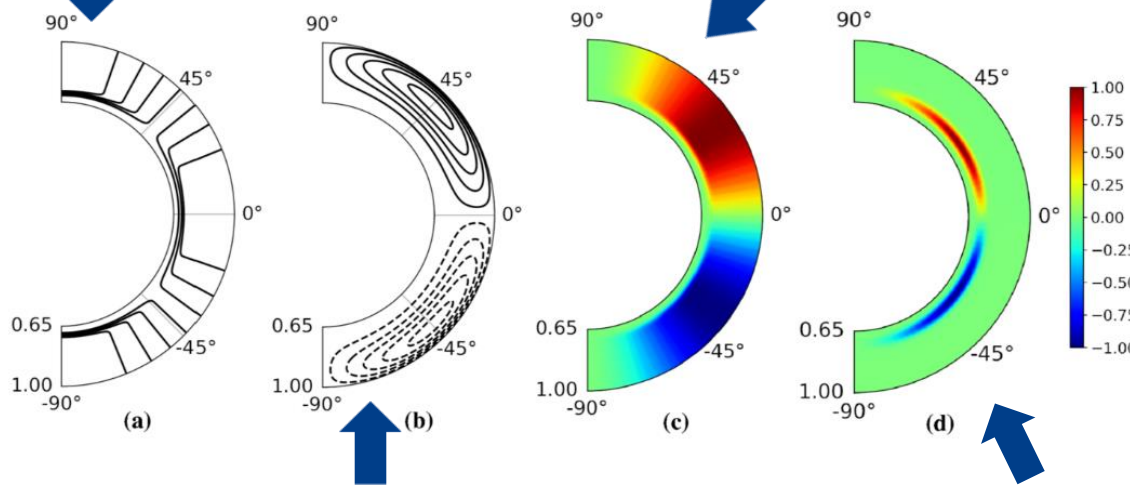
$$C_\Omega = \Omega_{\text{eq}} R_\odot^2 / \eta_t,$$

$$R_m = u_0 R_\odot / \eta_t,$$

$$C_\alpha^c = \alpha_{\text{max}}^c R_\odot / \eta_t,$$

$$C_\alpha^p = \alpha_{\text{max}}^p R_\odot / \eta_t.$$

$$\Omega(r, \Theta) = C_\Omega \left\{ \Omega_c + \frac{1}{2} \left[1 + \operatorname{erf} \left(\frac{r - r_c}{d} \right) \right] (1 - \Omega_c - c_2 \cos^2 \Theta) \right\} \quad \alpha^c(r, \Theta, t) = C_\alpha^c \frac{3\sqrt{3}}{4} \sin^2 \Theta \cos \Theta \left[1 + \operatorname{erf} \left(\frac{r - r_c}{d} \right) \right] \left[1 + \frac{|\mathbf{B}(r, \Theta, t)|^2}{B_0^2} \right]^{-1}$$



$$\mathbf{u}_p = \nabla \times (\psi(r, \Theta) \mathbf{e}_\phi)$$

$$\psi(r, \Theta) = R_m \left\{ -\frac{2}{\pi} \frac{(r - r_b)^2}{(1 - r_b)} \sin \left(\pi \frac{r - r_b}{1 - r_b} \right) \cos \Theta \sin \Theta \right\}$$

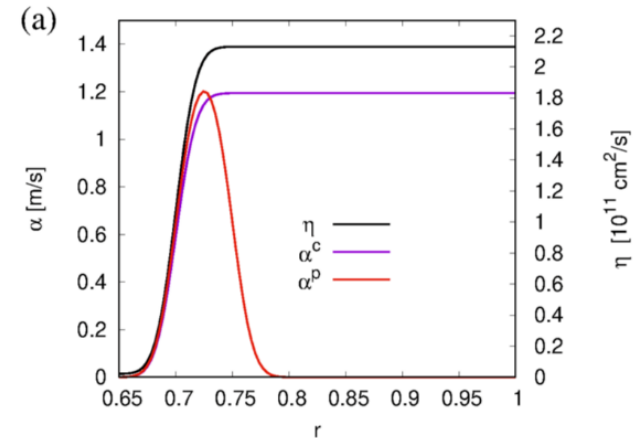
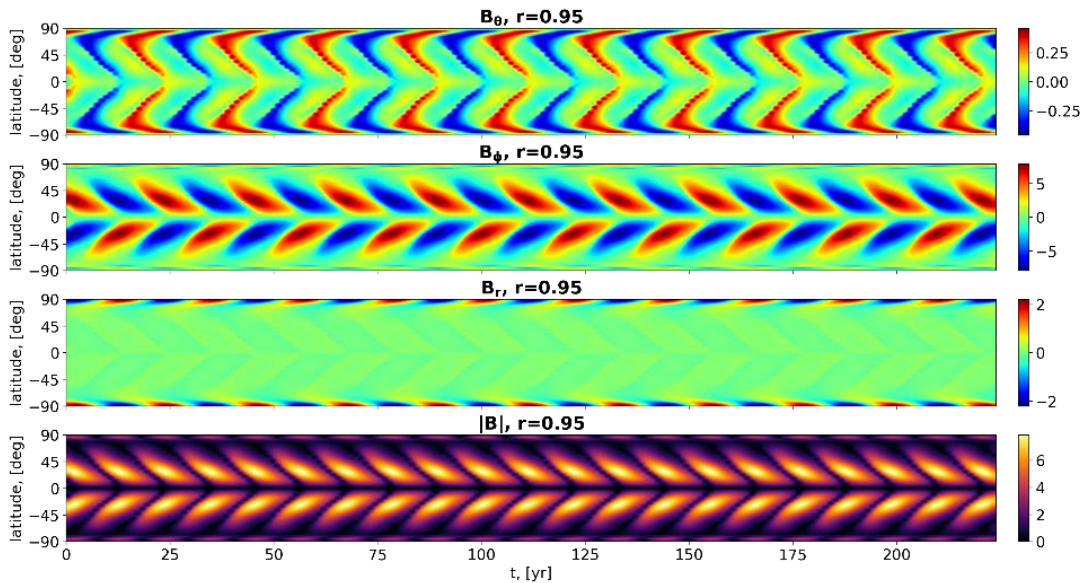
$$\alpha^p(r, \Theta, t) = C_\alpha^p \frac{1}{\sqrt{2}} \sin^2 \Theta \cos \Theta \left[1 + \operatorname{erf} \left(\frac{r - r_c}{d} \right) \right] \left[1 - \operatorname{erf} \left(\frac{r - r_d}{d} \right) \right] \times \frac{2|\mathbf{B}(r, \Theta, t)|^2}{1 + |\mathbf{B}(r, \Theta, t)|^4} \sin(2\pi t / T_f),$$

$$\alpha = \alpha^c + \alpha^p$$

Assumed to result from wave helicity

11.07 yr

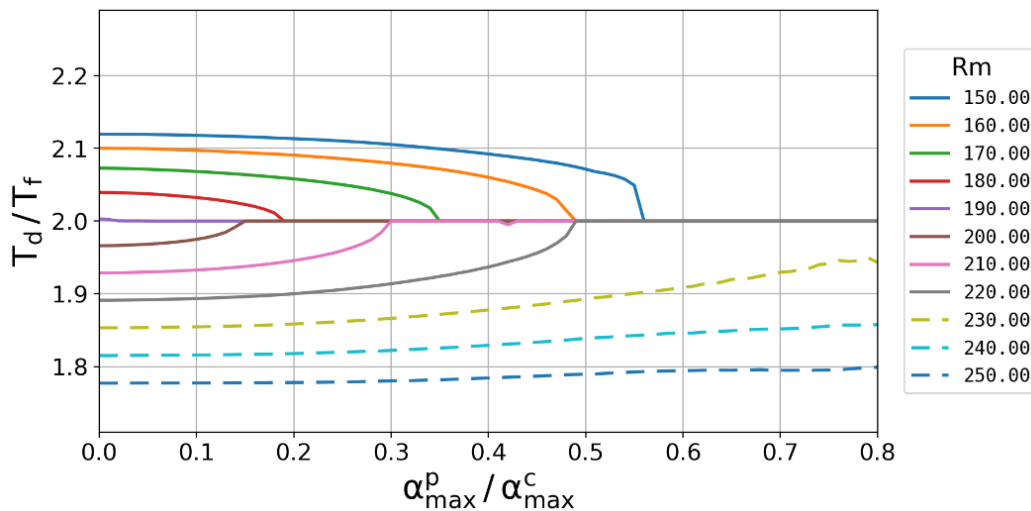
...shows a nice parametric resonance



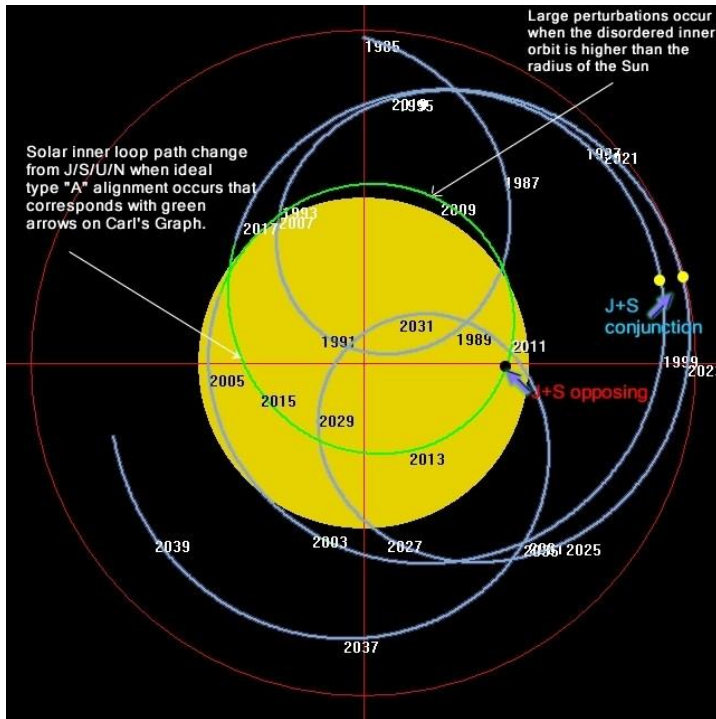
Much higher conductivity in the tachocline than in the convection zone



For a reasonable value $\alpha_0=1.3$ m/s, we need just **some dm/s** for the synchronized α -term to entrain the entire dynamo



Suess/de Vries cycle: A beat period between 22.14 and 19.86 yr ?

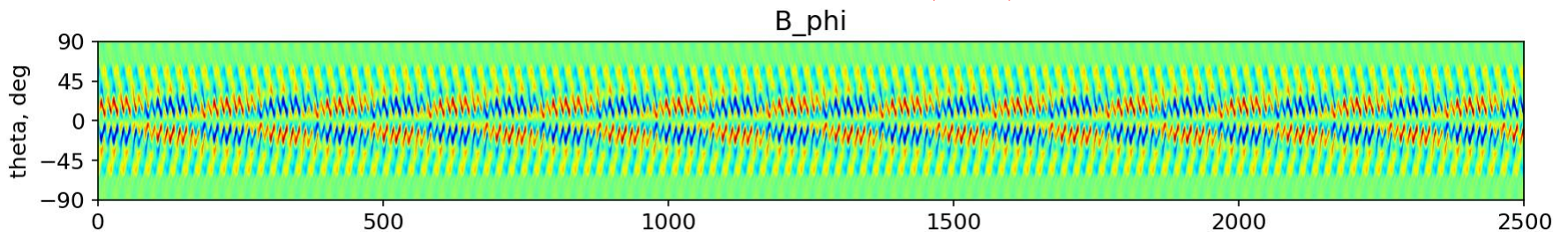


Tidal forcing → **22.14 years**
 Sun around barycenter → **19.86 years**
 (with unclear spin-orbit coupling ← Vidal and Cebren; Shirley ?)

Beat period: **193 years**
 $19.86 \times 22.14 / (22.14 - 19.86)$

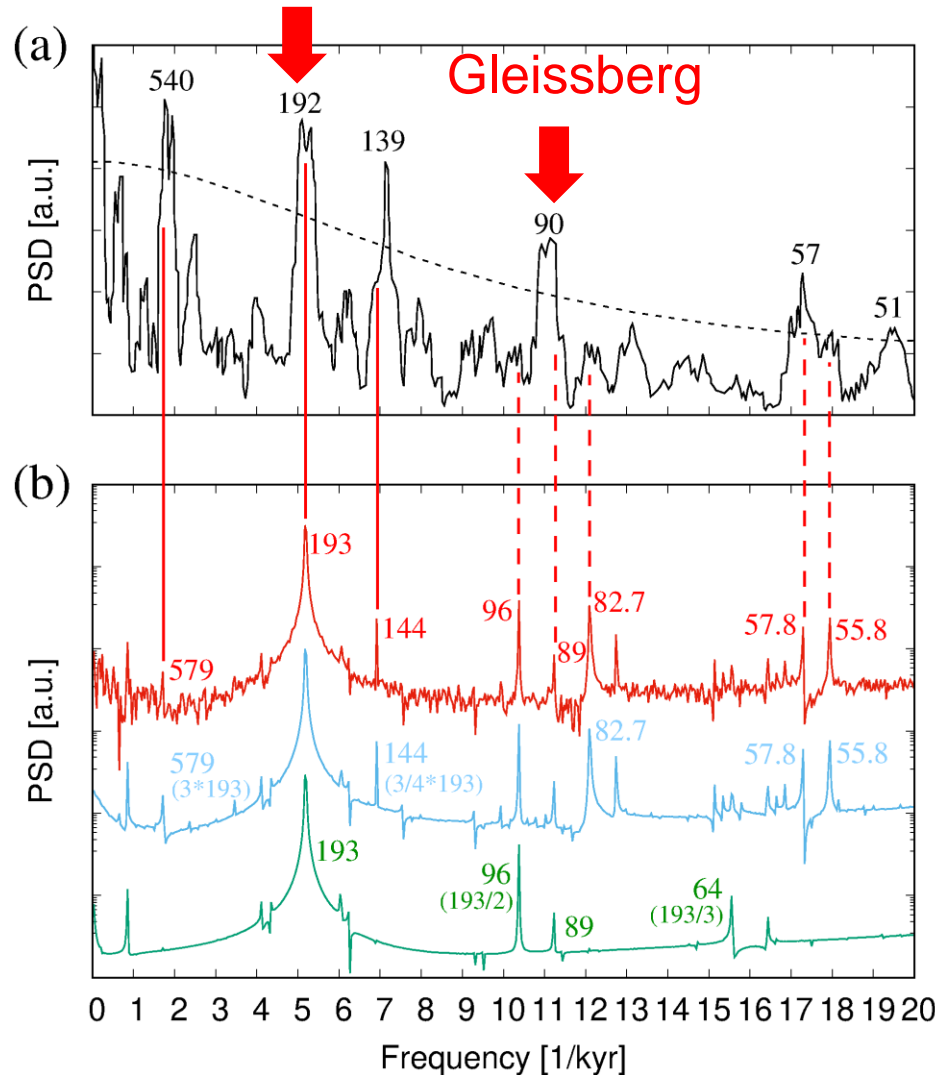


193 years: Suess-de Vries cycle



Comparison: numerical results - sediment data (Lake Lisan)

Suess-de Vries



Yearly sediment thicknesses over 8500 years (climate archive)

S. Prasad et al., *Geology* 32, 581 (2004)

1D α - Ω -dynamo model

...with some noise

...all planets

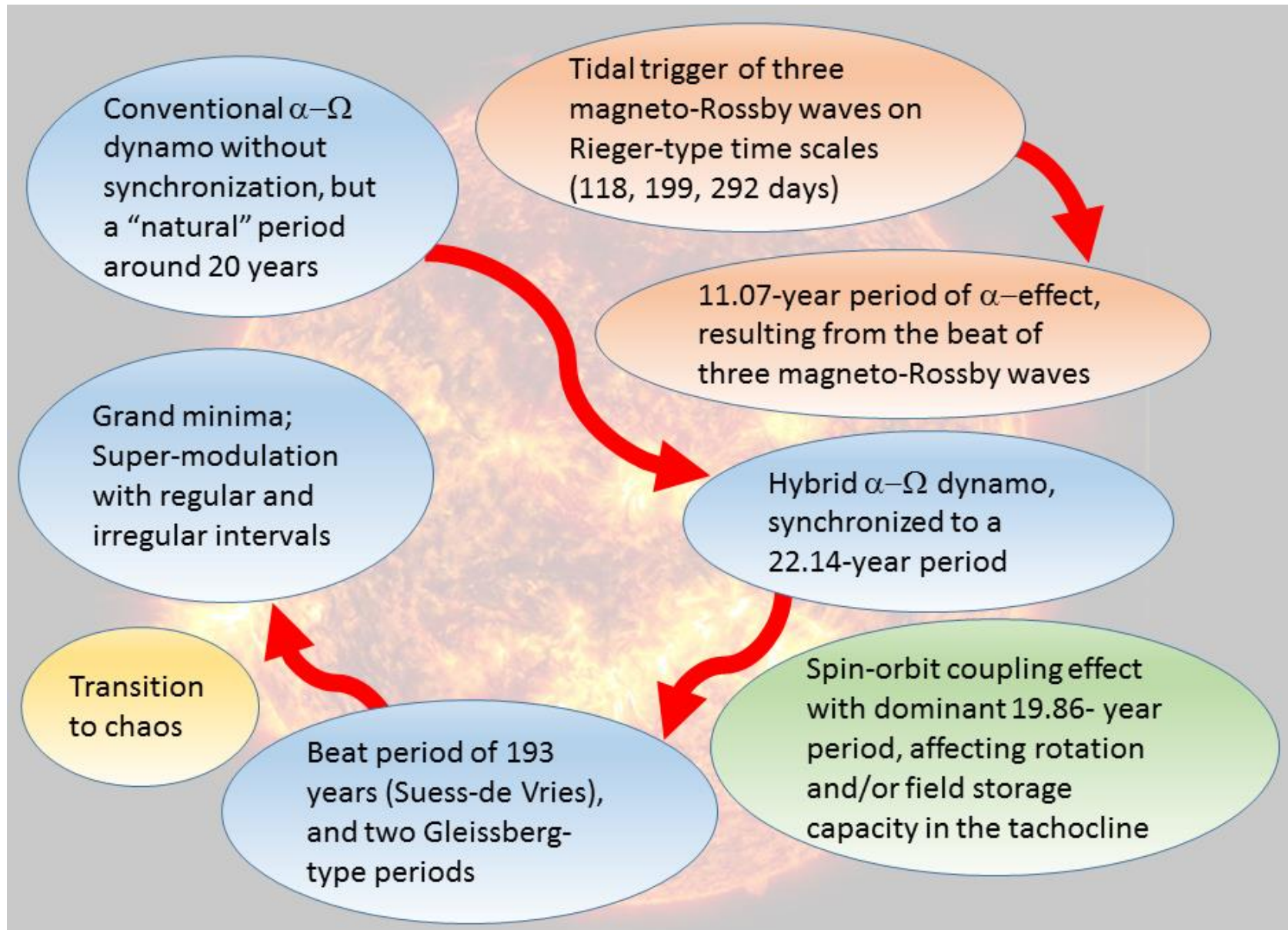
...only Jupiter and Saturn

F.S. et al., *Solar Physics* 296, 88 (2021); 299, 51 (2024)

Summary of our synchronized solar dynamo model

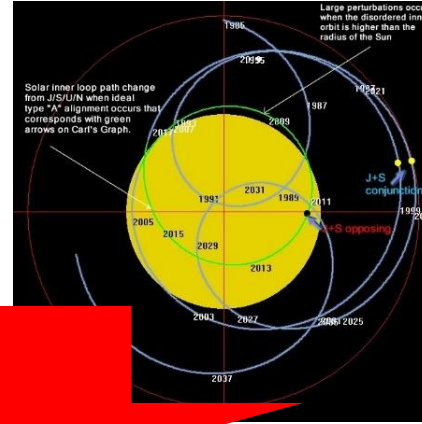
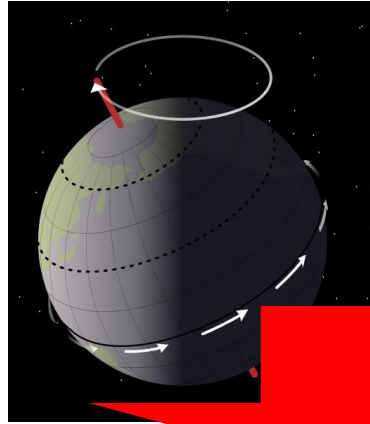
- General principle: Energy is „harvested“ on the shortest possible time-scales
- Various dynamo periods emerge as beat periods
- Three tidally triggered magneto-Rossby waves on Rieger-type time-scale → Schwabe/Hale
- Hale+Barycentric motion → Suess-de Vries (+Gleissberg)
- **Self-consistency**: The sharp Suess-de Vries peak at 193 years could hardly be explained without phase-stability of the primary Hale cycle at 22.14 years

Summary of our synchronized solar dynamo model

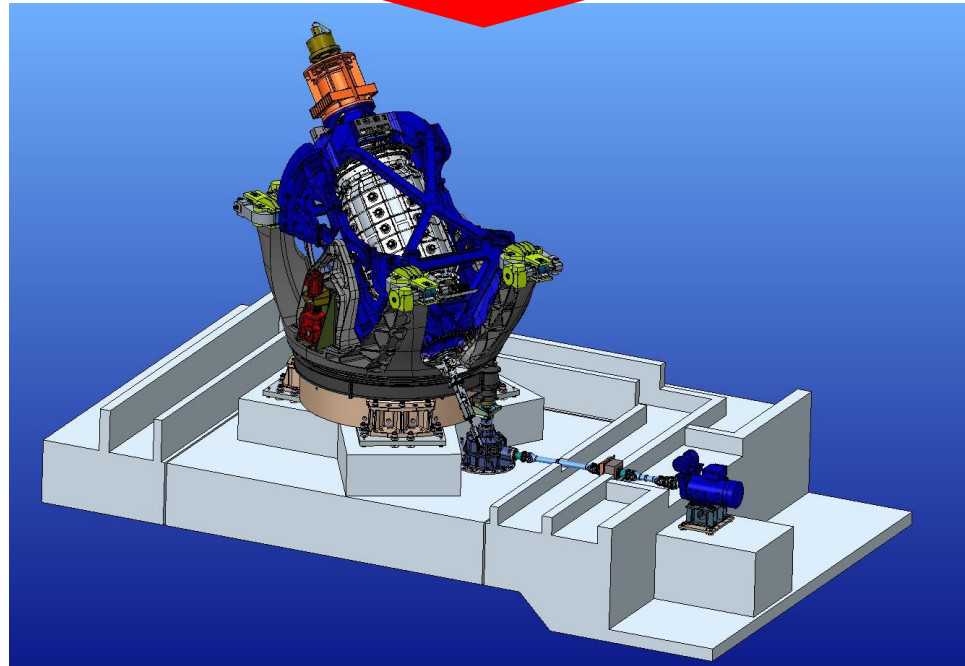


Precession driven DRESDYN dynamo: Two motivations

Influence of Milankovic cycles (precession, nutation, ellipticity) on the geodynamo



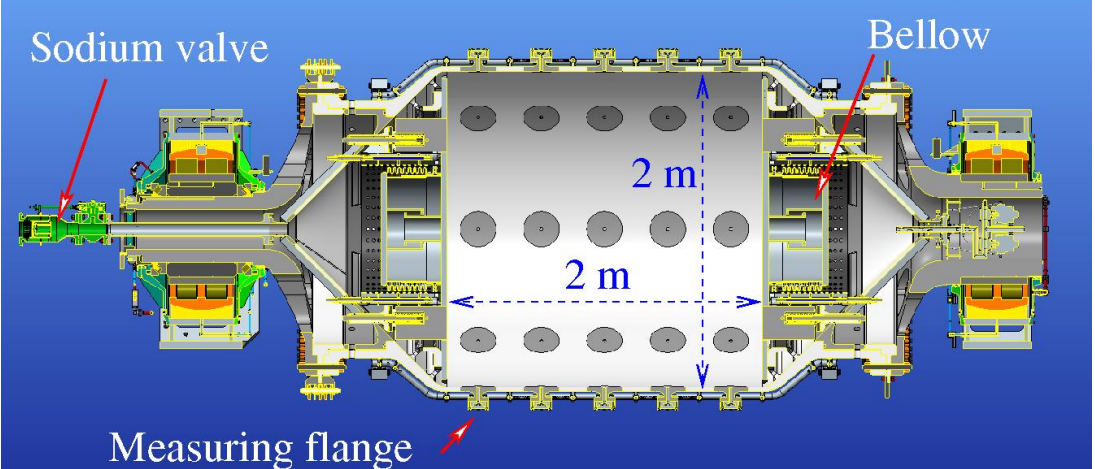
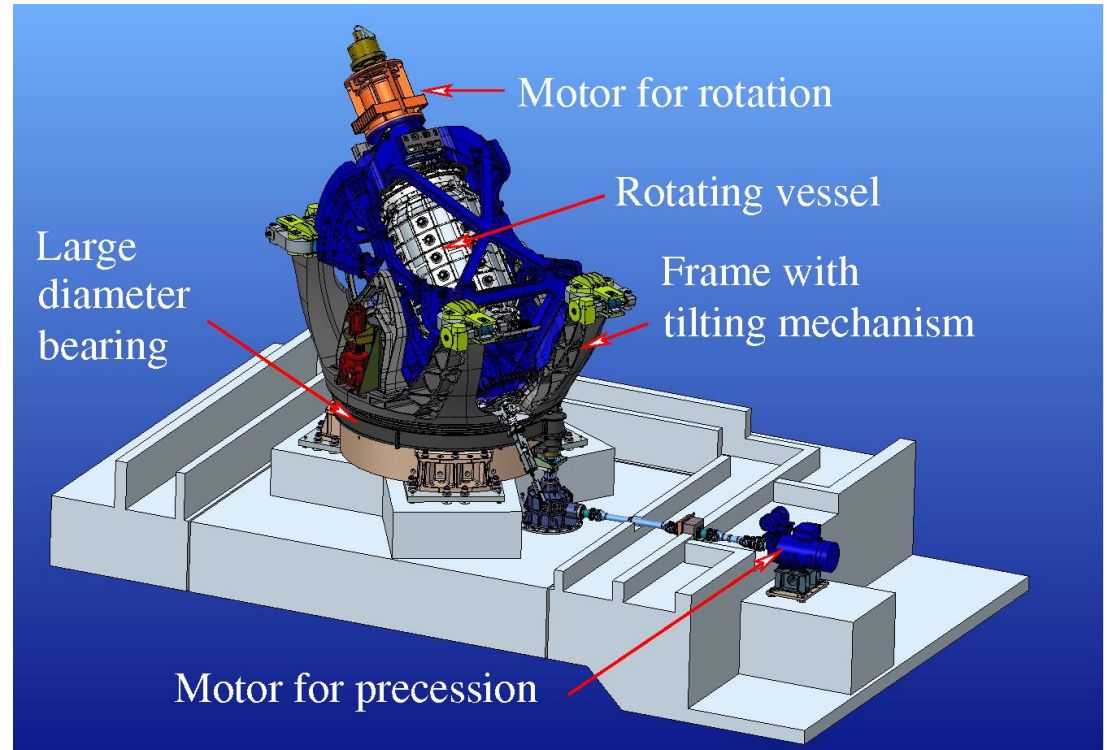
Influence of rosette-like motion on solar dynamo (spin-orbit coupling)



Precession driven dynamo within the DRESDYN project

Key parameters:

- Cylinder with 2 m diameter and 2 m height, 8 tons of liquid sodium
- Cylinder rotation: 10 Hz (will need some 800 kW motor power)
- Turntable rotation: 1 Hz
- **Magnetic Reynolds number ~ 700**
- **Gyroscopic torque onto the basement: 8 MNm !**



“Fundamental” problems due to huge gyroscopic torque

April 2013: drilling 7 holes (22 m deep)

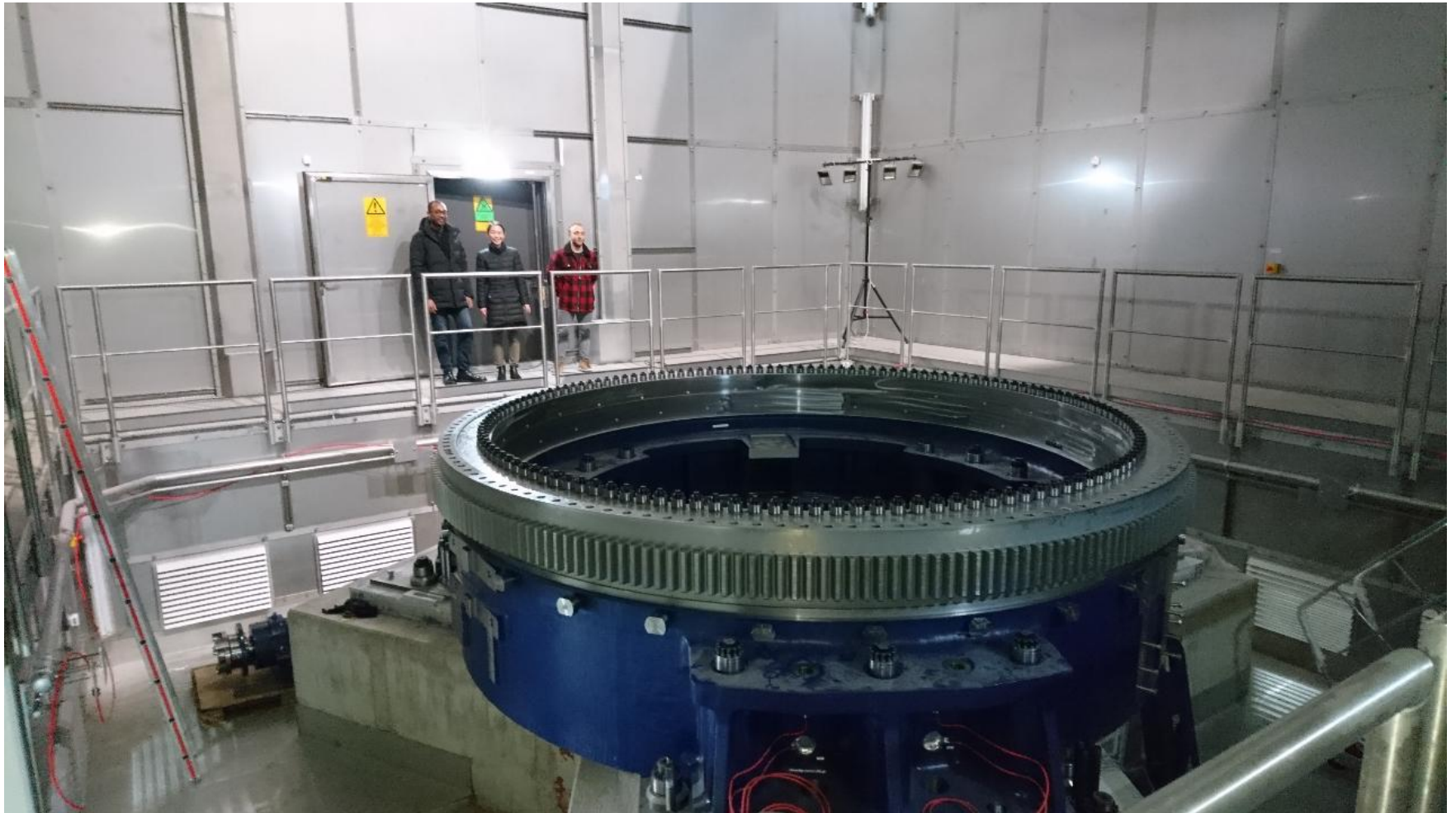


July 2013: Constructing the ferroconcrete basement



May 2015: The tripod for the dynamo within the containment (with stainless steel “wallpaper”)

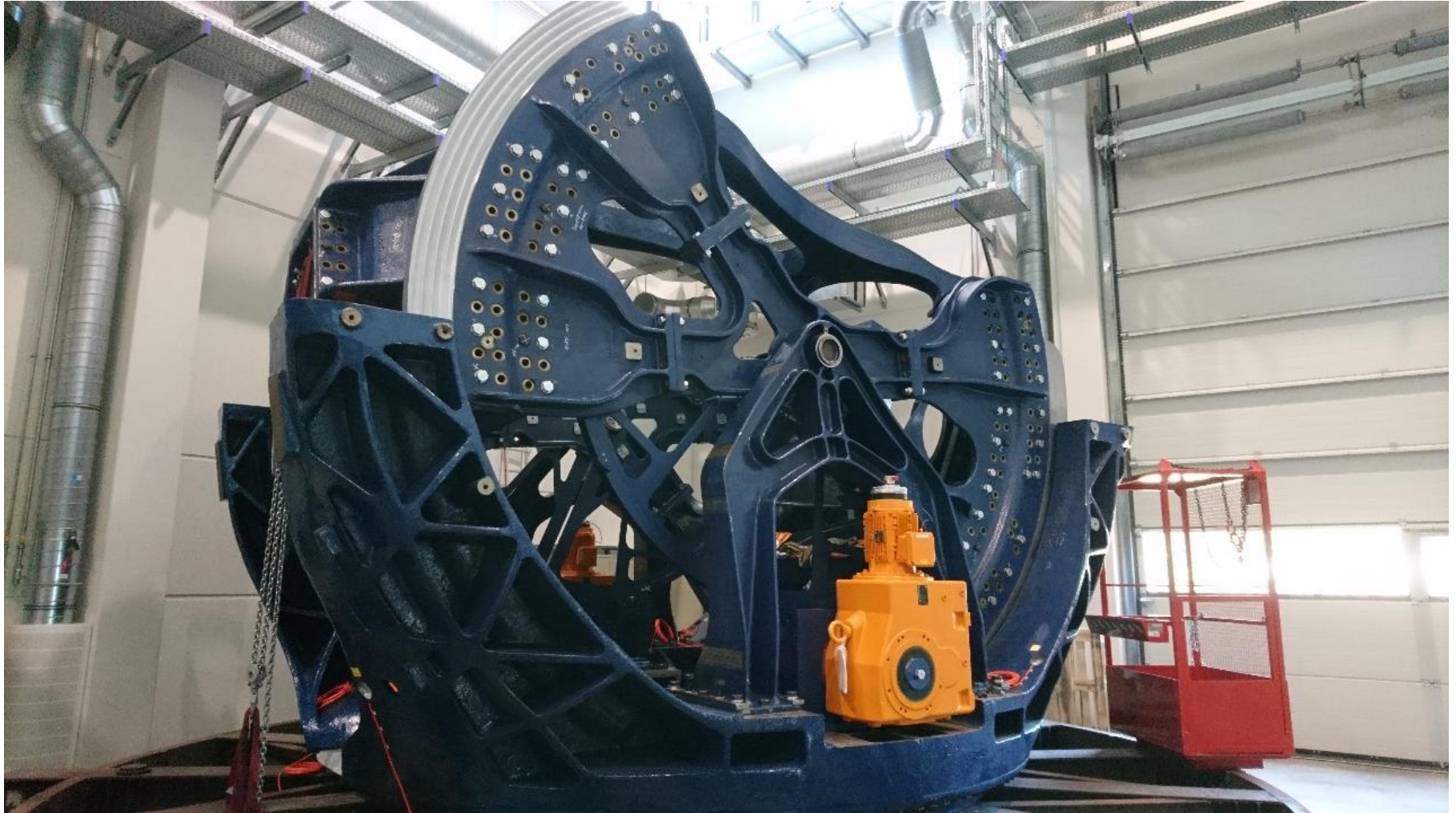
Large ball bearing installed (12/2018)



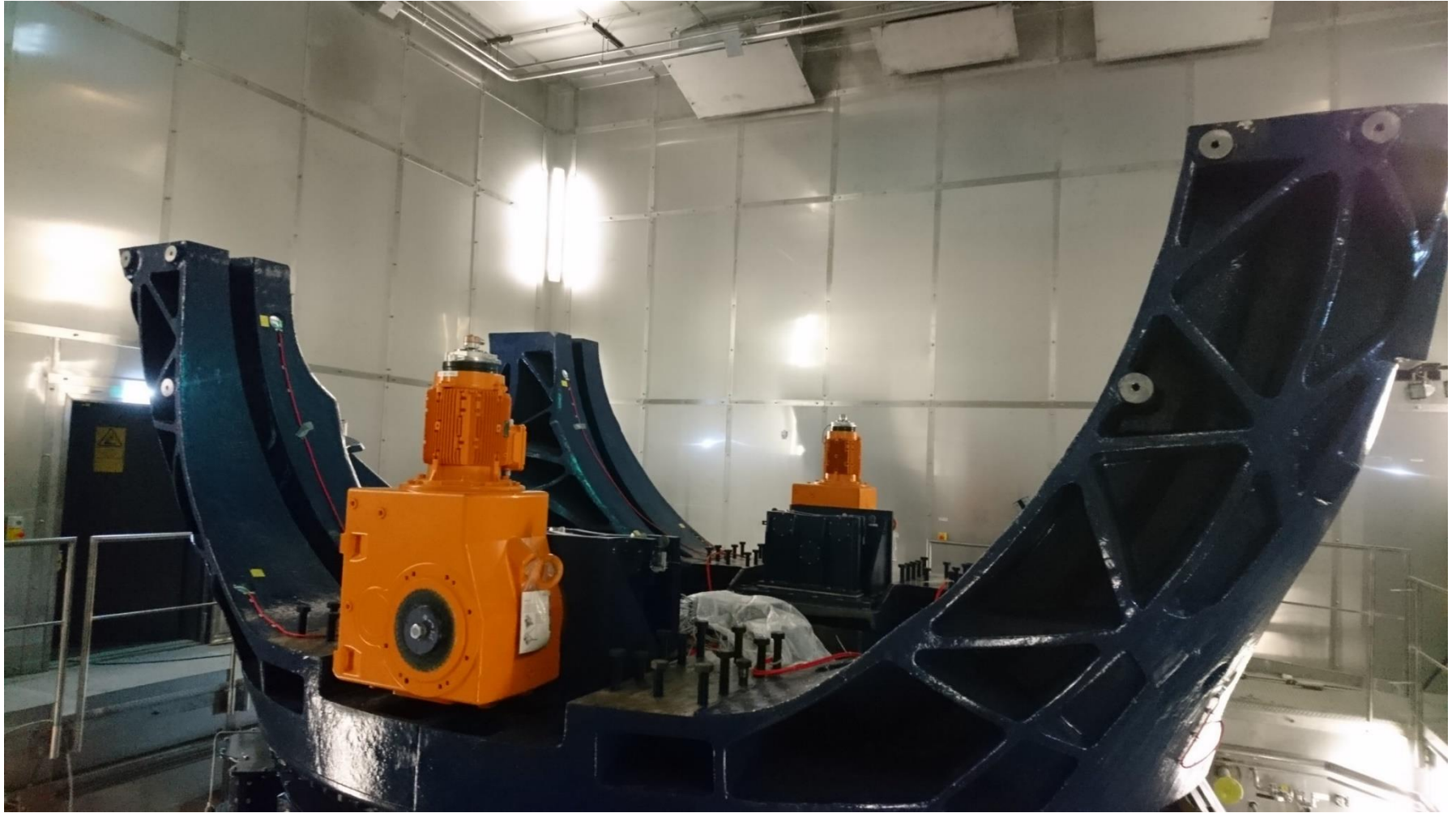
Traverse and pylons (01/2019)



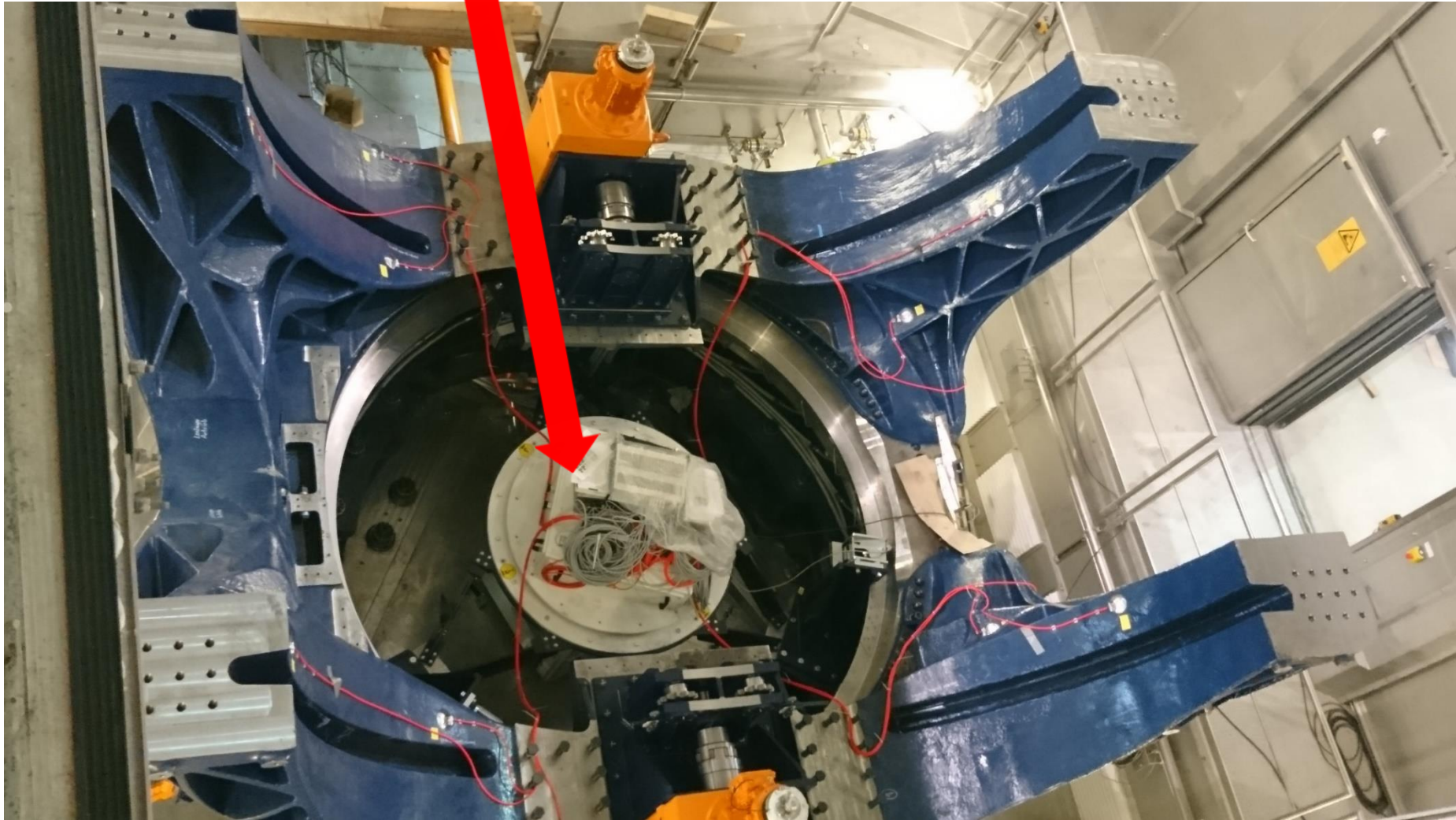
Test assembly of the tilting frame (07/2019)



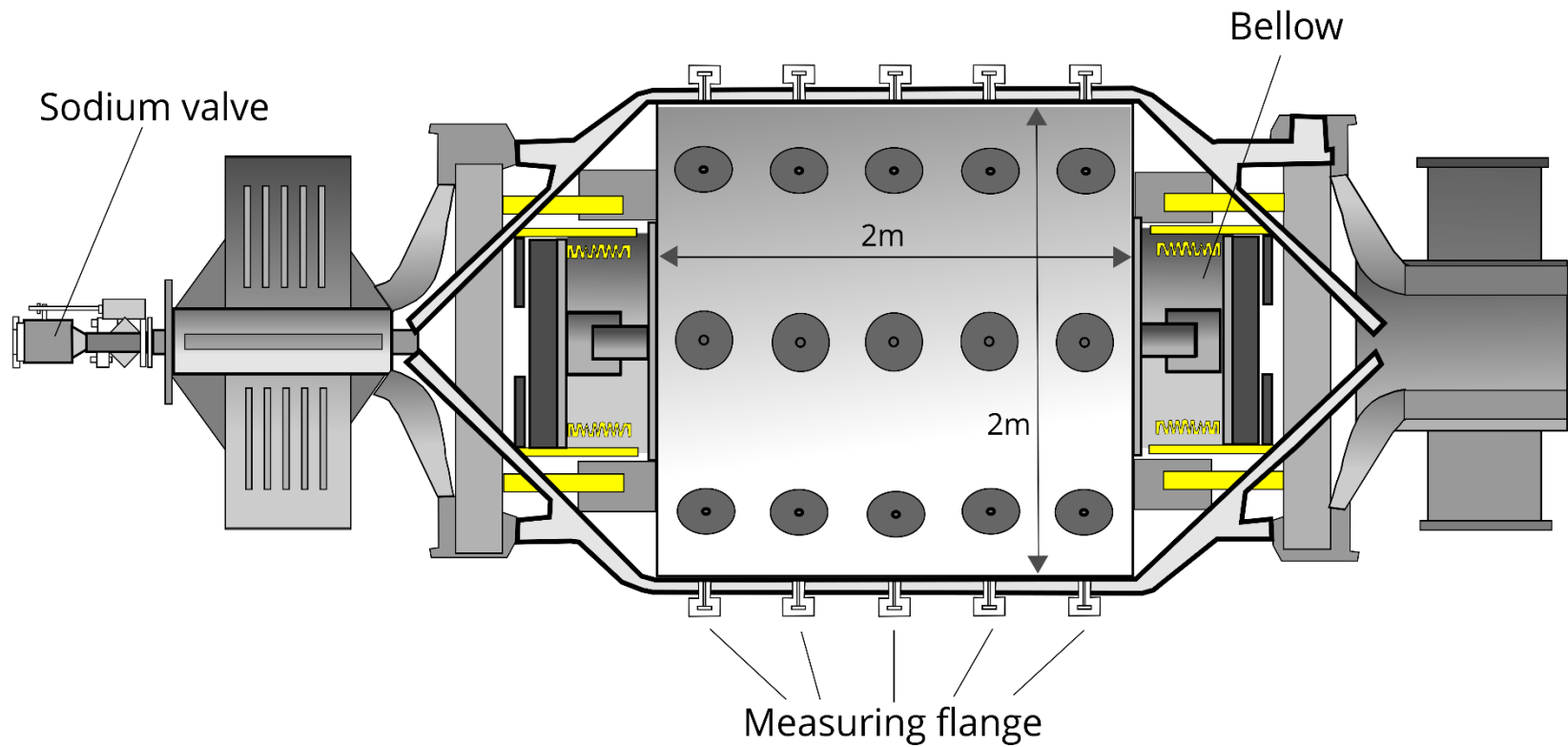
Pylons transferred to the containment (11/2019)



Pylons with central rotary connection (for 1 MW power and oil)



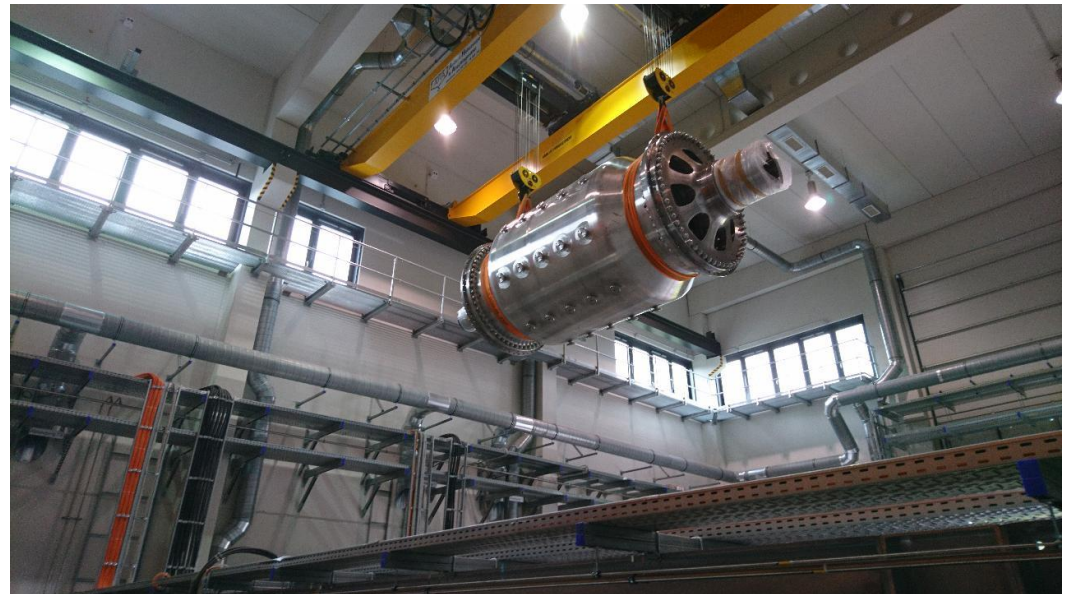
Rotation vessel with bearings



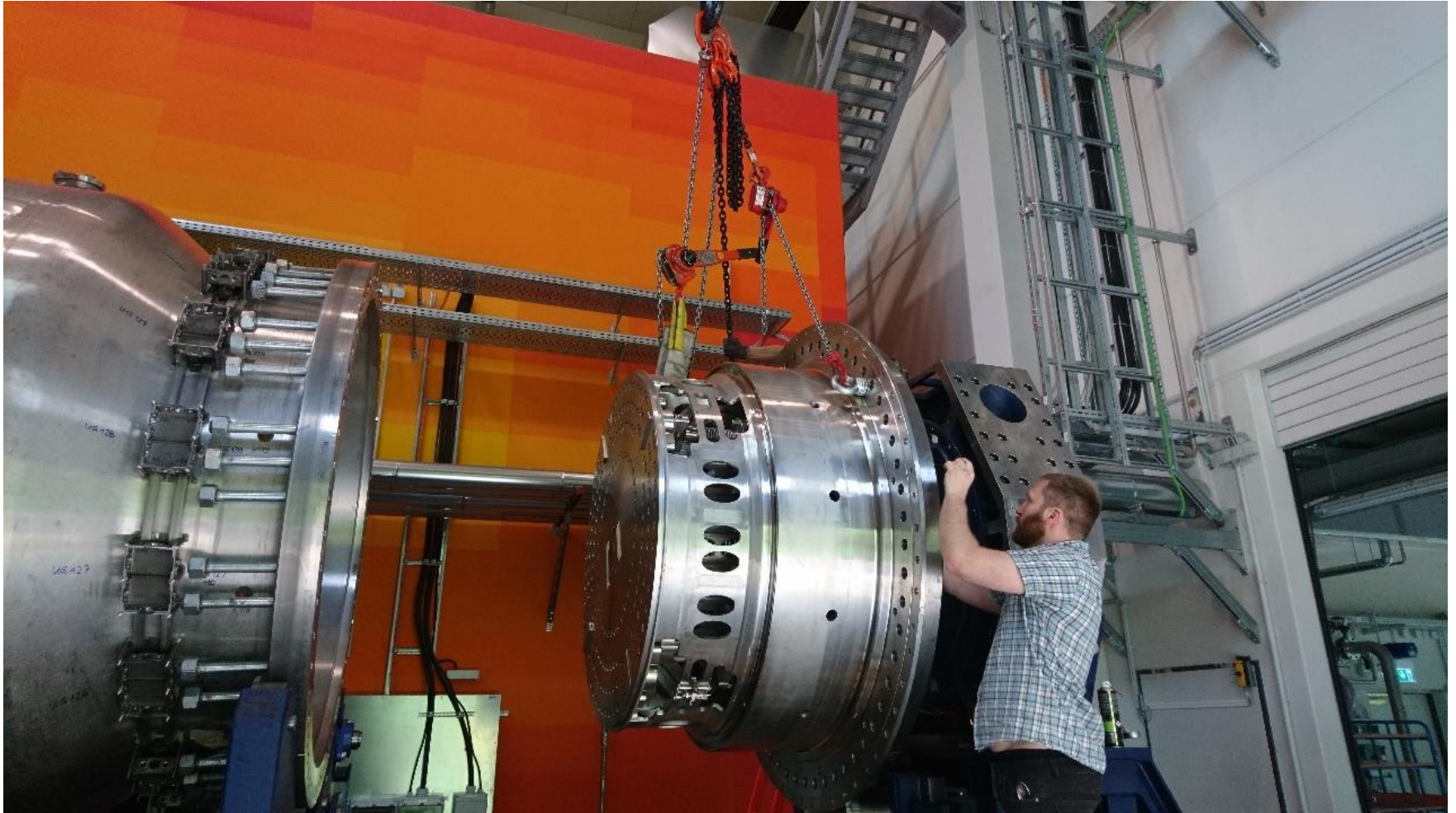
Pressure test (with 35 bar) of the rotation vessel (3/2019)



The vessel arrives at HZDR (July 3, 2020)



Assembly of the first conical end and the bearing (May 2022)

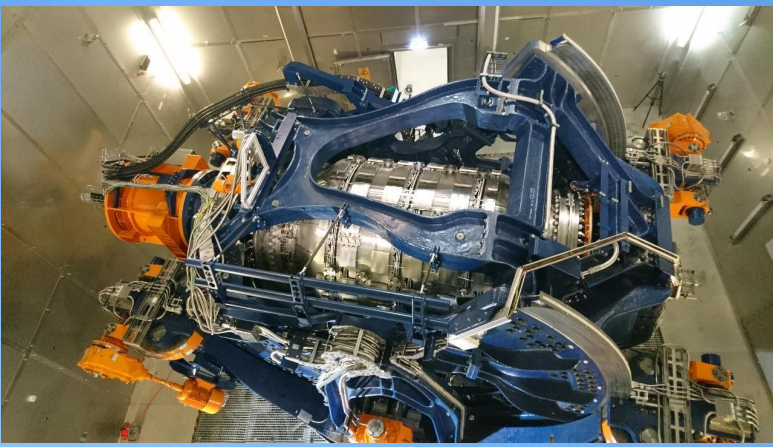


January 17, 2024: “Wedding” of frame and vessel

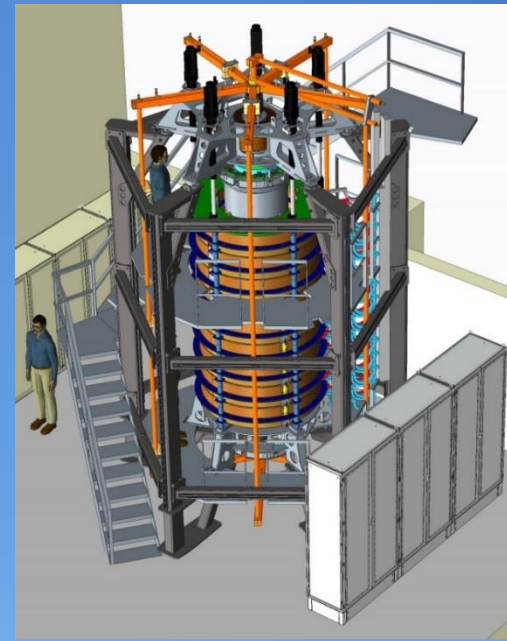


June 18, 2024: First precession (though very slowly, 0.05 Hz...)





Thank you
for your
attention!

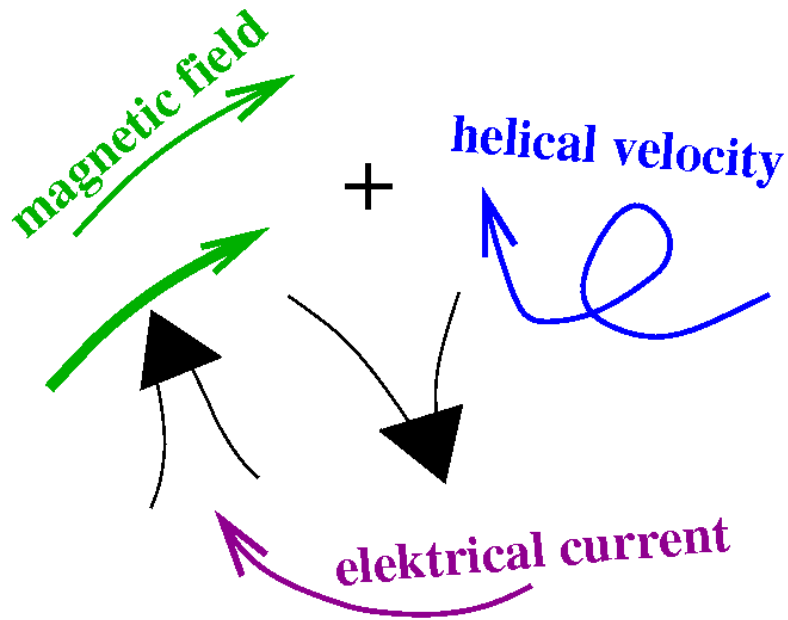




Geo- and astrophysical MHD: Basic mechanisms

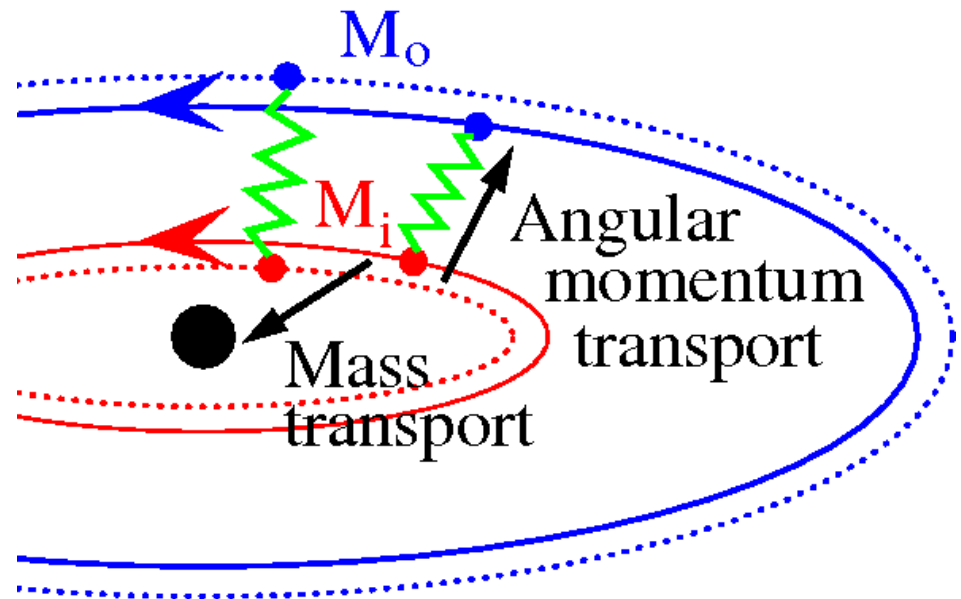
Homogeneous dynamo effect:

Self-excitation of magnetic fields in sufficiently strong, helical flows of conducting fluids



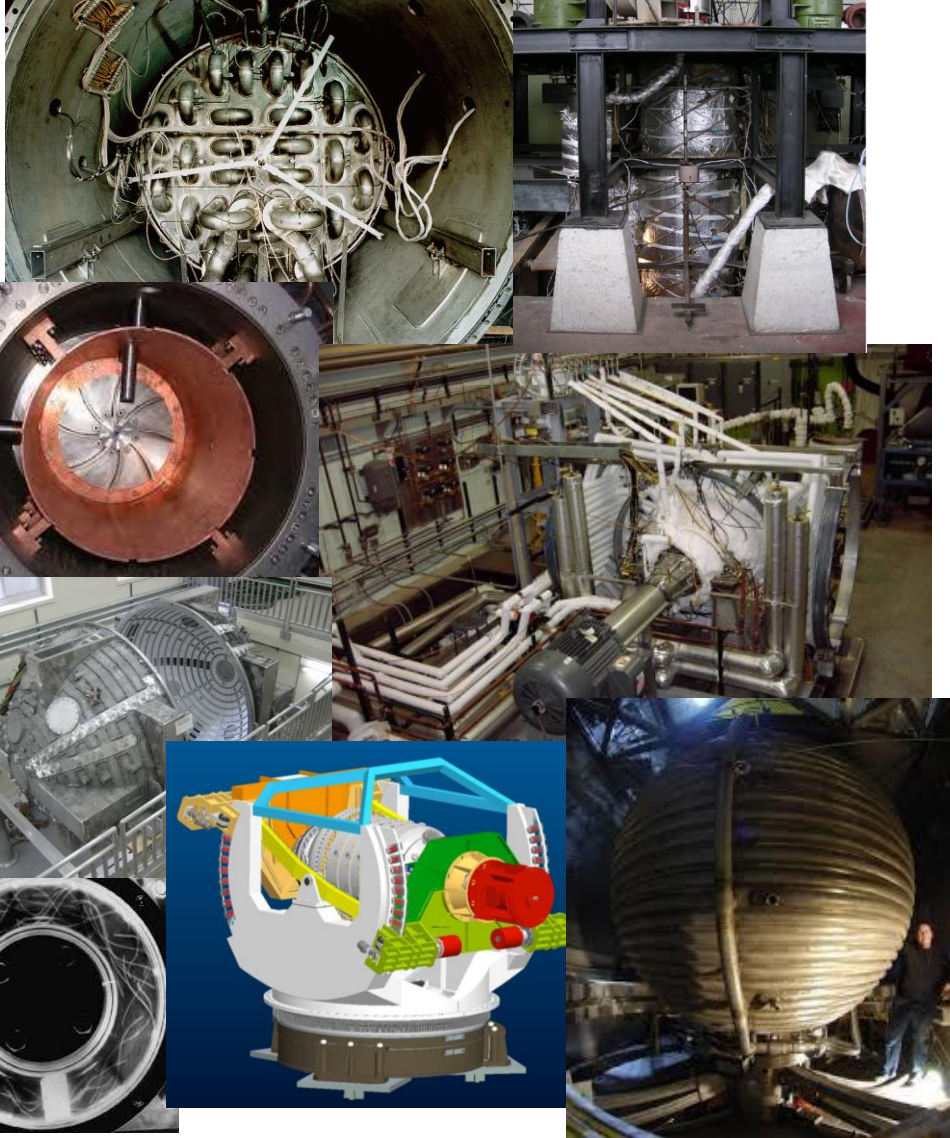
Magnetorotational instability (MRI):

Magnetic fields act like springs and trigger angular momentum transport in accretion disks around protostars or black holes

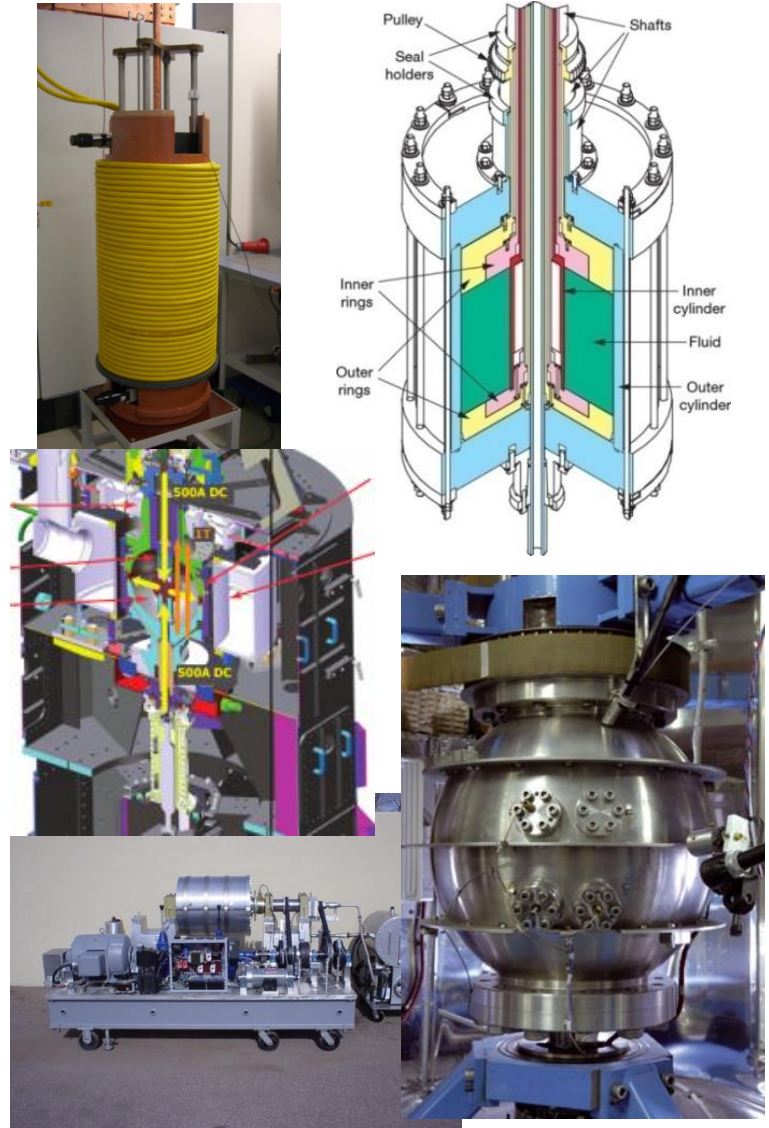


Previous, present, and future experiments

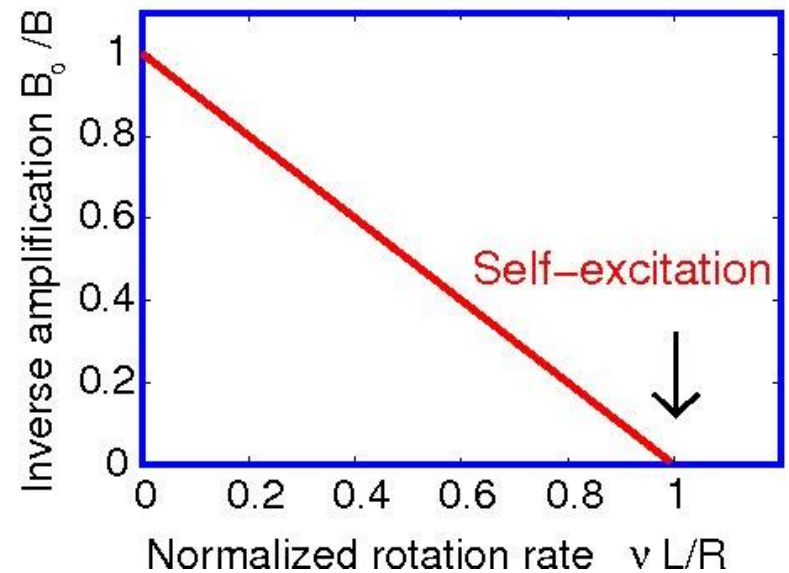
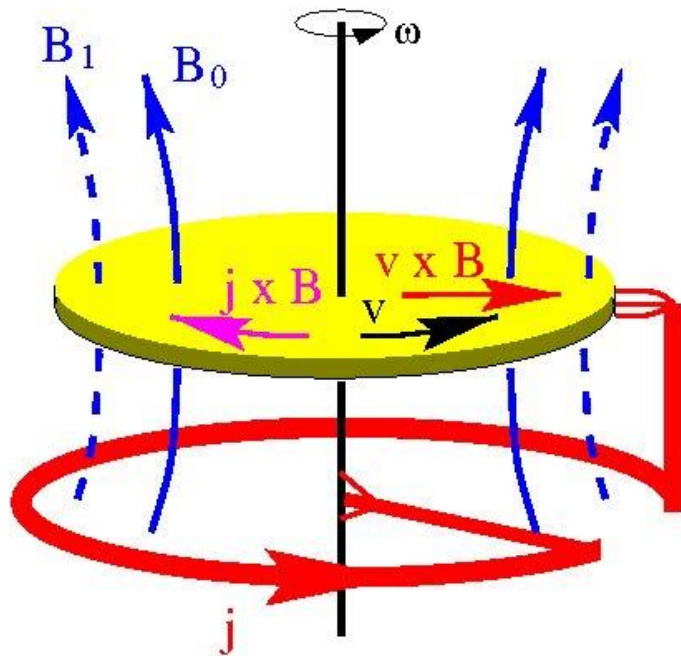
Dynamo effect



Magnetically triggered instabilities

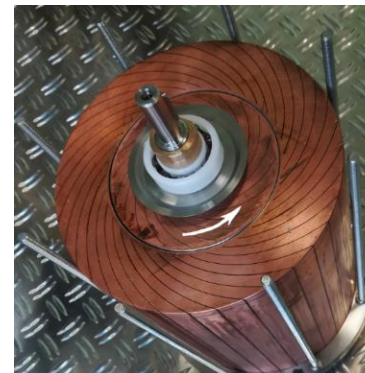


Principle of self-excitation: Illustrated at a disk dynamo model



Modified disk dynamos were recently built, and run, in Queretaro (Mexico) and in Grenoble

R. Avalos-Zúñiga,
J. Priede, Proc.
Royal Soc. A 479,
20220740 (2023)



T. Alboussière et
al. Proc. Royal
Soc. A 478,
20220374 (2023)

Hydromagnetic dynamos: Dimensionless parameters

$$\frac{\partial \mathbf{B}}{\partial t} = \nabla \times (\mathbf{v} \times \mathbf{B}) + \frac{1}{\mu_0 \sigma} \Delta \mathbf{B}$$

Governing parameter:
Magnetic Reynolds number

$$Rm = \mu_0 \sigma L V$$

$$\frac{\partial \mathbf{v}}{\partial t} + (\mathbf{v} \cdot \nabla) \mathbf{v} = -\frac{\nabla p}{\rho} + \frac{1}{\mu_0 \rho} (\nabla \times \mathbf{B}) \times \mathbf{B} + \nu \Delta \mathbf{v} + \mathbf{f}_{extern}$$

Governing parameters:
Reynolds, Hartmann

$$Re = \frac{LV}{\nu}$$

$$Ha = BL \sqrt{\frac{\sigma}{\rho \nu}}$$

Alternatively: Lundquist number

$$Lu = Pm^{1/2} Ha$$

...using the magnetic Prandtl number

$$Pm = \nu \mu_0 \sigma$$

Need for large-scale sodium facilities

Why sodium? Condition for magnetic self-excitation: Magnetic Reynolds number must be larger than ~ 10 :

$$Rm = \mu\sigma VL > Rm_{\text{crit}} \geq 10$$

(μ - magnetic permeability, σ - conductivity, V - typical velocity, L - typical size)

Sodium is the best liquid conductor with $\sigma \sim 10^7$ S/m $\rightarrow VL \sim 1$ m²/s

Why so large? Necessary power scales with $1/L$:

$$P \sim Rm^3 / L$$

Reasonable motor power (a few 100 kW) only with large facilities (~ 1 m)

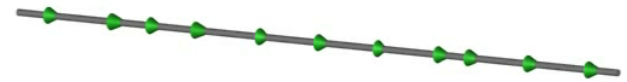
Karlsruhe dynamo experiment – Realizing an α^2 dynamo

α -effect: Under the influence of a **helical** flow, electrical currents are induced which are directed PARALLEL to the magnetic field

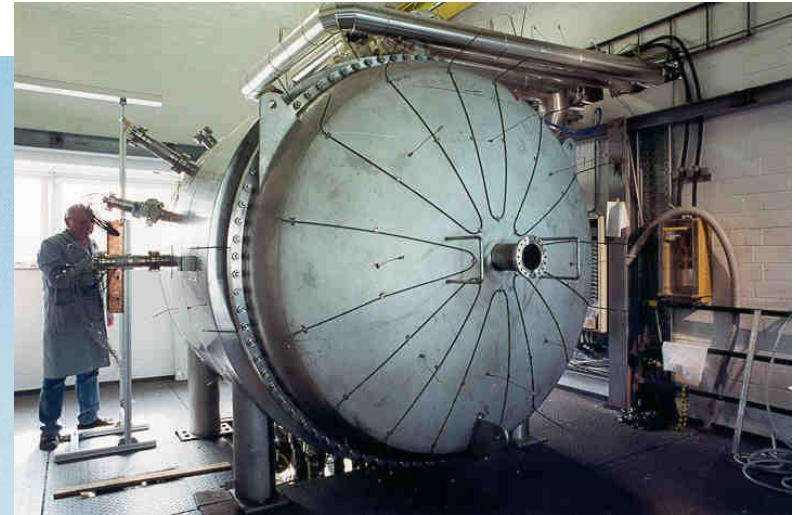
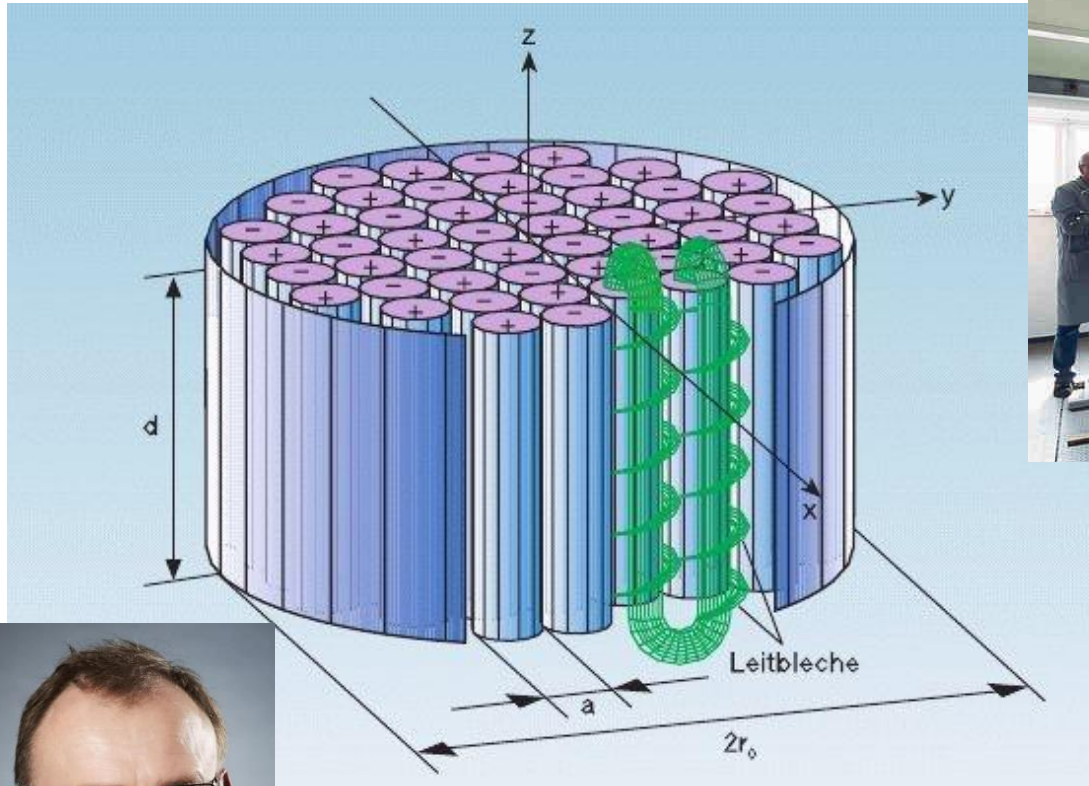


Max Steenbeck, Fritz Krause, Karl-Heinz Rädler:
BERECHNUNG DER MITTLEREN LORENTZ-FELDSTÄRKE FÜR EIN ELEKTRISCH LEITENDES MEDIUM IN TURBULENTER, DURCH CORIOLIS-KRÄFTE BEEINFLUSSTER BEWEGUNG

Zeitschrift für Naturforschung 21a, 369 (1966)



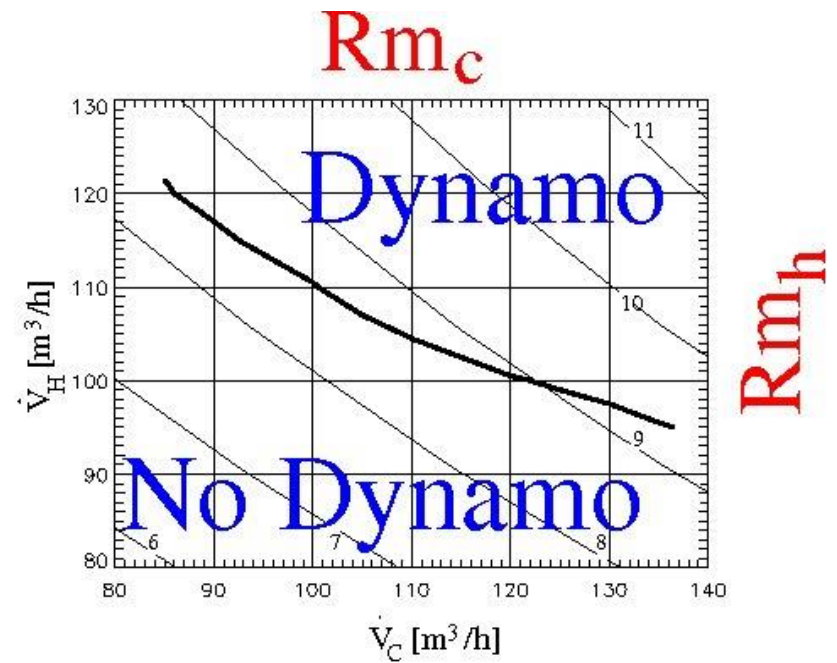
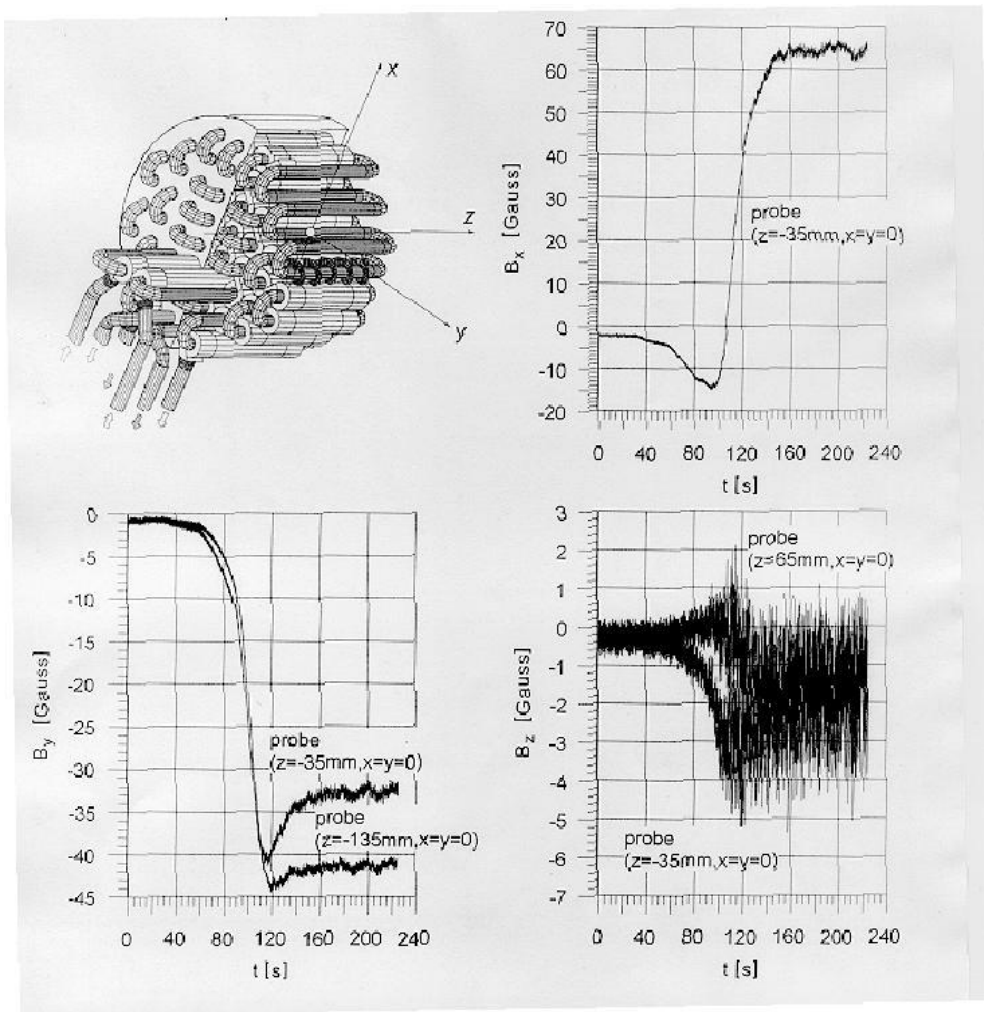
Karlsruhe Dynamo Experiment



A two-scale, α^2 type dynamo
(with anisotropic α), realized
by 52 spin-generators

Robert Stieglitz and Ulrich Müller, Phys. Fluids 13, 561 (2001)

Karlsruhe Dynamo Experiment



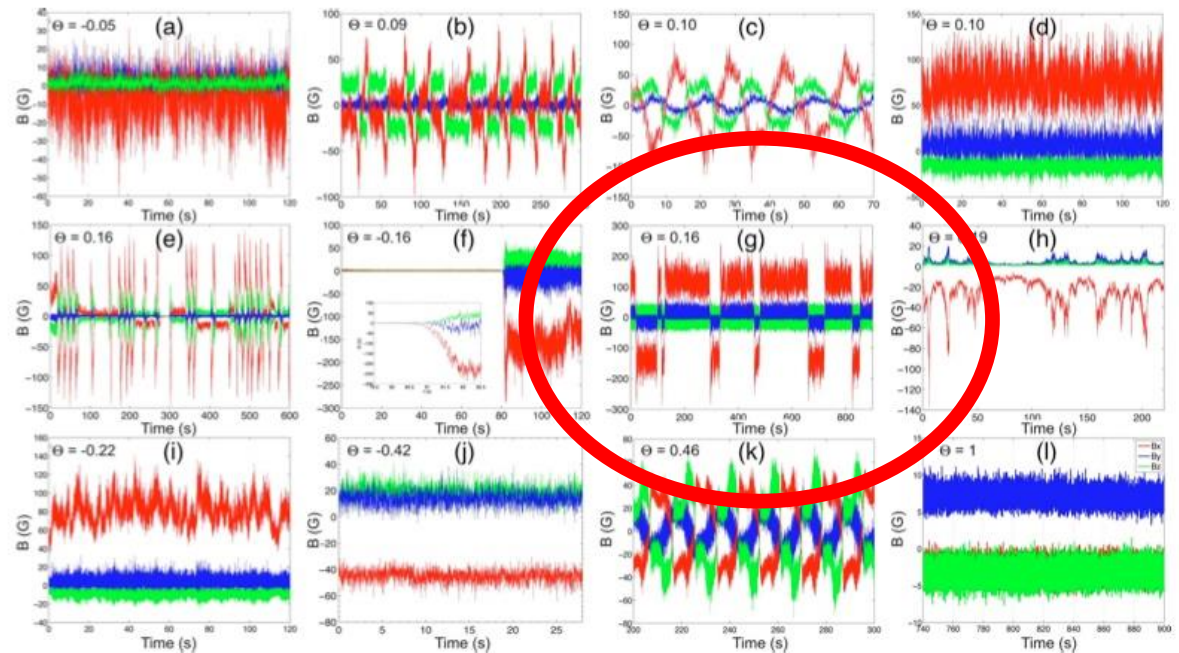
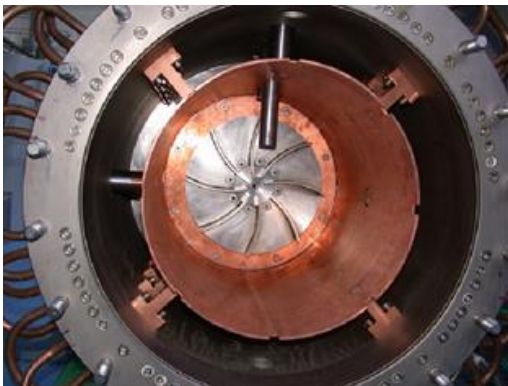
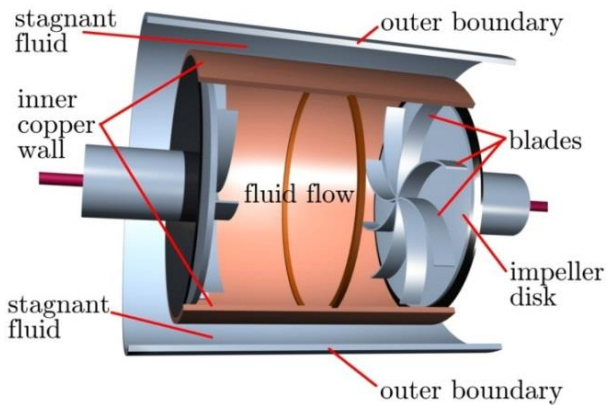
Again, very good agreement with numerical predictions

Rädler et al. Nonl. Proc. Geophys. 9, (2002), 171; Tilgner, Busse: Magnetohydrodynamics 38 (2002)

„Secret Fax“ from 19th December 1999, sent by Karl-Heinz Rädler

von-Kármán-Sodium (VKS) Experiment in Cadarache

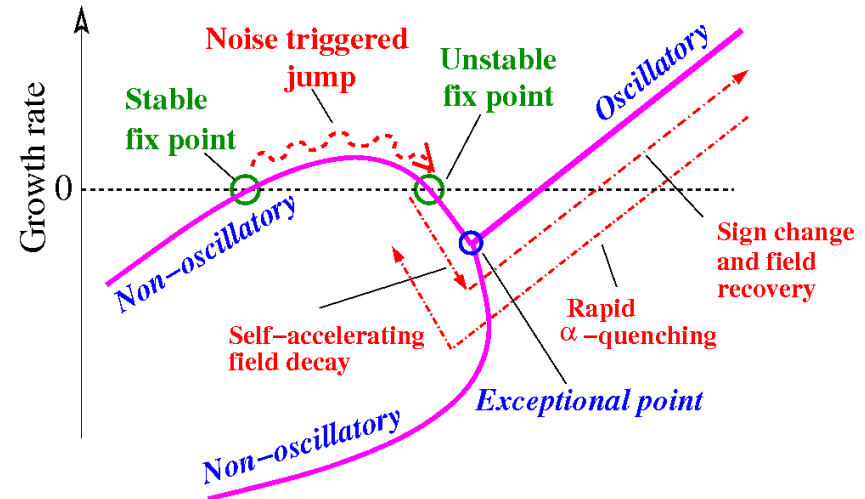
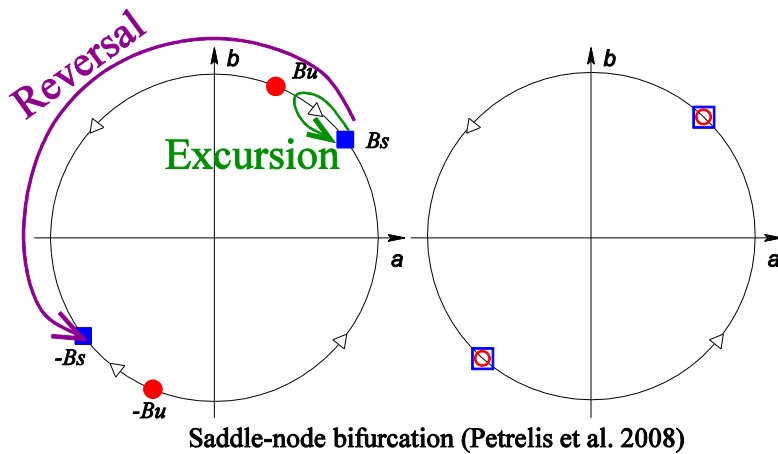
VKS has shown self-excitation and a wealth of wonderful dynamical effects, including **oscillations, reversals, burst, localized fields**....



Monchaux et al., Phys. Fluids 21 (2009), 035108

However: The dynamo works only if magnetic material is used for the disks...

Reversals: Two complementary pictures



Dynamical systems picture: Saddle-node bifurcation

$$\frac{d\Theta}{dt} = \alpha_0 + \alpha_1 \sin(2\Theta) + \text{noise}$$

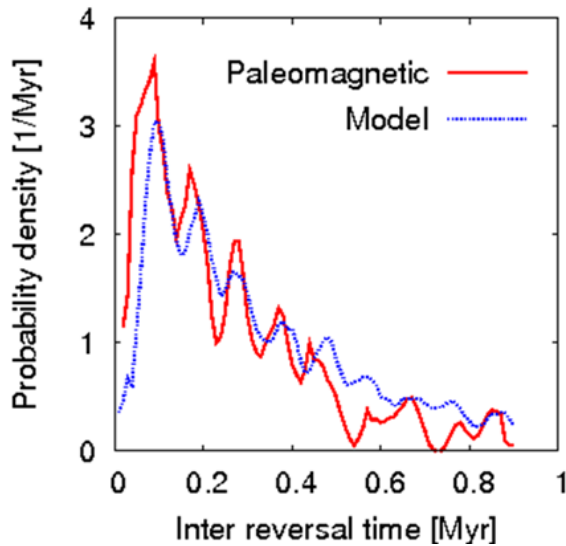
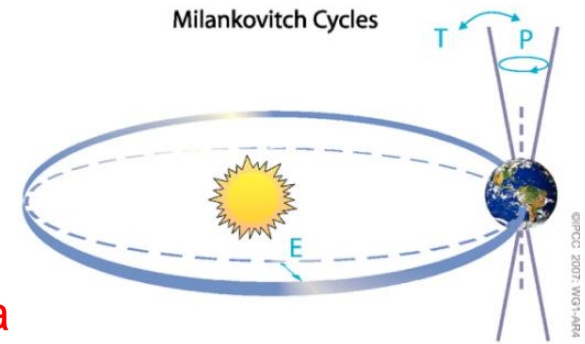
Petrelis et al., PRL 102 (2009), 144503

Spectral picture: Noise triggered relaxation oscillations in the vicinity of spectral exceptional points of non-self-adjoint dynamo operators

F.S. et al., PRE 67 (2003), 027302; PRL 94 (2005) 184506; Earth Planet. Sci.Lett. 243 (2006), 828; GAFD 101 (2007) 227; Fischer et al., Inverse Probl. 25 (2008) 065011

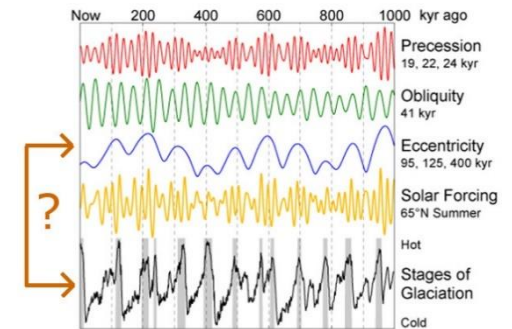
Role of mechanical forcings for the geodynamo (Milankovic cycles)

Strong indication for influence of variations of Earth's orbit parameters (precession, obliquity, excentricity) on the statistics of the geodynamo



Probability density of **inter-reversal times** shows maxima at multiples of the Milankovic cycle of Earth's orbit **eccentricity** (95 ka)

Connection with climate??



Consolini, De Michelis,
Phys. Rev. Lett. 90
(2003), 058503



Stochastic resonance

Changing moment of inertia when a 120 m water column is concentrated in ice sheets

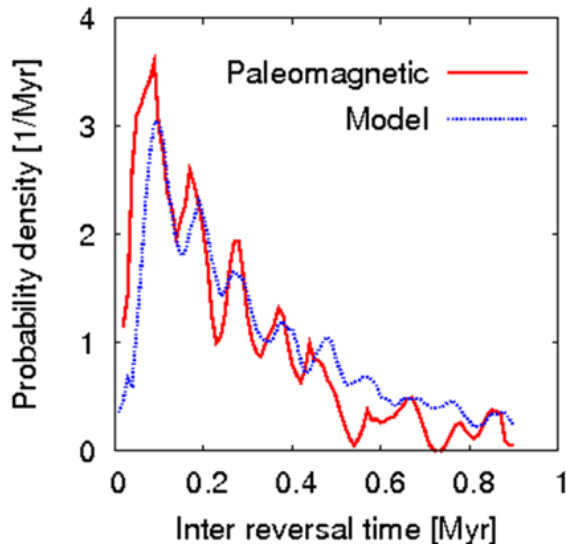
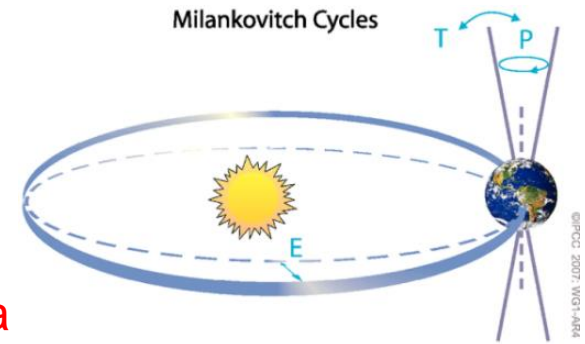
→ **Change of Earth's rotation period**

→ **Influence on geodynamo**

C.S.M. Doake: A possible effect of ice ages on the Earth's magnetic field, Nature 267 (1977), 415

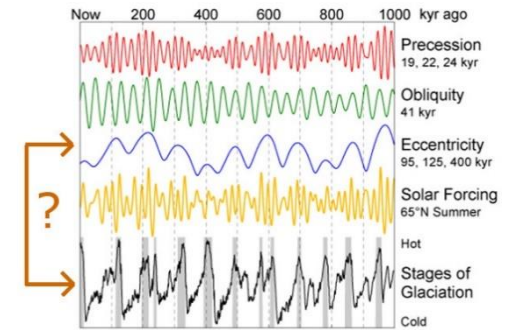
Role of mechanical forcings for the geodynamo (Milankovitch cycles)

Strong indication for influence of variations of Earth's orbit parameters (precession, obliquity, excentricity) on the statistics of the geodynamo



Probability density of **inter-reversal times** shows maxima at multiples of the Milankovitch cycle of Earth's orbit **eccentricity** (95 ka)

Connection with climate??



Consolini, De Michelis,
Phys. Rev. Lett. 90
(2003), 058503



Stochastic resonance

Alternative: Effect of eccentric Kepler orbits

→ **Fluid instabilities in ellipsoids**

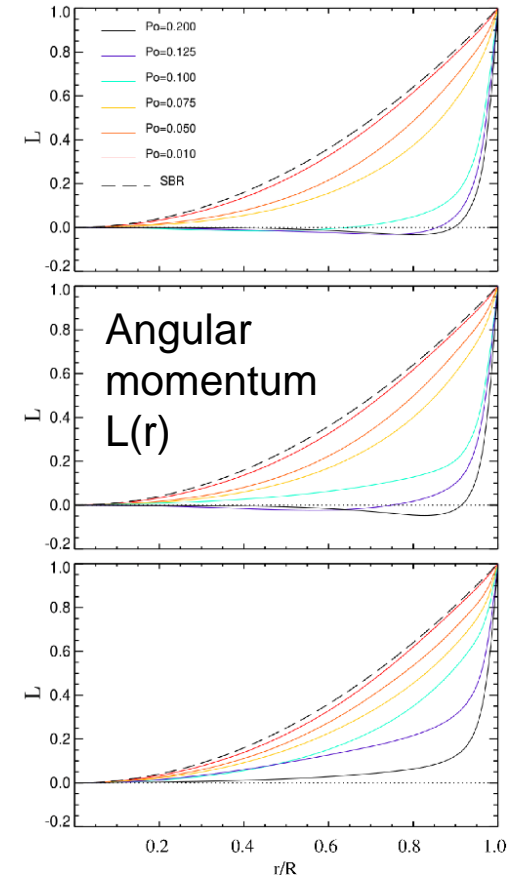
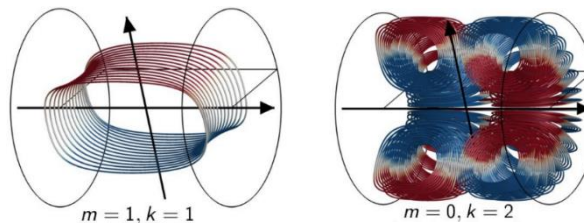
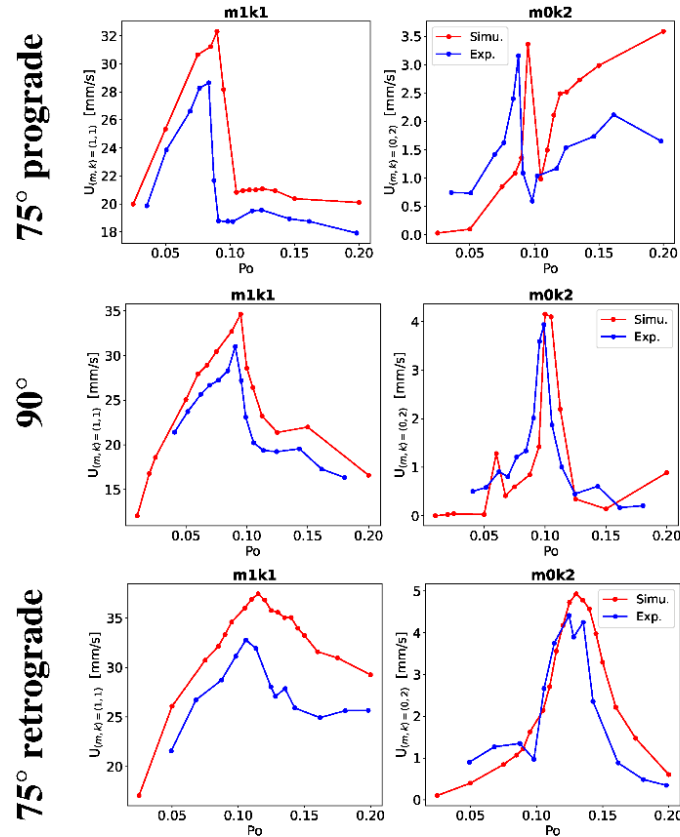
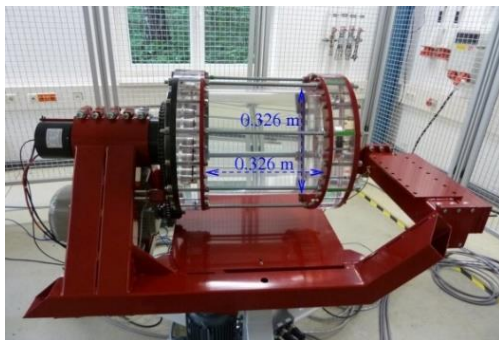
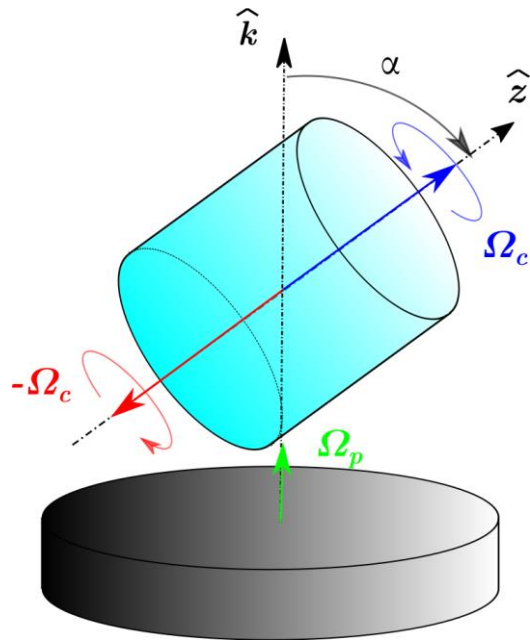
→ **Orbit-spin coupling for the case of tilted rotation axis**

Vidal and Cebron, JFM 833 (2017), 469;

Shirley and Mischna, Planet. Space Science 139 (2017), 3; Shirley, arXiv:2309.13076

Precession driven dynamo: Prospects for self-excitation

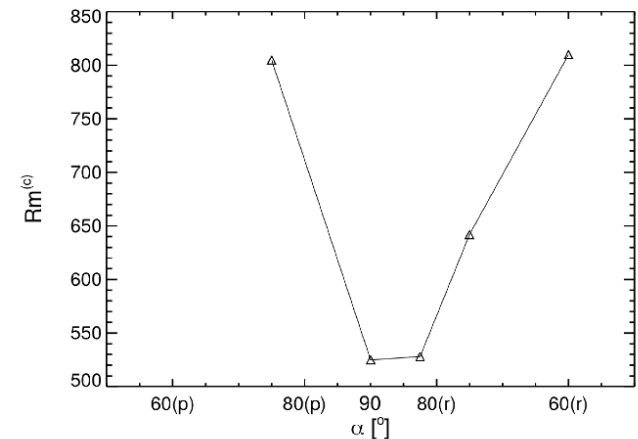
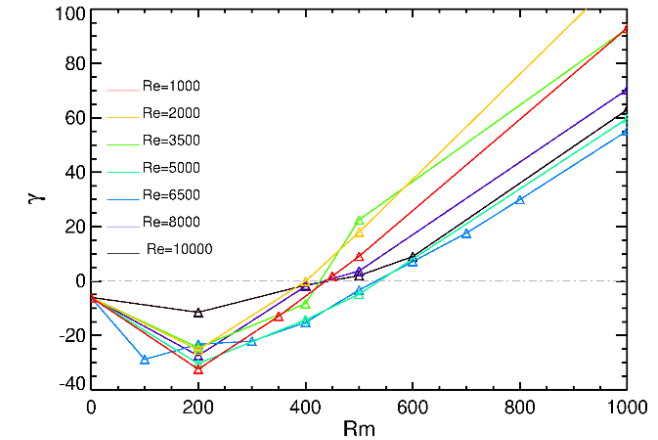
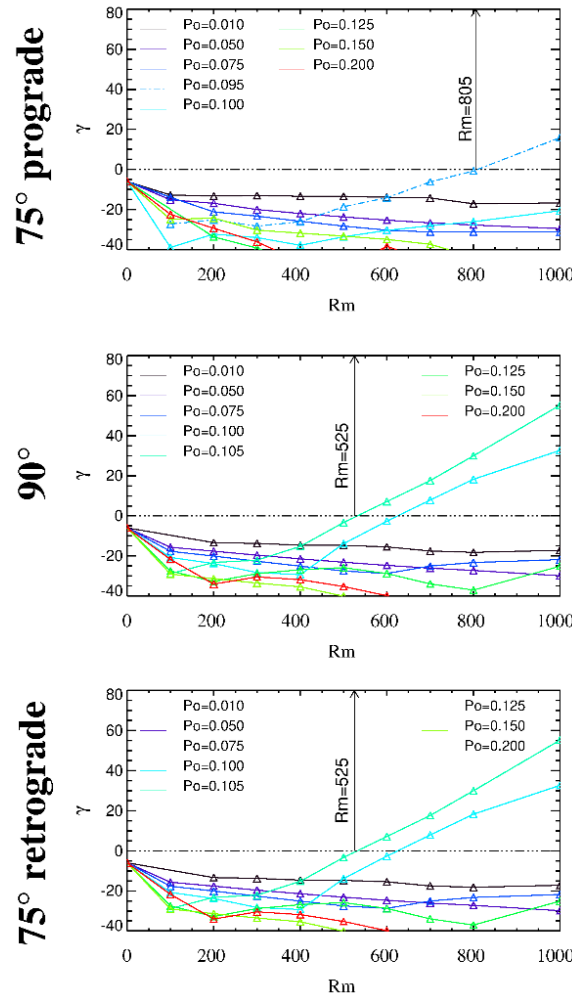
Good agreement of measured and simulated dynamo-relevant flow modes



Kumar et al., Phys. Fluids
35 (2023), 014114

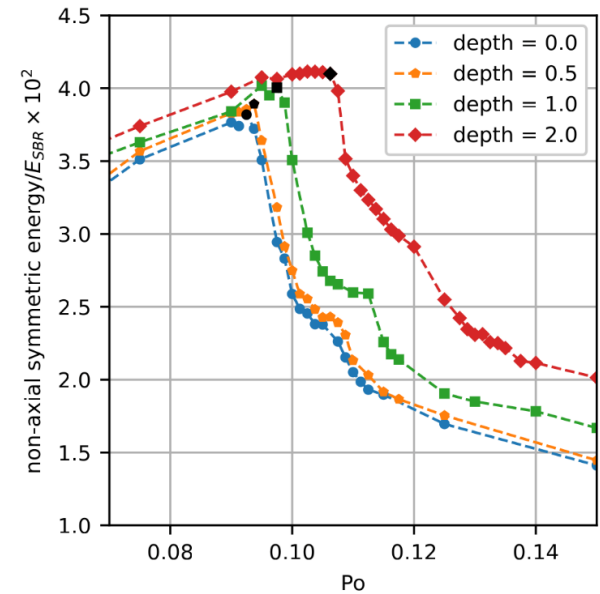
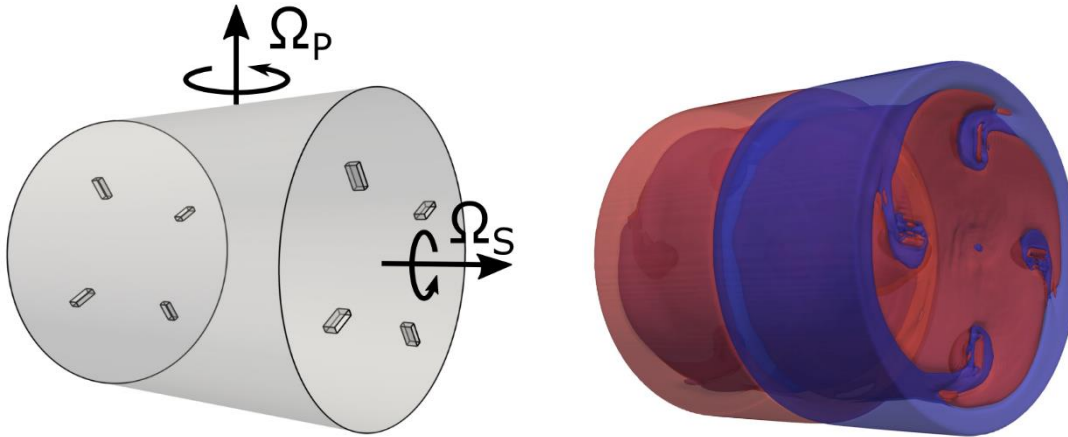
Precession driven dynamo: Prospects for self-excitation

In a narrow range of the precession ratio, **dynamo action is predicted for $Rm \sim 430$** ($Rm=700$ is technically feasible)

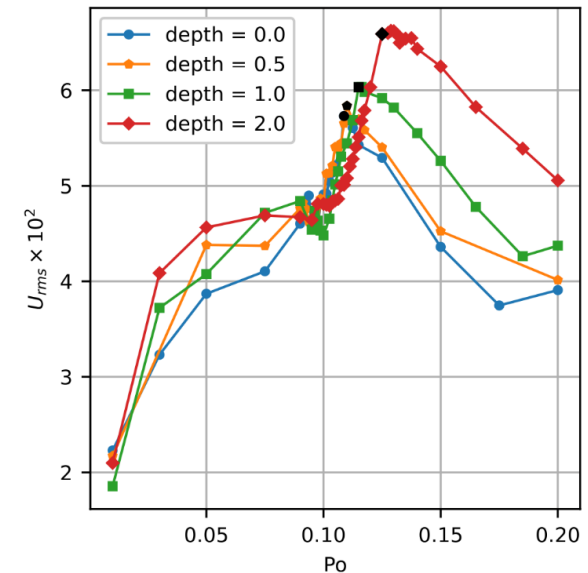


Giesecke et al., Phys. Rev. Lett. 120 (2018), 024502
 Kumar et al., Phys. Fluids 35 (2023), 014114

Role of inserted blades



- Transition between laminar and turbulent flow can be shifted to higher precession ratios
- Thereby, some 10-20 per cent more energy can be deposited into the dynamo-generating flow modes



Wilbert, Giesecke, Grauer, Phys. Fluids, 34, 096607 (2022)

Tilting machine in containment and sodium system are ready

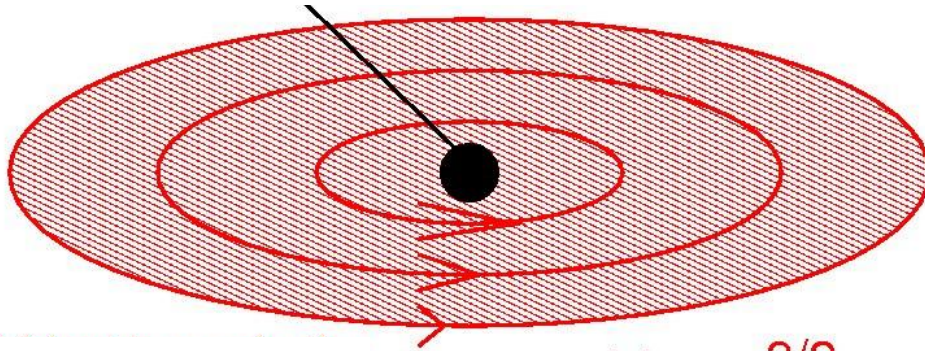


First experiments (with water) are planned for fall 2024



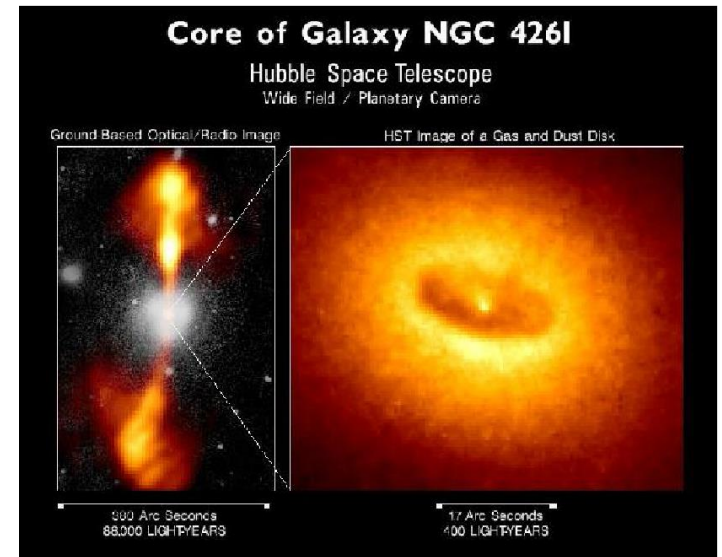
Magnetorotational instability: How do accretion discs work?

Central object (protostar, black hole)



Accretion disk

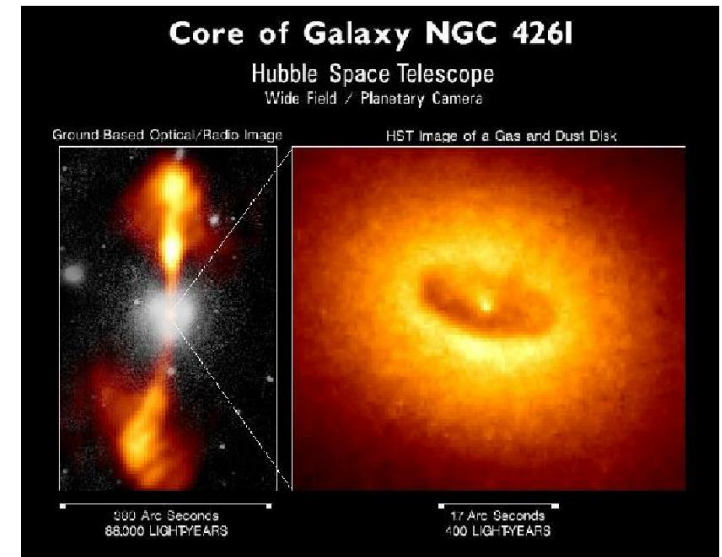
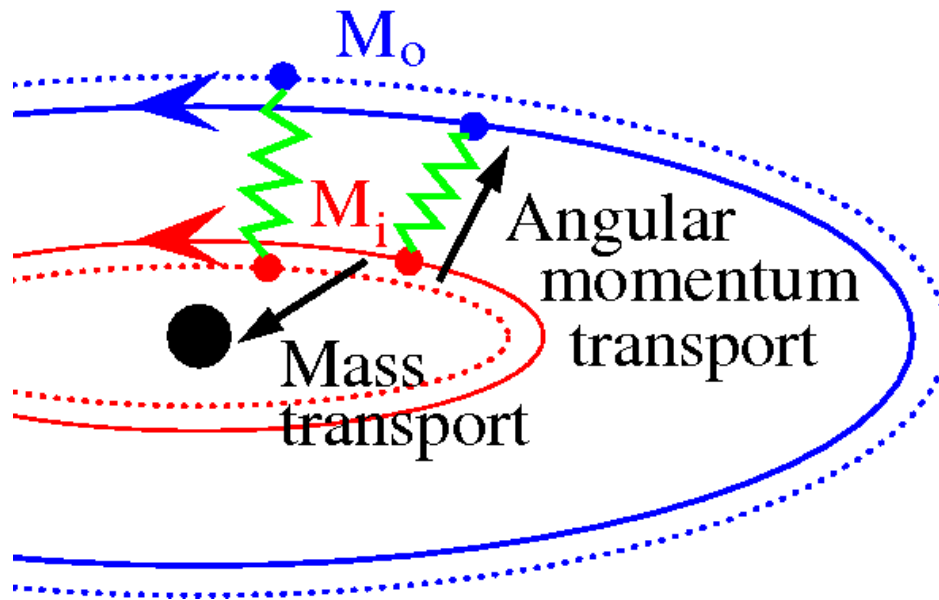
$$\Omega(r) \sim r^{-3/2}$$
$$\Omega(r)r^2 \sim r^{1/2}$$



Problem: Outward angular momentum transport is not explainable by normal viscosity

Turbulence could help. But: **Kepler rotation is hydrodynamically stable. Where does the turbulence come from?**

Magnetorotational instability: How do accretion discs work?



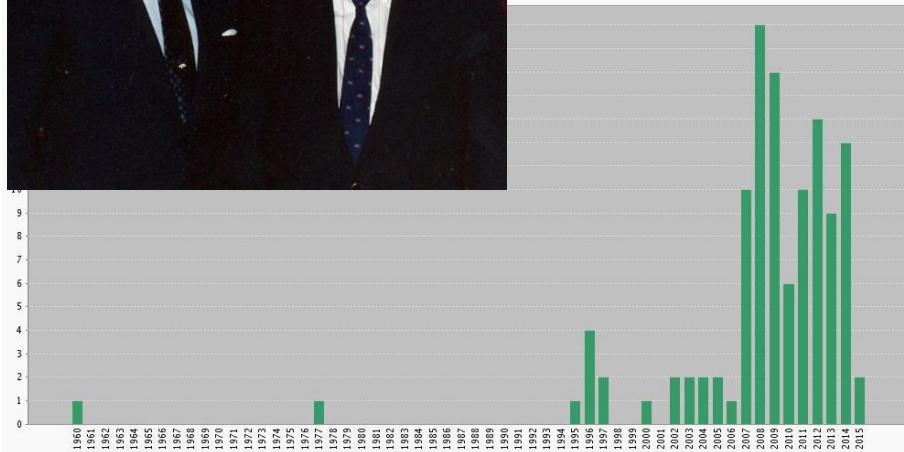
Solution: Magnetic fields act like springs and trigger angular momentum transport in accretion disks around protostars and black holes

(Citation) history of MRI

E.P. Velikhov



386 citations
since 1959



E.P. Velikhov: Sov. Phys.
JETP 9 (1959), 995

S.A. Balbus and J.F. Hawley

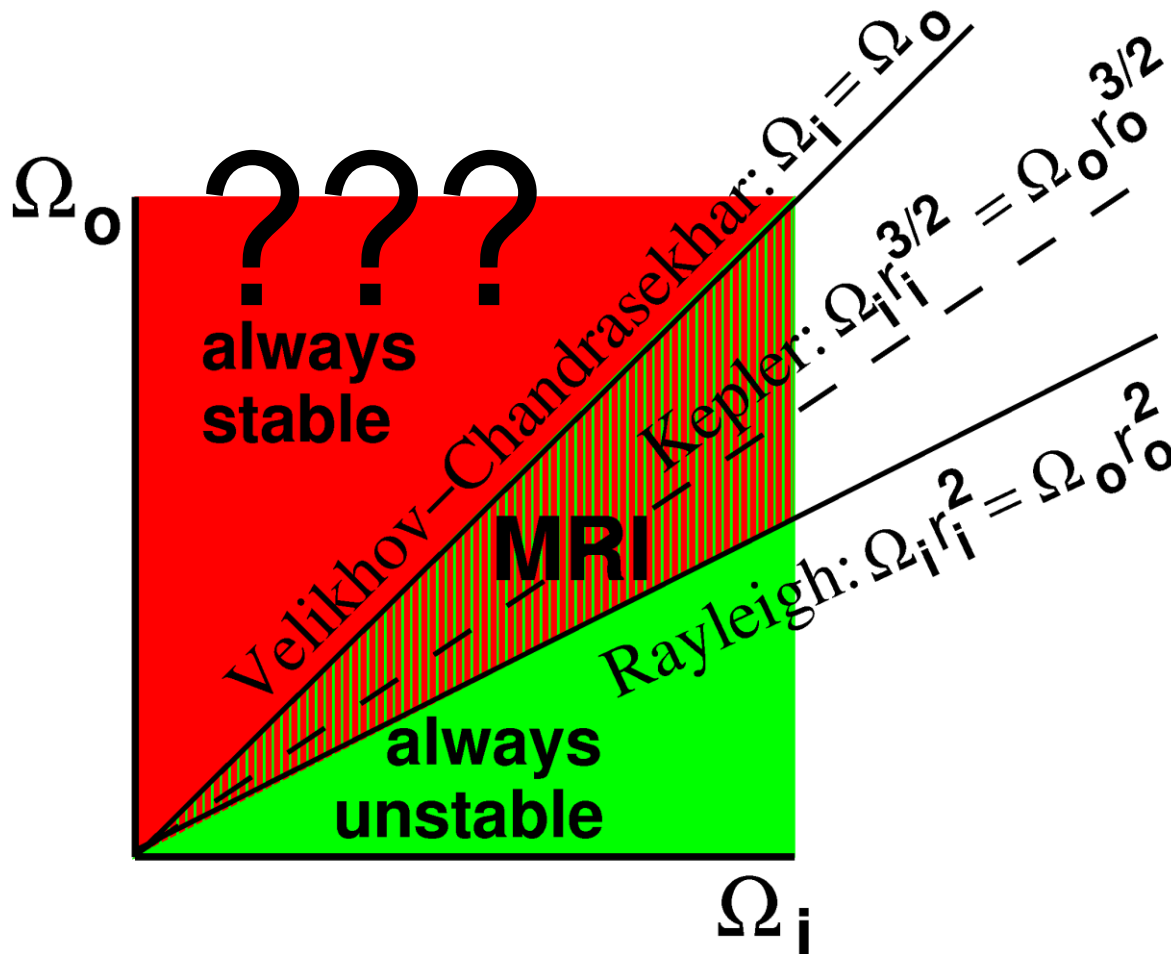


3470 citations
since 1991

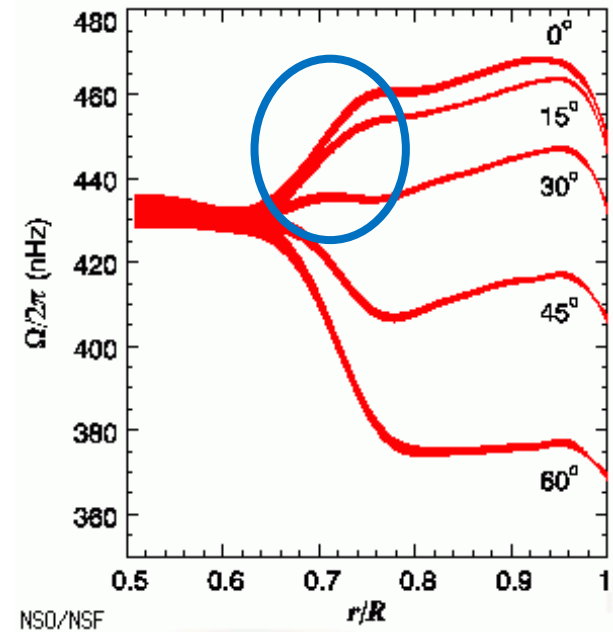


S.A. Balbus and J.F. Hawley:
ApJ 376 (1991), 214

Are rotational flows with positive shear always stable?



Possible relevance for the equator-near parts of the solar tachocline



MRI in the Maryland spherical Couette experiment ???

VOLUME 93, NUMBER 11

PHYSICAL REVIEW LETTERS

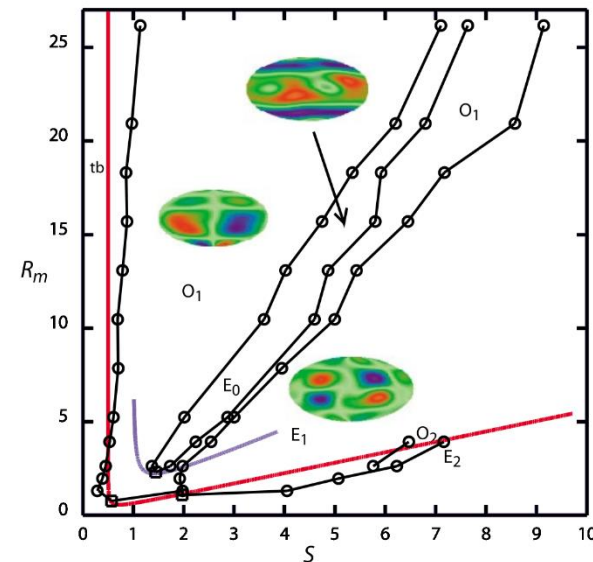
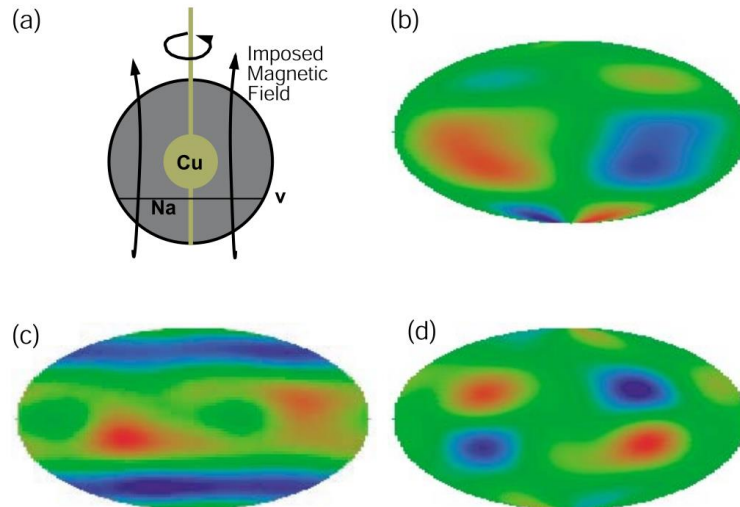
week ending
10 SEPTEMBER 2004

Experimental Observation and Characterization of the Magnetorotational Instability

Daniel R. Sisan, Nicolás Mujica, W. Andrew Tillotson, Yi-Min Huang, William Dorland, Adil B. Hassam, Thomas M. Antonsen, and Daniel P. Lathrop*

Department of Physics, IREAP, IPST, University of Maryland, College Park, Maryland 20742, USA
(Received 25 February 2004; published 10 September 2004)

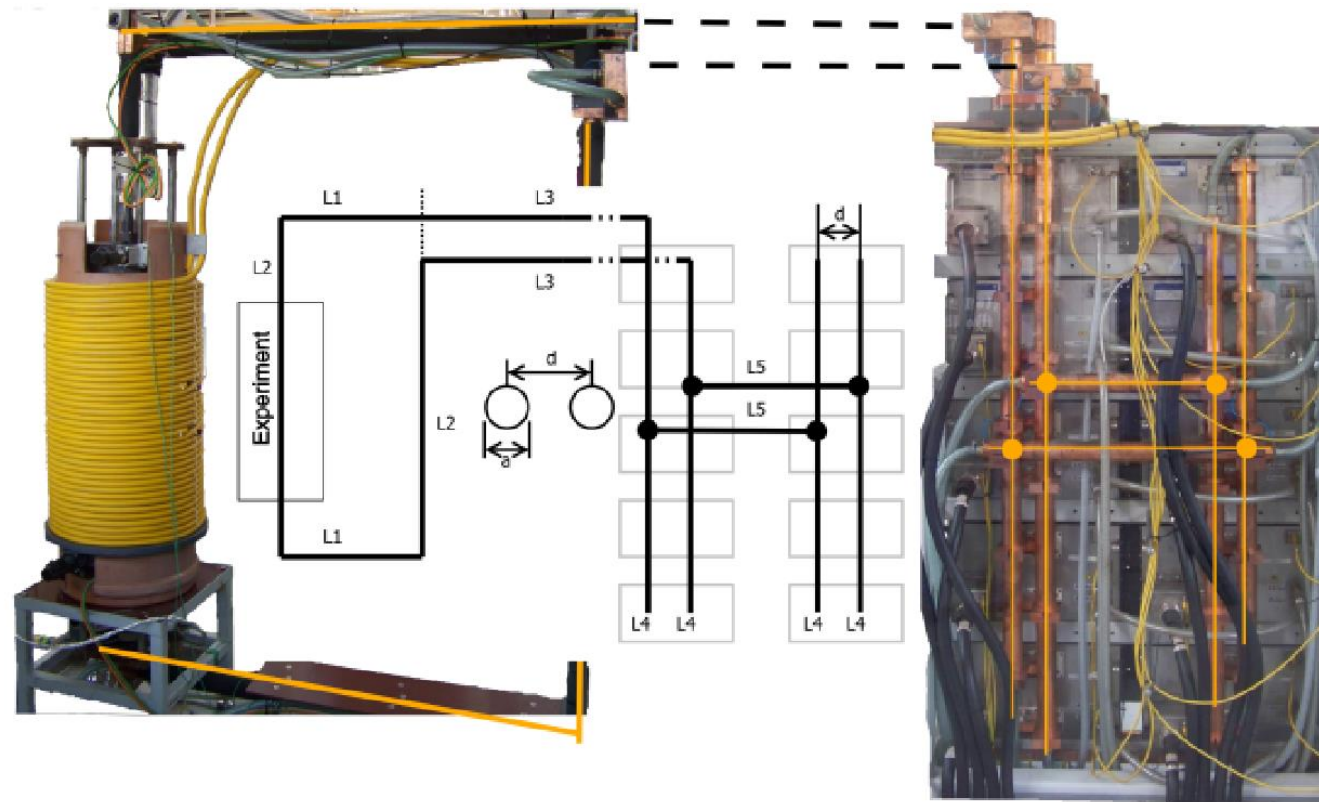
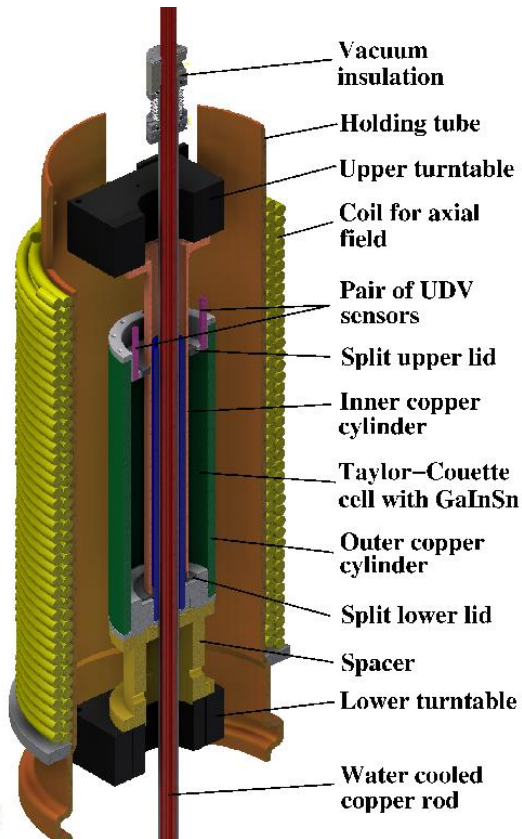
Differential rotation occurs in conducting flows in accretion disks and planetary cores. In such systems, the magnetorotational instability can arise from coupling Lorentz and centrifugal forces to cause large radial angular momentum fluxes. We present the first experimental observation of the magnetorotational instability. Our system consists of liquid sodium between differentially rotating spheres, with an imposed coaxial magnetic field. We characterize the observed patterns, dynamics, and torque increases, and establish that this instability can occur from a hydrodynamic turbulent background.



HZDR

The azimuthal MRI (AMRI): $m=1$ mode under influence of (pure) B_ϕ

New power supply provides currents up to 20 kA

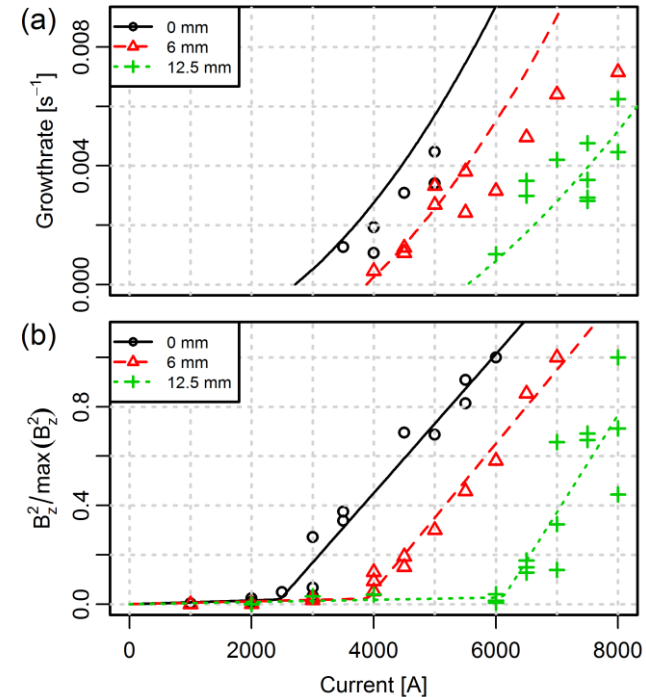
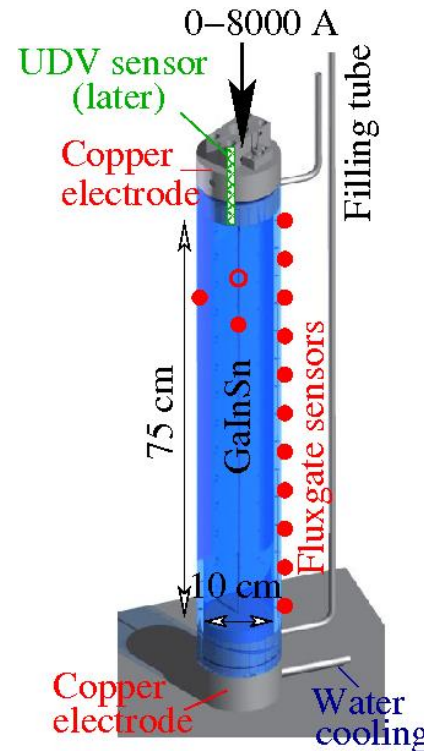
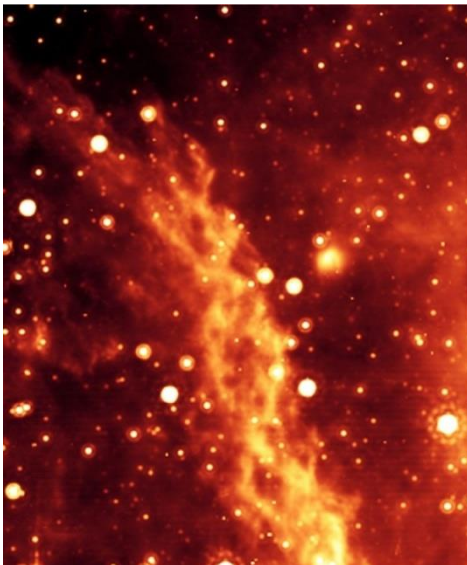


Very important: Simulation of the real geometry including the slight symmetry breaking of the applied magnetic field

Kink-type Tayler instability (TI)

Astrophysical motivation:

- Alternative mechanism of solar dynamo (Tayler-Spruit)
- Braking of neutron stars
- Instabilities in cosmic jets



First experiment at HZDR: Good correspondence of measured critical currents and growth rates of the TI with numerical simulations.

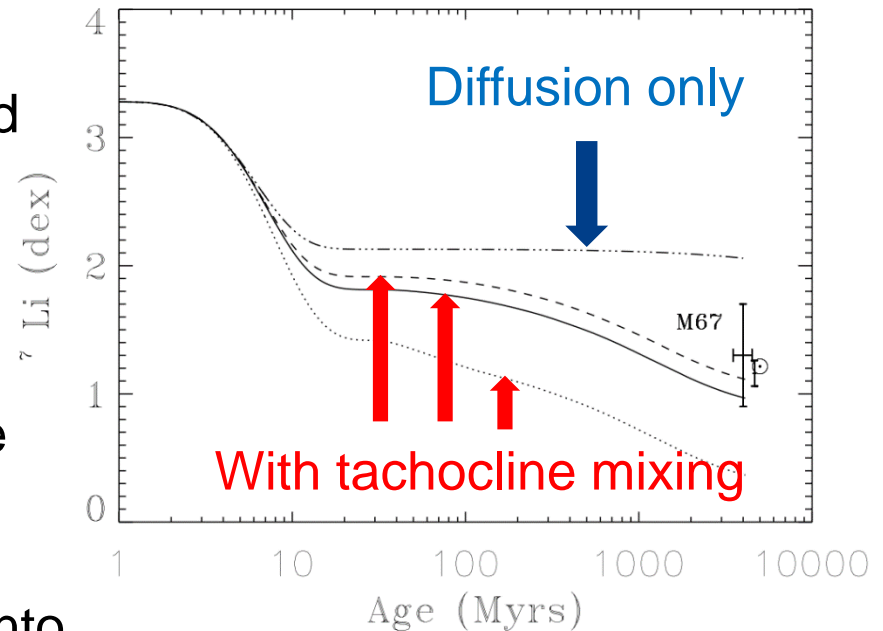
Seilmayer et al., PRL 108
(2012), 244501

This could solve Lithium depletion problem in the sun and stars

Lithium and Beryllium are destroyed by proton captures at very high temperatures ($\text{Li } 2.5 \times 10^6 \text{ K}$).

These elements survive in outer (colder) convection zone of sun-like stars. Their observed continuous decrease suggests a transport process from the convection zone into the radiation zone, where they are destroyed.

Transport mechanism needs to be rather slow (compared to turbulent convective motion).

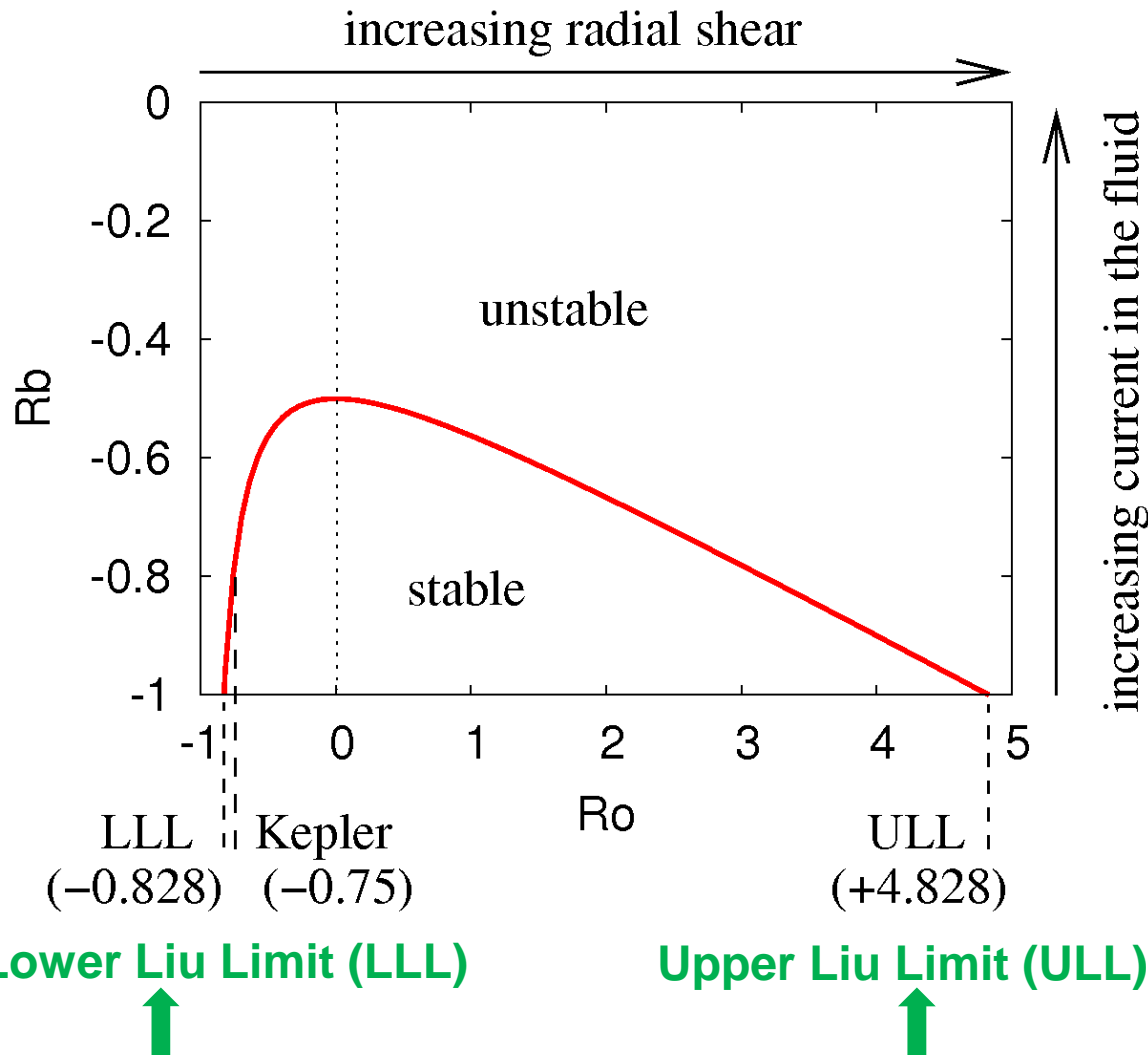


${}^7\text{Li}$ surface abundances in stars with solar mass and composition. Tachocline mixing with disk coupling time 10, 3, and 0.5 Myr, respectively. 5777 K at 4.6 Gyr

Piau and Turck-Chieze, ApJ 566, 419 (2002)

Rüdiger et al., MNRAS 399, 996 (2009)

Can magnetic fields destabilize rotations with positive shear?



$$Ro = \frac{r}{2\Omega} \frac{\partial \Omega}{\partial r}$$

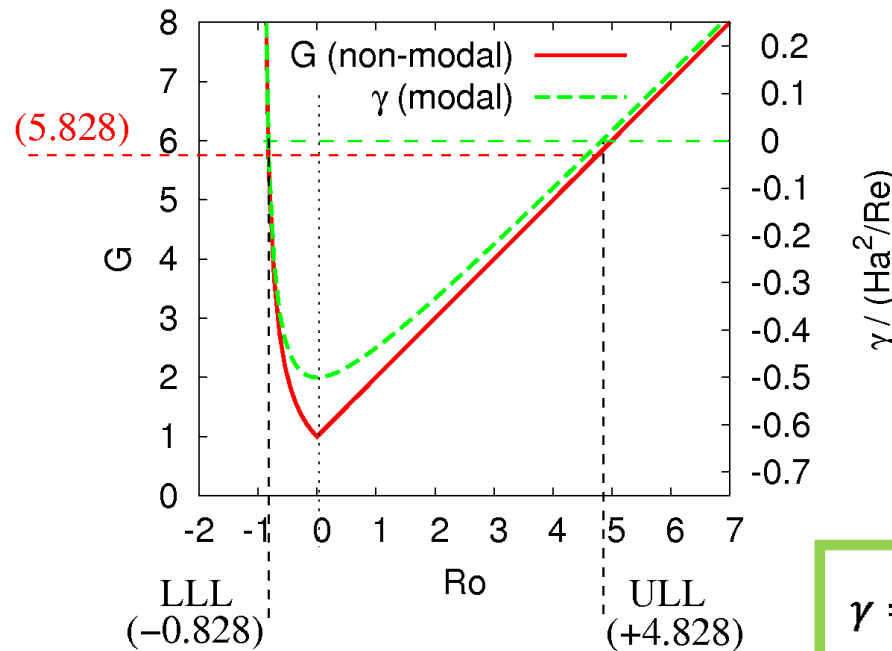
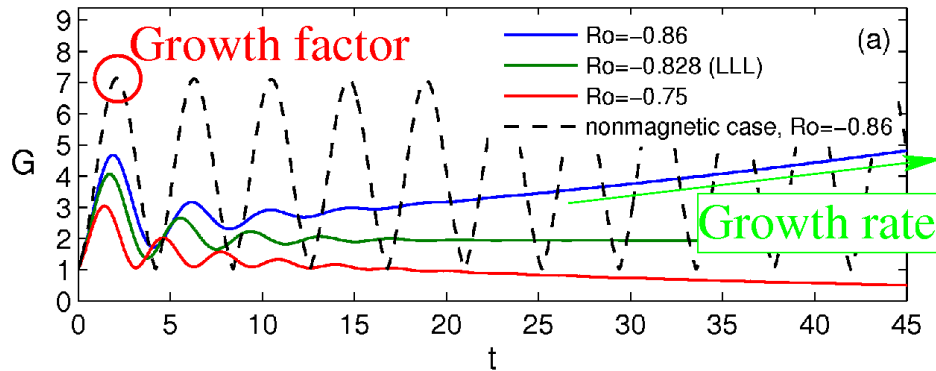
$$Rb = \frac{r}{2\omega_{A\phi}} \frac{\partial \omega_{A\phi}}{\partial r}$$

$$Rb = -\frac{1}{8} \frac{(Ro + 2)^2}{Ro + 1}$$

Kirillov and F.S., Phys. Rev. Lett. 111 (2013), 061103; JFM 760 (2014), 591

Liu, Goodman, Herron, Ji, Phys. Rev. E 74 (2006), 056302

Linking non-modal growth and dissipation-induced instabilities



Is there any physical reason behind LLL and ULL of the shear for the emergence of HMRI?

YES!

Analytical link between **non-modal growth factor G** of purely hydro-dynamic flows with **modal growth rate γ** of dissipation-induced HMRI

$$G_m = (1 + Ro)^{\text{sgn}(Ro)}$$

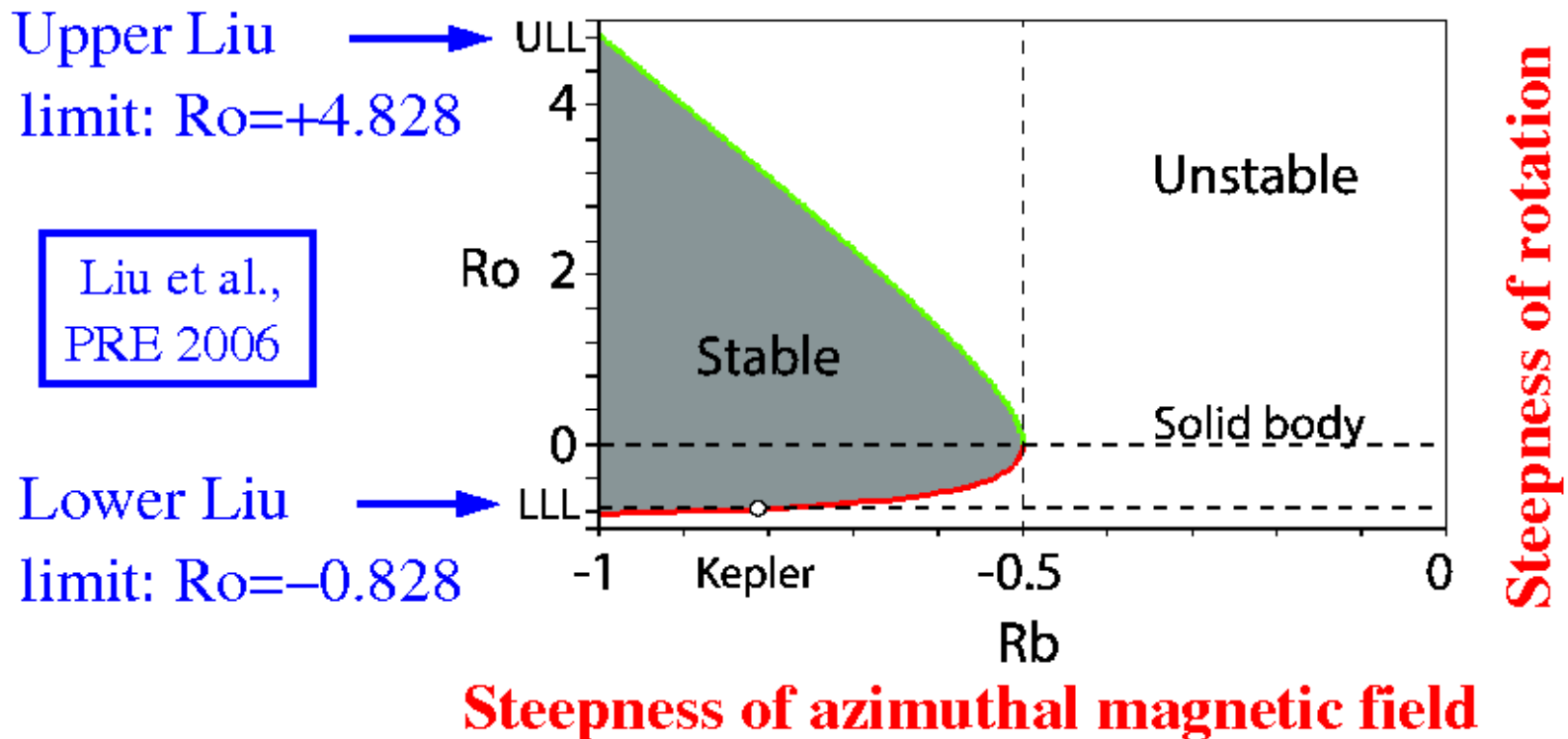
$$\gamma = \frac{Ha^2}{Re} \left[\frac{(Ro + 2)^2}{8(1 + Ro)} - 1 \right] = \frac{Ha^2}{Re} \left[\frac{(G_m + 1)^2}{8G_m} - 1 \right]$$

Destabilizing Kepler flows with appropriate combination of MRI and TI

WKB-Analysis of the complete viscous and resistive MRI/TI problem for arbitrary azimuthal modes

Main results:

$$Rb = -\frac{1}{8} \frac{(Ro + 2)^2}{Ro + 1}$$

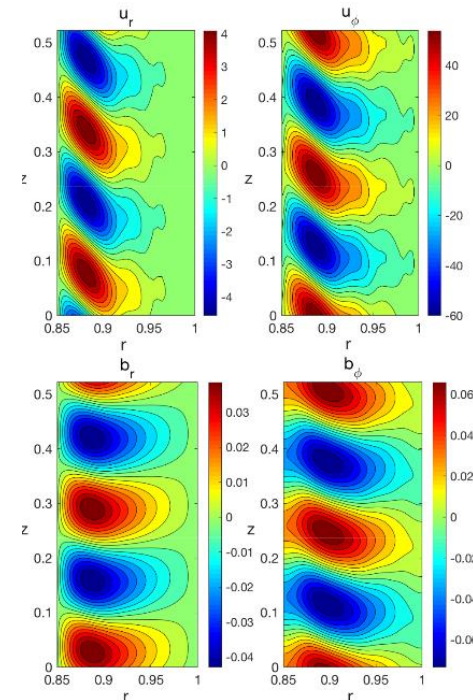
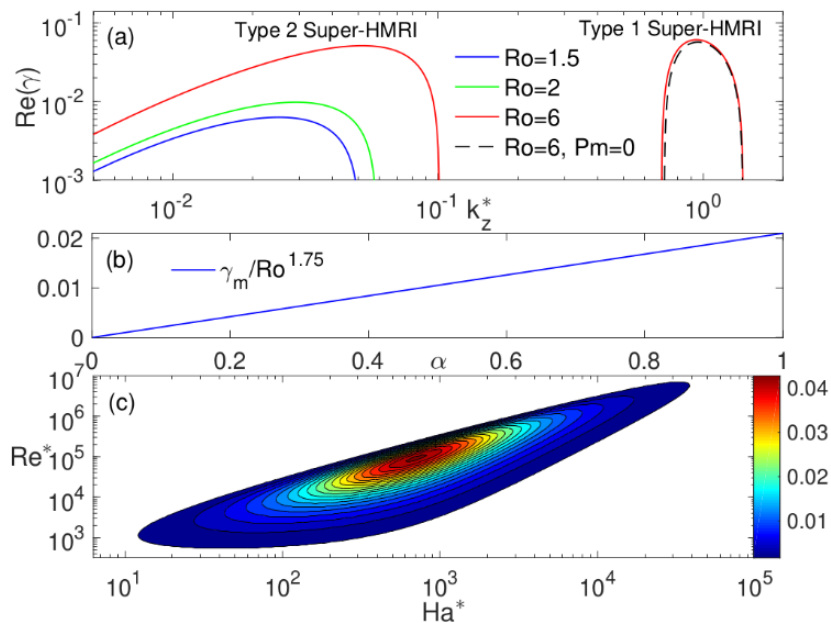


Kirillov and Stefani, Phys. Rev. Lett. 111 (2013), 061103;
arXiv:1307.1576; arXiv:1401.8276

New instability for rotating flow with positive shear

Super-HMRI:

- Axi-symmetric: $m=0$
- Scales with Rm and Lundquist
- Requires B_φ and B_z
- Double-diffusive! Not for $Pm=1$
- Works for arbitrarily weak shear!



Super-HMRI should also be detectable in the new MRI/TI experiment...

...and seems also to work for the near-equator parts of the tachocline!

Mamatsashvili, F.S., Hollerbach, Rüdiger, Phys. Rev. Fluids 4 (2019), 103905

Planned experiment: Technical aspects

Parameters:

- $r_{in}=0.2$ m
- $r_{out}=0.4$ m
- $h=2$ m

- $f_{in}=20$ Hz
- $f_{out}=6$ Hz

- $B_z=150$ mT

- $Rm = 40$
- $Lu = 8$

